

AD-A243 553



Lin (2)

NAVAL POSTGRADUATE SCHOOL

Monterey, California



DTIC
ELECTE
DEC 8 1991
S C D

THESIS

A CAD MODEL FOR THE AXIAL INDUCTIVE STRIP
WITH FINITE THICKNESS CENTERED IN
HOMOGENEOUS FINLINE WITH $w/b=1$

by

Dimitris Dariotis

December 1990

Thesis Advisor:

Jeffrey B. Knorr

Approved for public release; distribution is unlimited

91-18402



91-18402

Approved for public release; distribution is unlimited.

**A Circuit Model for Inductive Strip with Finite Thickness Centered in
Homogeneous Finline with $w/b=1$**

by

**Dimitrios Dariotis
Lieutenant, Hellenic Navy
B.S., Hellenic Naval Academy, 1982**

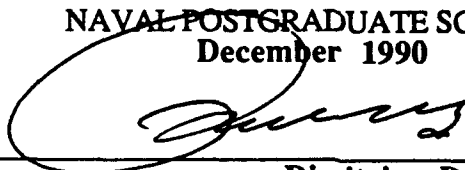
Submitted in partial fulfillment of the requirements for the
degree of

MASTER OF SCIENCE IN ELECTRICAL ENGINEERING

from the

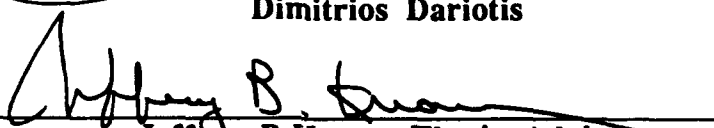
**NAVAL POSTGRADUATE SCHOOL
December 1990**

Author:

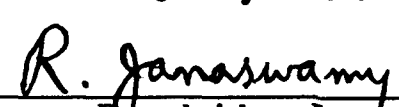


Dimitrios Dariotis


Approved by:



Jeffrey B. Knorr, Thesis Advisor



Ramakrishna Janaswamy, Second reader



**Michael A. Morgan, Chairman
Department of Electrical and Computer Engineering**

ABSTRACT

This thesis describes a CAD compatible circuit model for an inductive strip with finite metal thickness centered in finline with $w/b=1$. Scattering coefficients predicted by the circuit model are in good agreement with those predicted by an electromagnetic model based on Maxwell's equations. Filter simulations using the circuit model predict responses which are in good agreement with laboratory measurements.

TABLE OF CONTENTS

I. INTRODUCTION.....	1
A. BACKGROUND.....	1
B. OBJECTIVE	2
C. RELATED WORK.....	2
II. SCATTERING COEFFICIENTS FOR THE INDUCTIVE STRIP.....	5
A. CONCEPT	5
B. BACKGROUND.....	5
III. A CAD MODEL FOR THE INDUCTIVE STRIP.....	8
A. BACKGROUND.....	8
B. CIRCUIT MODEL.....	9
C. SCALING THE MODEL FOR ALL THE FREQUENCY BANDS	17
D. MODEL ACCURACY.....	20
IV. EXPERIMENTAL VALIDATION.....	23
V. CONCLUSIONS AND RECOMMENDATIONS	32
A. CONCLUSIONS.....	32
B. RECOMMENDATIONS	32
APPENDIX A.....	33
APPENDIX B.....	40
APPENDIX C.....	70
REFERENCES.....	79
INITIAL DISTRIBUTION LIST.....	81

Accession for	
NTIS Serial	
DTIC Tab	
Unannounced	
Justification	
By	
Distribution	
Availability Codes	
Dist	Special
A-1	

LIST OF FIGURES

Figure 1.	Inductive strip in finline.....	4
Figure 2.	Model for the inductive strip with finite thickness.	10
Figure 3.	A Touchstone program for the inductive strip.	11
Figure 4.	Inductance versus strip length for metal thickness.	14
Figure 5.	Inductance versus strip length with metal thickness $t=5$ mils.....	15
Figure 6.	Inductance versus strip length with metal thickness $t=50$ mils.	15
Figure 7.	Coefficient A_1 versus metal thickness	16
Figure 8.	A_2 coefficient versus metal thickness.....	16
Figure 9.	A CAD model for the finline for all the frequency bands.....	18
Figure 10.	A CAD model for the finline for all the frequency bands (cont.).....	19
Figure 11.	Magnitude $ S_{11} $ versus Frequency for $T=200$ mils, $t=45$ mils.....	21
Figure 12.	Phase versus Frequency for $T=200$ mils and $t=45$ mils.....	22
Figure 13.	Filter with three resonators.....	24
Figure 14.	Finline Filter Model Program.....	25
Figure 15.	Finline Filter Model program (cont.).	26
Figure 16.	Finline Filter Model program (cont.).	27
Figure 17.	Experimental response for the X-Band filter [Ref 9].....	28
Figure 18.	Filter response from the finline filter model	28
Figure 19.	Experimental response for the Ku Band filter [Ref 11].....	29
Figure 20.	Model response for the Ku Band filter.	29
Figure 21.	Experimental response for the Ka band filter [Ref 11].	30
Figure 22.	Model response for the Ka Band filter.....	30
Figure 23.	Experimetal response for the E Band filter [Ref 11].	31
Figure 24.	Model response for the E Band filter.	31
Figure 25.	Magnitude of S_{11} versus frequency for strip length $T=0.1$ mm.	33
Figure 26.	Angle Θ_{11} versus frequency for strip length $T=0.1$ mm.	33
Figure 27.	Magnitude of S_{11} versus frequency for strip length $T=0.2$ mm.	34
Figure 28.	Angle Θ_{11} versus frequency for strip length $T=0.2$ mm.....	34
Figure 29.	Magnitude of S_{11} versus frequency for strip length $T=0.5$ mm.	35
Figure 30.	Angle Θ_{11} versus frequency for strip length $T=0.5$ mm.	35

Figure 31.	Magnitude S11 versus frequency for strip length $T=1\text{mm}$	36
Figure 32.	Angle Θ_{11} versus frequency for strip length $T=1\text{ mm}$	36
Figure 33.	Magnitude of S11 versus frequency for strip length $T=2\text{ mm}$	37
Figure 34.	Angle Θ_{11} versus frequency for strip length $T=2\text{ mm}$	37
Figure 35.	Magnitude for S11 versus frequency for strip length $T=5\text{ mm}$	38
Figure 36.	Angle Θ_{11} versus frequency for strip length $T=5\text{ mm}$	38
Figure 37.	Magnitude of S11 for strip with thickness $t=5\text{ mils}$ [Ref 10].....	39
Figure 38.	Angle of the S11 for strip with thickness $t=5\text{ mils}$ [Ref 10].	39
Figure 39.	Plots for WR(28), $w/b=1$, $T=0.1\text{ mm}$, $t=0\text{ mils}$	40
Figure 40.	Plots for WR(28), $w/b=1$, $T=0.1\text{ mm}$, $t=1\text{ mils}$	41
Figure 41.	Plots for WR(28), $w/b=1$, $T=0.1\text{ mm}$, $t=2\text{ mils}$	42
Figure 42.	Plots for WR(28), $w/b=1$, $T=0.1\text{ mm}$, $t=5\text{ mils}$	43
Figure 43.	Plots for WR(28), $w/b=1$, $T=0.1\text{ mm}$, $t=50\text{ mils}$	44
Figure 44.	Plots for WR(28), $w/b=1$, $T=0.2\text{ mm}$, $t=0\text{ mils}$	45
Figure 45.	Plots for WR(28), $w/b=1$, $T=0.2\text{ mm}$, $t=1\text{ mils}$	46
Figure 46.	Plots for WR(28), $w/b=1$, $T=0.2\text{ mm}$, $t=2\text{ mils}$	47
Figure 47.	Plots for WR(28), $w/b=1$, $T=0.2\text{ mm}$, $t=5\text{ mils}$	48
Figure 48.	Plots for WR(28), $w/b=1$, $T=0.2\text{ mm}$, $t=50\text{ mils}$	49
Figure 49.	Plots for WR(28), $w/b=1$, $T=0.5\text{ mm}$, $t=0\text{ mils}$	50
Figure 50.	Plots for WR(28), $w/b=1$, $T=0.5\text{ mm}$, $t=1\text{ mils}$	51
Figure 51.	Plots for WR(28), $w/b=1$, $T=0.5\text{ mm}$, $t=2\text{ mils}$	52
Figure 52.	Plots for WR(28), $w/b=1$, $T=0.5\text{ mm}$, $t=5\text{ mils}$	53
Figure 53.	Plots for WR(28), $w/b=1$, $T=0.5\text{ mm}$, $t=50\text{ mils}$	54
Figure 54.	Plots for WR(28), $w/b=1$, $T=1\text{ mm}$, $t=0\text{ mils}$	55
Figure 55.	Plots for WR(28), $w/b=1$, $T=1\text{ mm}$, $t=1\text{ mils}$	56
Figure 56.	Plots for WR(28), $w/b=1$, $T=1\text{ mm}$, $t=2\text{ mils}$	57
Figure 57.	Plots for WR(28), $w/b=1$, $T=1\text{mm}$, $t=5\text{ mils}$	58
Figure 58.	Plots for WR(28), $w/b=1$, $T=1\text{ mm}$, $t=50\text{ mils}$	59
Figure 59.	Plots for WR(28), $w/b=1$, $T=2\text{ mm}$, $t=0\text{ mils}$	60
Figure 60.	Plots for WR(28), $w/b=1$, $T=2\text{ mm}$, $t=1\text{ mils}$	61
Figure 61.	Plots for WR(28), $w/b=1$, $T=2\text{ mm}$, $t=2\text{ mils}$	62
Figure 62.	Plots for WR(28), $w/b=1$, $T=2\text{ mm}$, $t=5\text{ mils}$	63
Figure 63.	Plots for WR(28), $w/b=1$, $T=2\text{ mm}$, $t=50\text{ mils}$	64

Figure 64. Plots for WR(28), $w/b=1$, $T=5$ mm, $t=0$ mils.....	65
Figure 65. Plots for WR(28), $w/b=1$, $T=5$ mm, $t=1$ mils.....	66
Figure 66. Plots for WR(28), $w/b=1$, $T=5$ mm, $t=2$ mils.....	67
Figure 67. Plots for WR(28), $w/b=1$, $T=5$ mm, $t=5$ mils.....	68
Figure 68. Plots for WR(28), $w/b=1$, $T=5$ mm, $t=50$ mils.....	69
Figure 69. Magnitude for WR(28) with $w/b=1$, $T=15$ mils, $t=0$ mils.....	71
Figure 70. Angle for WR(28) with $w/b=1$, $T=15$ mils, $t=0$ mils.....	71
Figure 71. Magnitude for WR(8) with $w/b=1$, $T=30$ mils, $t=0$ mils.....	74
Figure 72. Angle for WR(8) with $w/b=1$, $T=30$ mils, $t=0$ mils.....	74
Figure 73. Model response for the Ka band filter with $t=0$ mils.....	78
Figure 74. Model response for the E band filter with $t=0$ mils.	78

LIST OF TABLES

TABLE 1. INDUCTANCE (μH) FOR BEST MATCH BETWEEN MODEL AND SHIH'S DATA.....	13
TABLE 2. COEFFICIENTS A1, A2 FOR THE INDUCTANCE	13
TABLE 3. FILTERS SPECIFICATIONS	24
TABLE 4. S-DATA FOR STRIP LENGTH $T=0.1\text{ MM}$	33
TABLE 5. S-DATA FOR STRIP WITH LENGTH $T=0.2\text{ MM}$	34
TABLE 6. S-DATA FOR STRIP LENGTH $T=0.5\text{ MM}$	34
TABLE 7. S-DATA FOR STRIP LENGTH $T=1\text{ MM}$	35
TABLE 8. S-DATA FOR STRIP LENGTH $T=2\text{ MM}$	36
TABLE 9. S-DATA FOR STRIP LENGTH $T=5\text{ MM}$	37
TABLE 10. S-DATA FOR WR(28), $w/b=1$, $T=15\text{ MILS}$ $t=0\text{ MILS}$	70
TABLE 11. S-DATA FOR WR(28), $w/b=1$, $T=15\text{ MILS}$, $t=0\text{ MILS}$ FROM [REF.10].....	70
TABLE 12. S-DATA FOR WR(8), $w/b=1$, $T=30\text{ MILS}$, $t=0\text{ MILS}$ FROM [REF. 9]....	72
TABLE 13. S-DATA FOR WR(8), $w/b=1$, $T=30\text{ MILS}$, $t=0\text{ MILS}$	73
TABLE 14. WORST ERROR FOR METAL THICKNESS $t=0\text{ MILS}$	75
TABLE 15. WORST ERROR FOR METAL THICKNESS $t=1\text{ MILS}$	75
TABLE 16. WORST ERROR FOR METAL STRIP $t=2\text{ MILS}$	76
TABLE 17. WORST ERROR FOR METAL THICKNESS $t=5\text{ MILS}$	76
TABLE 18. WORST ERROR FOR METAL THICKNESS $t=50\text{ MILS}$	77

ACKNOWLEDGEMENTS

I would like to thank Prof. Jeffery B. Knorr for his continued support and guidance. I would also like to thank my wife Tina for her help and moral support and my son Jason-Dimitris for his patience.

I. INTRODUCTION

A. BACKGROUND

It is known from the theory of transmission lines that for efficient transmission, coaxial lines, rectangular waveguides and circular waveguides are usually used. The coaxial line generally is used at frequencies below 5 GHz while rectangular waveguide is used for applications above 5 GHz. Circular waveguides are widely used in situations where the transmitted or received waves are elliptically polarized.

In millimeter wave applications, small sections of transmission lines are often used to realize inductance and capacitance. Microwave integrated circuits for example, are built using planar transmission lines. The importance of millimeter wave systems has increased very quickly during the last twenty years. This importance is more powerful in military applications. Applications such as short range communication with link privacy and precise tracking guidance systems for missiles are improved with the use of the millimeter waves.

Microstrips are often used in the design of microwave integrated circuits to improve the advantages provided by them above 3 GHz. According to Meier [Ref. 1], the advantages include reduced size, production uniformity, reliability, and improved electrical performance. However, integrated circuits at centimeter wavelengths (3-30 GHz) have some fundamental problems which have limited the use of microstrip to fabricate such circuits. The problems are radiation loss, higher mode propagation, and spurious coupling. The above problems become more significant as the operating frequency is raised. To overcome the above problems and other difficulties, integrated finline is often used as a medium for constructing millimeter wave circuits. Figure 1, on page 4 shows a

cross-sectional view of finline, a 3-dimensional view of an inductive strip with finite thickness, and a cross-sectional view of an inductive strip with finite thickness in the waveguide.

The structure of the finline consists of axial metal fins inserted in a rectangular waveguide so that the fin surface is parallel to the narrow waveguide wall. As disadvantages for the integrated finline, we mention that, due to the high field concentration at the edges of the strip, the finline must be used for applications with low and medium power.

Modeling is a powerful capability, the use of which started just recently, to develop microwave computer assisted design (CAD) programs. The goal of CAD programs is to be used as a tool in the design process for microwave circuits. It can be said that such programs are successful if they can predict what one would observe experimentally.

B. OBJECTIVE

The first objective of this research is to measure the scattering coefficients of E-plane inductive metal strips of finite thickness and $w/b=1$. The second objective is to use measured scattering coefficients to develop a CAD model for the axial inductive strip with finite thickness centered in the finline with $w/b=1$.

C. RELATED WORK

There have been a number of studies about finline and the inductive strip in finline in the microwave laboratory of NPS. Initially, analysis of the finline using the spectral domain method was published by Knorr and Shayda in 1980 [Ref. 2]. Miller did experimental measurements of scattering coefficients of inductive strips and published data in his thesis in December 1980 [Ref. 3]. A 1981 paper by Knorr presents experimental and numerical data for a shorting septum [Ref. 4]. Experimental and numerical results for

inductive strips were published by Deal in his thesis in March 1984 [Ref. 5], and by Knorr and Deal in October 1985 [Ref. 6]. A 1988 report by Knorr presents a circuit model for an inductive strip centered in a unilateral finline with $w/b=1$ [Ref. 7]. Lately, a CAD model for inductive strips with infinitesimally thin metal in homogeneous finline was published by Knorr in a March 1990 report [Ref. 8] and by Morua in his thesis work in June 1990 [Ref. 9].

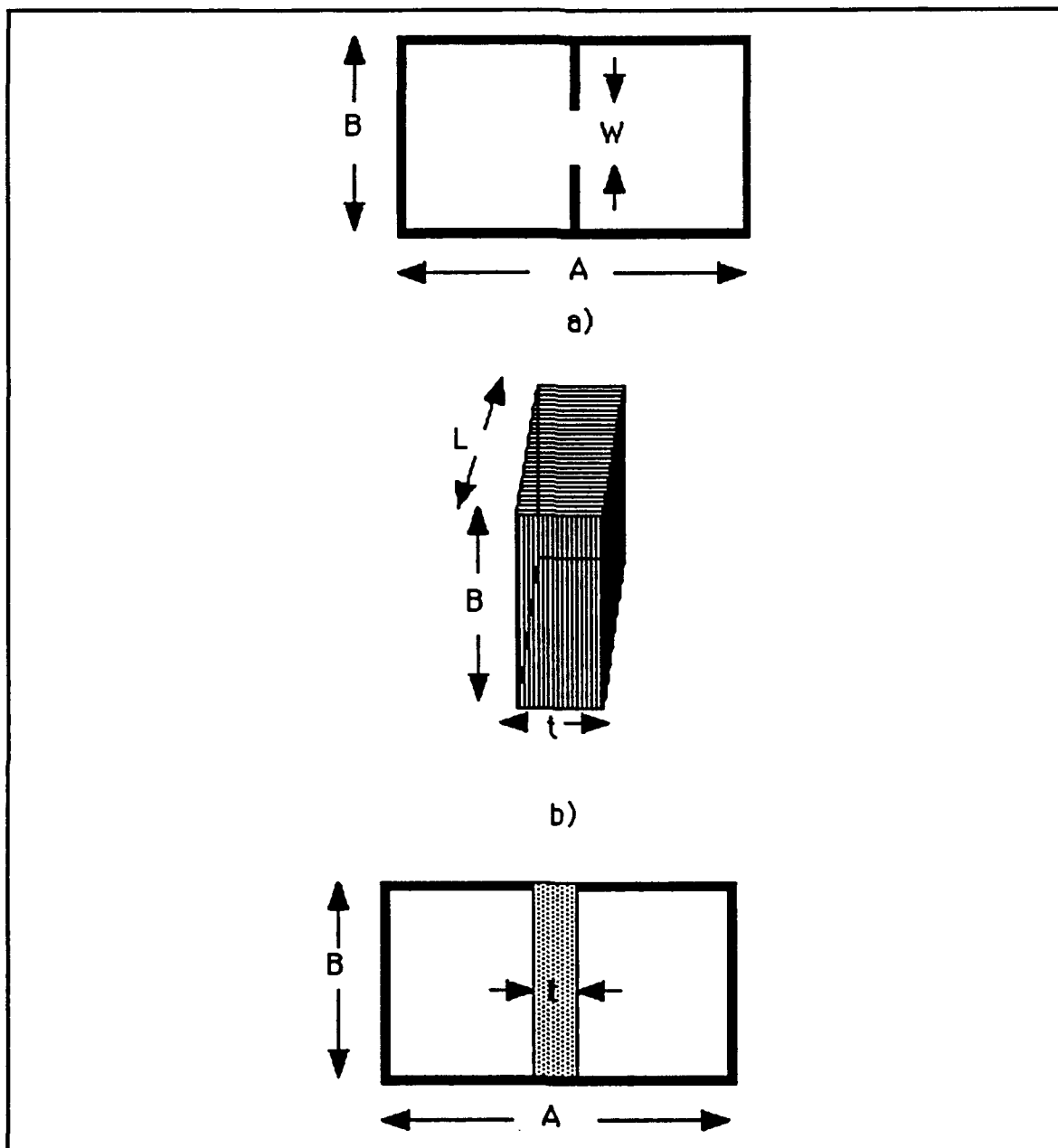


Figure 1. Inductive strip in finline.: a) cross-sectional view of a finline b) inductive strip with finite thickness c) cross sectional view of strip with finite thickness centered in the rectangular waveguide.

II. SCATTERING COEFFICIENTS FOR THE INDUCTIVE STRIP

A. CONCEPT

As mentioned before, the objective of this research is to develop a CAD model for the inductive strip with finite thickness. The already existing models, mentioned above, are for inductive strips with infinitesimally thin metal. The starting point for these models was the scattering coefficients developed by the spectral domain method. The greatest problem of this research was to find a way to measure the scattering coefficients of E-plane inductive strips with finite thickness. At the beginning, with the help of the Mechanical Engineering Department, strips with $w/b=1$ and strip length $t=50, 100, 200$ mils were machined. Each of those strips was constructed with thickness $t=90, 45$ mils and $b=400$ mils for use with the WR(90) waveguide. However, it was subsequently decided to use the curves of scattering coefficients ($|S_{11}|, \theta_{11}$) versus strip length for different strip thickness for the Ka band which were published by Yi-Chi Shih in July 1984 [Ref. 10], for the following reasons: a) The dimensions of the machined strips were different than those we requested. b) It was a problem to put the strips into WR(90) waveguide and to center them. c) The generated error of the procedure used to measure the S-parameters. It was also decided that the scattering coefficients measured in the laboratory would be used for validation of Yi-Chi Shih's work [Ref. 10].

B. BACKGROUND

It is known from network theory that in microwave applications it is quite useful to work with the scattering matrix. In our problem, the network has two ports (input, output) which means that the scattering matrix is as follows:

$$S = \begin{bmatrix} S_{11} & S_{12} \\ S_{21} & S_{22} \end{bmatrix} \quad (1)$$

where S_{11} , S_{12} , S_{21} , S_{22} are the scattering coefficients of the two-port network.

When the network is lossless and reciprocal, the following equations are valid:

$$|S_{21}| = \sqrt{1 - |S_{11}|^2} \quad (2)$$

$$\Theta_{21} = \Theta_{11} \pm \frac{\pi}{2} \quad (3)$$

$$S_{12} = S_{21} \quad (4)$$

$$|S_{11}| = |S_{22}| \quad (5)$$

If the network is symmetric, the following equation is valid:

$$\Theta_{11} = \Theta_{22} \quad (6)$$

If we substitute the above relations into the scattering matrix, we obtain:

$$S = \begin{bmatrix} |S_{11}| e^{j\Theta_{11}} & \sqrt{1 - |S_{11}|^2} e^{j[\Theta_{11} - (2n+1)\frac{\pi}{2}]} \\ \sqrt{1 - |S_{11}|^2} e^{j[\Theta_{11} - (2n+1)\frac{\pi}{2}]} & |S_{11}| e^{j\Theta_{11}} \end{bmatrix}, n=0, 1 \quad (7)$$

In this case, the network is assumed to be lossless, reciprocal, and symmetric which means that the scattering matrix is completely determined if the $|S_{11}|$ and Θ_{11} are known. We used the curves that Yi-Chi Shih [Ref. 10] published to determine the magnitude and angle of S_{11} for inductive strips with length $T=0.1, 0.2, 0.5, 1, 2, 5$ mm. Each of these strips had thickness $t=0, 1, 2, 5, 50$ mils. In Appendix A there are tables containing the

data and plots of $|S_{11}|$ and Θ_{11} as a function of frequency for different strip lengths and metal thicknesses. In Appendix A are also included the curves derived from Shih's work [Ref. 10] for the magnitude and angle of the reflection coefficient for inductive strips of thickness $t=5$ mils centered in the WR (28) rectangular waveguide.

III. A CAD MODEL FOR THE INDUCTIVE STRIP

A. BACKGROUND

It is known that the dominant mode for the rectangular waveguide is the TE₁₀ mode; the E-field exists in the y dimension of the waveguide. When a septum or a strip is put in the waveguide, a potential is generated by the E-field between the upper and lower walls and current flows on the surface of the strip. This results in a storage of magnetic energy. This discontinuity in the rectangular waveguide appears as an inductive reactance.

In a March 1990 report by Knorr [Ref. 8] one can see that a homogeneous finline can be represented by a rectangular waveguide having the same impedance and wavelength. That means, if one measures the finline cut-off wavelength and the impedance, an equivalent rectangular waveguide can be constructed from the following equations:

$$\frac{a_{eq}}{a} = \frac{\lambda_c}{2a} \quad (8)$$

$$\frac{b_{eq}}{b} = \frac{Z_{ov}}{120\pi} \left(\frac{a_{eq}}{a} \right) \left(\frac{a}{2b} \right) \quad (9)$$

where, λ_c and Z_{ov} are the cut-off wavelength and the impedance of the homogeneous finline, a_{eq} and b_{eq} are the dimensions of the equivalent waveguide, and a and b the dimensions of the finline. In this research, the finline have $w/b=1$, where w/b is the ratio of the fin gap to finline height. So, we have: $a_{eq}=a$ and $b_{eq}=b$.

Knorr describes in his work [Ref. 8] the inductive strip in finline as a strip region, a discontinuity region, and a finline region. The proposed model for the strip region consists

of two sections of below-cut off rectangular waveguides. These two waveguides represent the spaces between the inductive strip and the narrow waveguide walls. In order to take into account the thickness of the inductive strip, the width of each of the above waveguides must be $w=a/2-t/2$, where a is the finline width and t is the thickness of the strip. The discontinuity region is modeled by using an inductor and a capacitor to take into account the stored electromagnetic energy mentioned above. Finally, the finline region is modeled by using an ideal transformer to model the impedance step from rectangular waveguide ($w/b=1$) to the finline with $w/b<1$.

In this case, because the finlines have $w/b=1$, we do not need to match the unloaded waveguide with the finline using the above transformer because the voltage power impedance of the unloaded waveguide is equal to the voltage power impedance of the finline. Figure 2, on page 10 shows the equivalent circuit for the inductive strip with finite thickness centered in finline with $w/b=1$.

B. CIRCUIT MODEL

In order to simulate the equivalent circuit model described in figure 2 on page 10, Touchstone software is used. First, data files for strip length $T=0.1, 0.2, 0.5, 1, 2, 5$ mm were created. The thickness of each of them is $t=0, 1, 2, 5, 50$ mils. Then a Touchstone program (Figure 3, on page 11) was written for the equivalent circuit using as parameters, the inductance L and the capacitance C .

As Morua discovered in his thesis work [Ref 9], a match between data and model can be achieved by changing only the inductance while the capacitance remains constant. Morua discovered that the capacitance changes only when w/b changes. In this work, the same observation has occurred, and for this reason, the equation for the capacitance that Morua found in his thesis work was used [Ref 9]. Because in this case $w/b=1$, the capacitance for the WR(28) is constant and is equal $C=0.0008297$ PF.

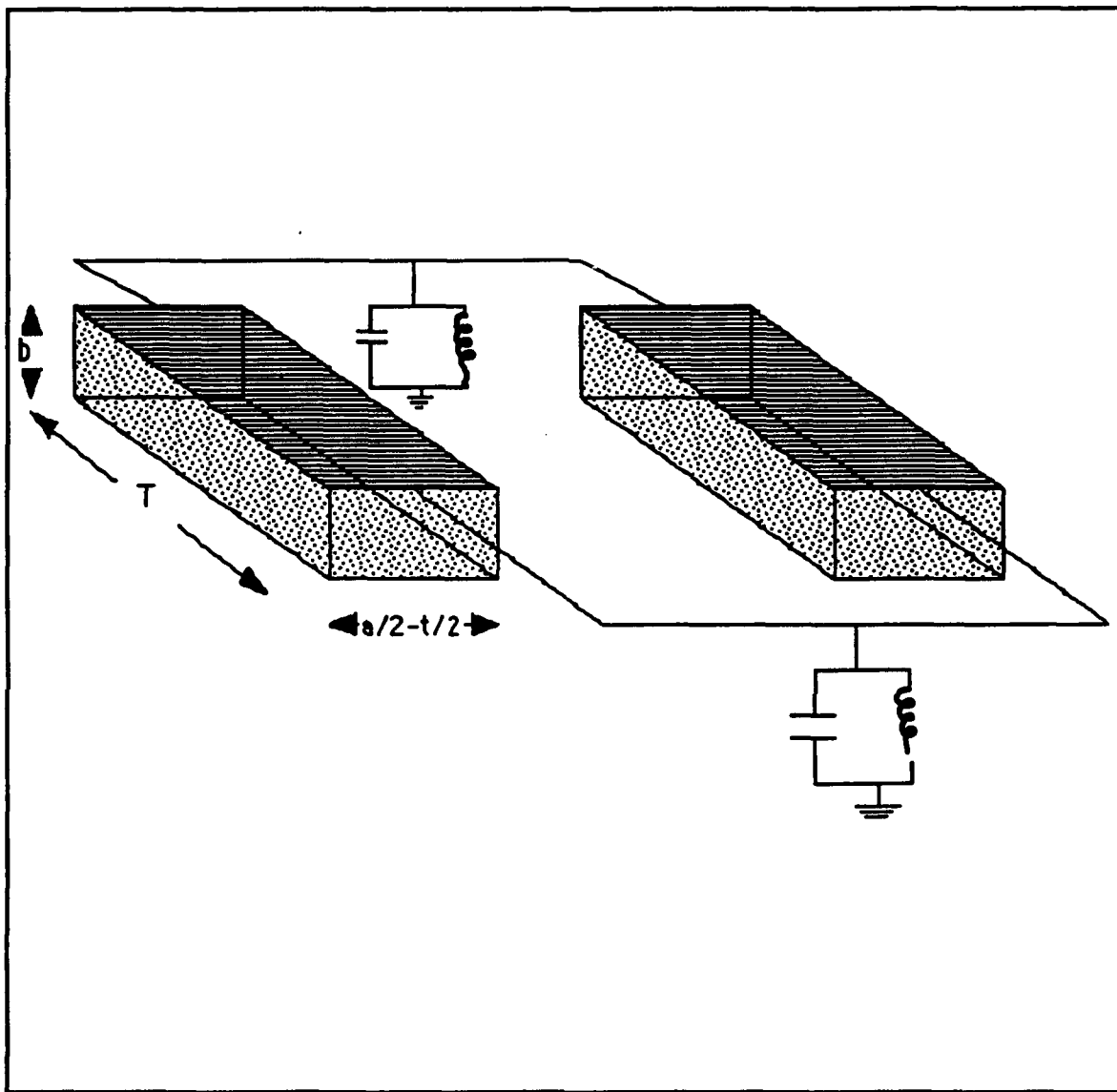


Figure 2. Model for the inductive strip with finite thickness centered in finline with $w/b=1$.

```

! USER: DARIOTIS DIMITRIS
! DATE: SEP-16-90
! CIRCUIT: MODEL FOR THE INDUCTIVE STRIP WITH FINITE METAL
! THICKNESS CENTERED IN THE FINLINE WITH W/B=1

```

```

DIM
FREQ GHZ
RES OH
IND NH
CAP PF
LNG MIL
TIME PS
COND /OH
ANG DEG

```

```

VAR
A=280
B=140
R=3.3937      ISTRIP LENGTH
t= 0          IMETAL THICKNESS
L=5.74
C=0.0008297

```

```

EQN
Ac=0.5*(A-t)
Lg=R/2

```

```

CKT
CAP 1 0 C^C
IND 1 0 L^L
RWG 1 2 A^Ac B^B L^Lg ER=1 RIIO=1
DEF2P 1 2 D
D 1 2
D 1 2
D 3 2
D 3 2
DEF2P 1 3 STRIPA
S2PA 1 2 0 KA1A.s2p
DEF2P 1 2 KA1A

```

```

RWGT 1 A=280 B=140 ER=1 RIIO=1
DEFIP 1 WEDGE

```

```

TERM
STRIPA WEDGE WEDGE

```

```

PROC1

```

```

OUT
STRIPA S11 SC1
STRIPA MAG[S11] GR1
STRIPA ANG[S11] GR1A
KA1A S11 SC2
KA1A MAG[S11] GR1
KA1A ANG[S11] GR1A

```

```

FREQ
SWEEP 26 40 0.5

```

```

GRID
RANGE 26 40 1

```

Figure 3. A Touchstone program for the inductive strip with finite thickness centered in finline with $w/b=1$.

The values of the inductances that successfully match between model and data are given in Table 1, on page 13. These values are plotted as a function of strip length, keeping constant the thickness t using the Cricket graph program. Figure 4, on page 14 shows the graph of inductance versus strip length for metal thickness $t=0, 1, 2, 5, 50$ mm. As we can see from Figure 4, all the curves have exponential form. To find a mathematical formula for the inductance, we approach these curves by using the Logarithmic method of the Ckricet Graph software. Figures 5 and 6, on page 15 show two examples of the above method for inductive strips with thickness $t=5, 50$, mils.

It can be observed that all the mathematical formulas that approach the curves of inductance versus strip length for constant thickness, have the following shape:

$$L = A_1 - A_2 \log T \quad (10)$$

where A_1 and A_2 are real numbers and T is the strip length. In Table 2 on page 13 the values of the above coefficients are given for different metal thicknesses.

To find a general formula for the inductance for all the strip lengths and thicknesses, one must find mathematical expressions for the above two coefficients A_1 and A_2 . First, plot the values of the A_1 and A_2 versus the strip thickness and then use two different methods to approach these curves. Shih's curves [Ref. 10] were for metal thickness $t=0, 1, 2, 5, 50$ mils. As can be seen, there are only 5 points and the last two (5, 50) were very far from each other. That is the reason (in order to be more accurate), two methods were used. The first method utilized the Matlab software. The coefficients A_1 and A_2 were plotted versus thickness and then the Fitfun application of the Matlab was used in order to approach the curves. The second was made with the help of the best fit software of the Hewlett Packard computer. In Figures 7 and 8, on page 16 we can see these methods.

The dotted line represents the plot of data, (five points) the continuous line is the Matlab result and the dashed line is the HP result.

TABLE 1. INDUCTANCE (nH) FOR BEST MATCH BETWEEN MODEL AND SHIH'S DATA

	t=0 mils	t=1 mils	t=2 mils	t=5 mils	t=50 mils
T=0.1 mm	7.65	7.18	6.75	5.8	2
T=0.2 mm	7.15	6.7	6.2	5.5	1.95
T=0.5 mm	6.3	5.9	5.6	5	1.65
T=1 mm	5.8	5.4	5.2	4.6	1.45
T=2 mm	5.5	5.1	4.9	4.3	1.3
T=5 mm	4.9	4.7	4.6	3.9	1.2

TABLE 2. COEFFICIENTS A1, A2 FOR THE INDUCTANCE

Thickness, t (mils)	A1	A2
0	8.4682	1.5881
1	7.9040	1.4628
2	7.3052	1.2438
5	6.4280	1.1130
50	2.3258	0.5354

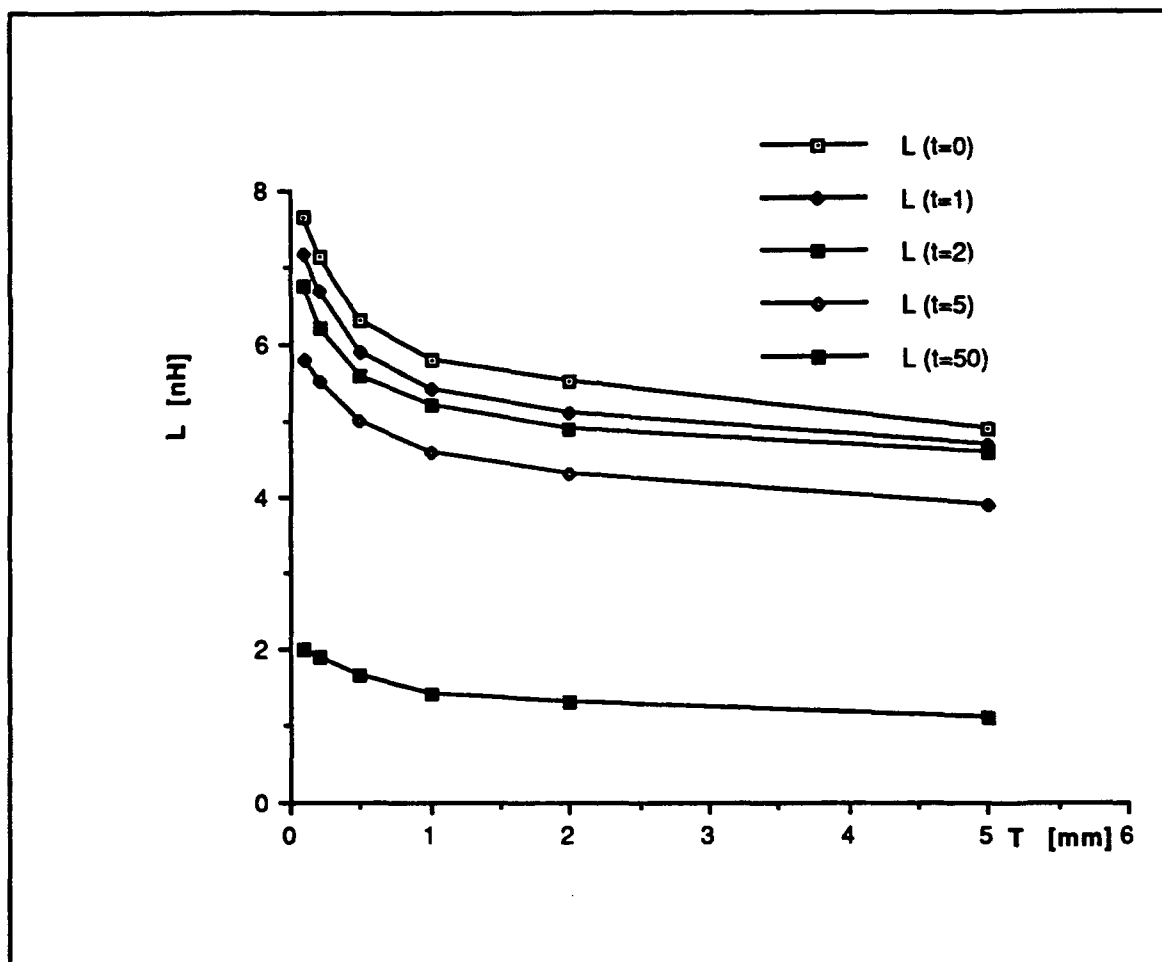


Figure 4. Inductance versus strip length for metal thickness $t=0, 1, 2, 5, 50$ mils.

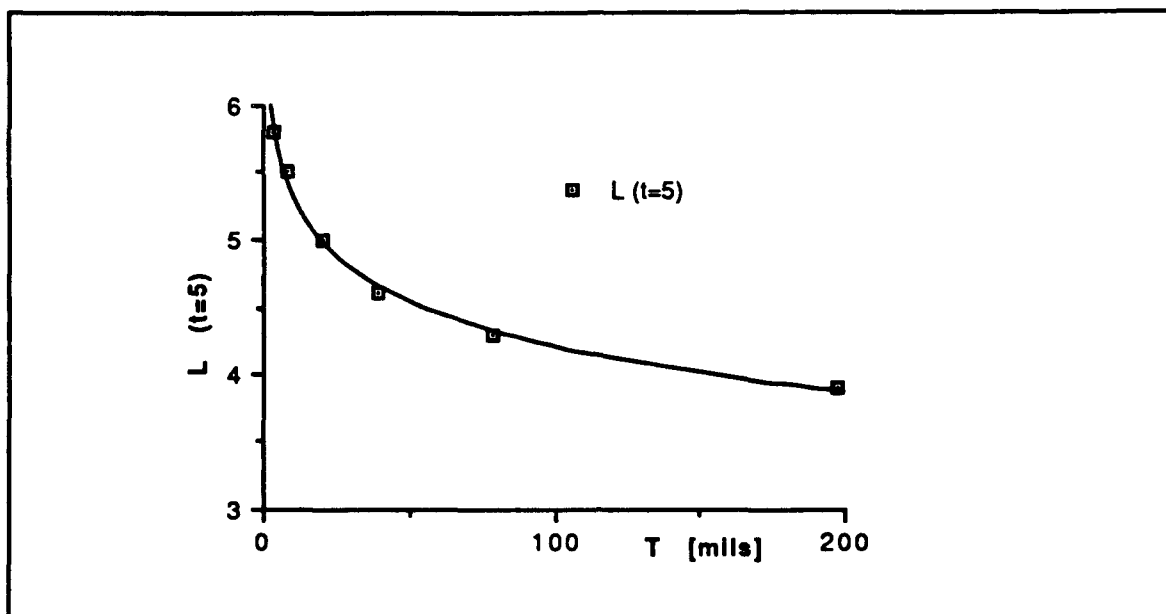


Figure 5. Inductance versus strip length with metal thickness $t=5$ mils.

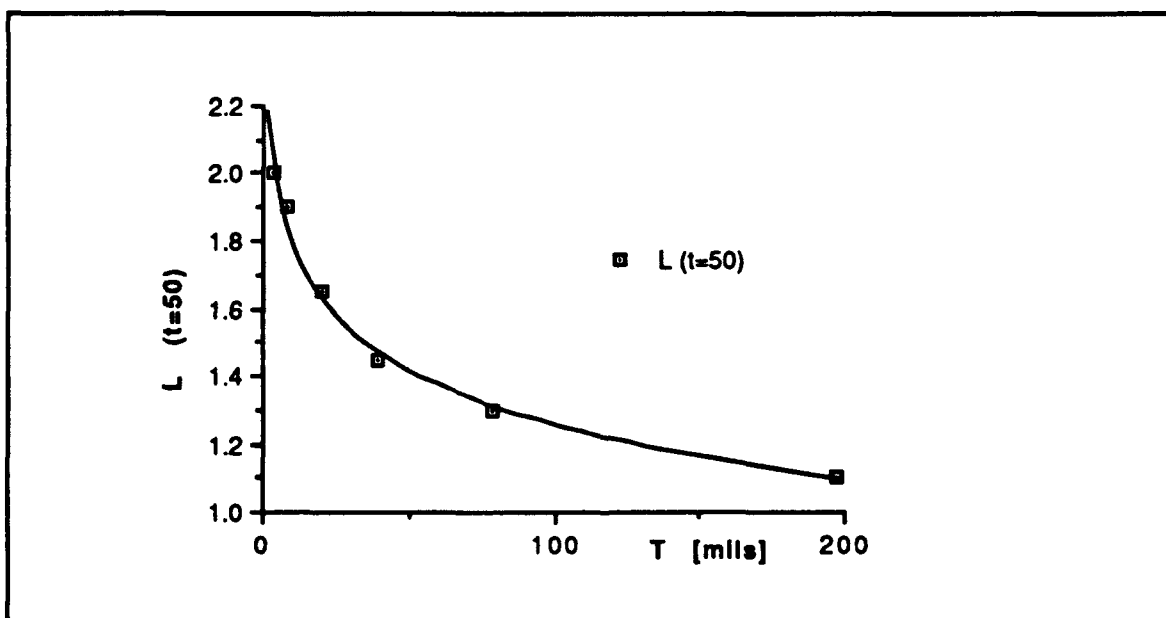


Figure 6. Inductance versus strip length with metal thickness $t=50$ mils.

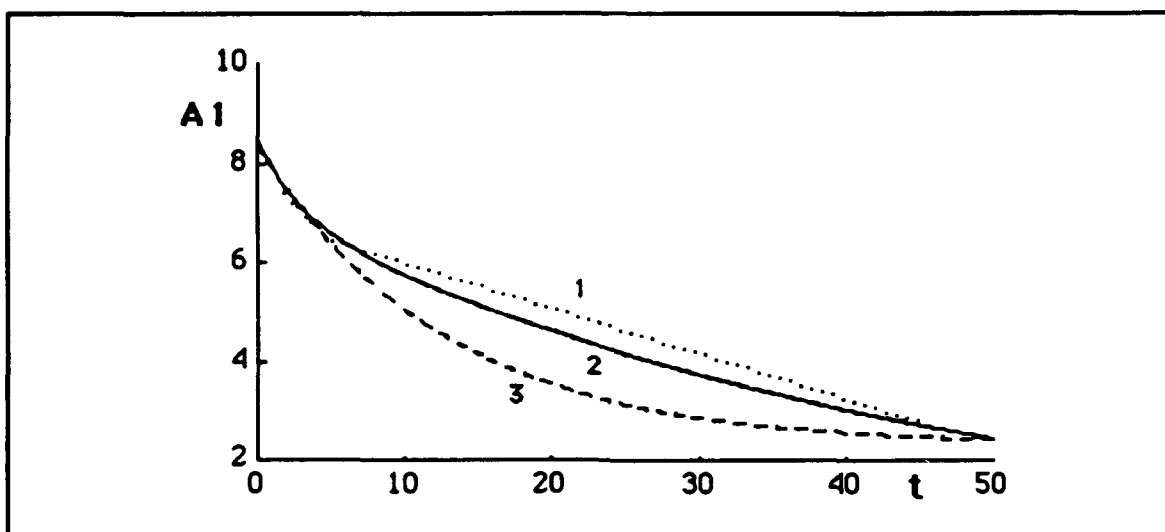


Figure 7. Coefficient A1 versus metal thickness: 1) plot of data 2) Matlab approximation 3) Hewlett Packard approximation.

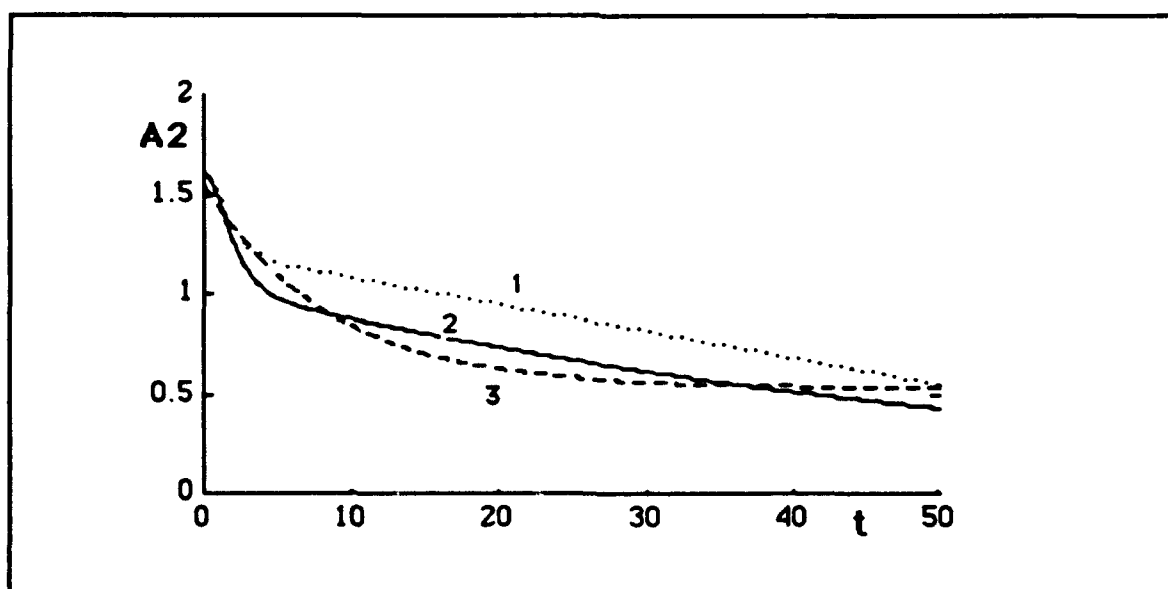


Figure 8. A2 coefficient versus metal thickness: 1) plot of data 2) Matlab approximation 3) Hewlett Packard approximation.

As observed, for both of the coefficients the HP approach is closer to the exponential form. For this reason, this method was chosen to define the coefficients A_1 and A_2 . The formulas for the coefficients A_1 and A_2 given by the above method are:

$$A_1 = 2.3258 + 6.0338e^{-0.0797t} \quad (11)$$

$$A_2 = 0.53542 + 1.0103e^{-0.1197t} \quad (12)$$

If we substitute (11) and (12) in the general formula for the inductance, we have:

$$L = 2.3258 + 6.0338e^{-0.0797t} - [0.53542 + 1.0103e^{-0.1197t}] \log(T) \text{ nH.} \quad (13)$$

where the strip length T , and thickness, t , are in mils.

To see the result obtained by using the general formulas for the inductance and capacitance, a Touchstone file was created, using these formulas (Figure 9) on page 18 and the obtained values of magnitude and angle were compared to the values from Shih's curves [Ref. 10]. Appendix B, contains some plots of magnitude and angle as well as the corresponding Smith chart diagrams comparing model predictions with Shih's data.

C. SCALING THE MODEL FOR ALL THE FREQUENCY BANDS

The developed model works only in the Ka band because the scattering data which are used to define the model, were computed in the Ka band. In order to modify the model to work for any frequency, the scaling method described by Knorr in his March 1990 report [Ref.9] was used. The scaling principle states that if all dimensions and wavelength are scaled by the same factor, the electrical performance will remain unchanged. Using this method, the two general equations for the inductance and capacitance are modified as:

$$L = \left(\frac{b}{140}\right) f_1 \left(\frac{280T}{a}\right) \text{ nH} \quad (14)$$

$$C = 0.5 \left(\frac{a}{b}\right) \left(\frac{a}{280}\right) 0.0008297 \text{ pF} \quad (15)$$

where a, b, t, and T are in mils and f_1 is the analytic expression for the inductance of a strip centered in the WR(28) waveguide. Figures 9 and 10 give a Touchstone program for the model that works for all the frequency bands.

```
! USER:  DARIOTIS DIMITRIS
! DATE:   SEP-16-90
! CIRCUIT: MODEL FOR THE INDUCTIVE STRIP WITH FINITE METAL
!          THICKNESS CENTERED IN THE FINLINE WITH W/B=1

DIM
FREQ GHZ
RES OH
IND NH
CAP PF
LNG MIL
TIME PS
COND /OH
ANG DEG

VAR
A=280
B=140
R=3.3937
t= 0
! L=5.74
C=0.0008297
EQN

Ac=0.5*(A-t)
Lg=R/2
```

Figure 9. A CAD model for the finline for all the frequency bands.

```

D1=(2.3258+6.0338*EXP(-0.0797*280*√A))*B/140
D2=(0.53542+1.0103*EXP(-0.1197*280*√A))*B/140
! FORMULA FOR THE INDUCTANCE

L=D1-D2*LOG(280*R/A)

CKT
! STRIP #1
CAP 1 0 C^C
IND 1 0 L^L
RWG 1 2 A^Ac B^B L^Lg ER=1 RHO=1
DEF2P 1 2 D
D 1 2
D 1 2
D 3 2
D 3 2
DEF2P 1 3 STRIPA
S2PA 1 2 0 KA1A.s2p
DEF2P 1 2 KA1A

RWGT 1 A=280 B=140 ER=1 RHO=1
DEF1P 1 WEDGE
TERM
STRIPA WEDGE WEDGE

PROC!

OUT
STRIPA S11 SC1
STRIPA MAG[S11] GR1
STRIPA ANG[S11] GR1A
KA1A S11 SC2
KA1A MAG[S11] GR1
KA1A ANG[S11] GR1A

FREQ
SWEEP 26 40 0.5

GRID
RANGE 26 40 1
GR1 0 1 .1
GR1A 90 180 10

```

Figure 10. A CAD model for the finline for all the frequency bands (cont.).

D. MODEL ACCURACY

An error function is used to define the accuracy of the model. As error function we define:

$$\text{Error} = \frac{|\text{Model value} - \text{Computed value}|}{\text{Computed value}} \times 100$$

The above formula is used to compare Shih's data [Ref. 10] with the data generated by the model. In Appendix C, there are tables that give the values of the error function for the worst cases using inductive strips with lengths $T=0.1, 0.2, 0.5, 1, 2, 5$ mm and thickness for each of them $t=0, 1, 2, 5, 50$ mils. As we can see, in these tables we have about 9% worst error at the edges of Ka band only when the strip length T is smaller than 0.1 mm and the thickness t is smaller than 1 mil. For greater values of thickness and strip length, the worst error is about 1.5%.

Another problem about accuracy, is how accurate are Shih's curves [Ref. 10] that were used to determine the scattering coefficients to develop the CAD model for the inductive strip. As mentioned before, strips that were machined with the help of the Mechanical Engineering department, were used to validate Shih's curves. In figures 11 and 12 Shih's data is compared with the laboratory measured data in X band, for inductive strips with strip length $T=200$ mils and thickness $t=45$ mils. Because Shih's work was in the Ka band (26-40 GHz) it was necessary to convert the Ka band data to X band with the scaling method that is mentioned above.

Another method to examine the accuracy of Shih's data used to build the CAD model, is to compare $|S_{11}|$, Θ_{11} generated by this model for a finline with zero strip metal thickness and $w/b=1$ to the data generated by Morua's CAD model [Ref.9] for the same

finline which was based on the spectral domain data. In Appendix C two comparisons for the magnitude $|S_{11}|$, and angle Θ_{11} are shown. In the first case, the strip has length $T=30$ mils in WR(8) and in the second case, the strip has length $T=15$ mils in WR(28). In Appendix C also, there are tables containing the scattering data generated by the CAD model and spectral domain method. As a result from all the above comparisons, we can say that the data generated by the model are very close to the X band data derived from Shih's work and to the spectral domain data.

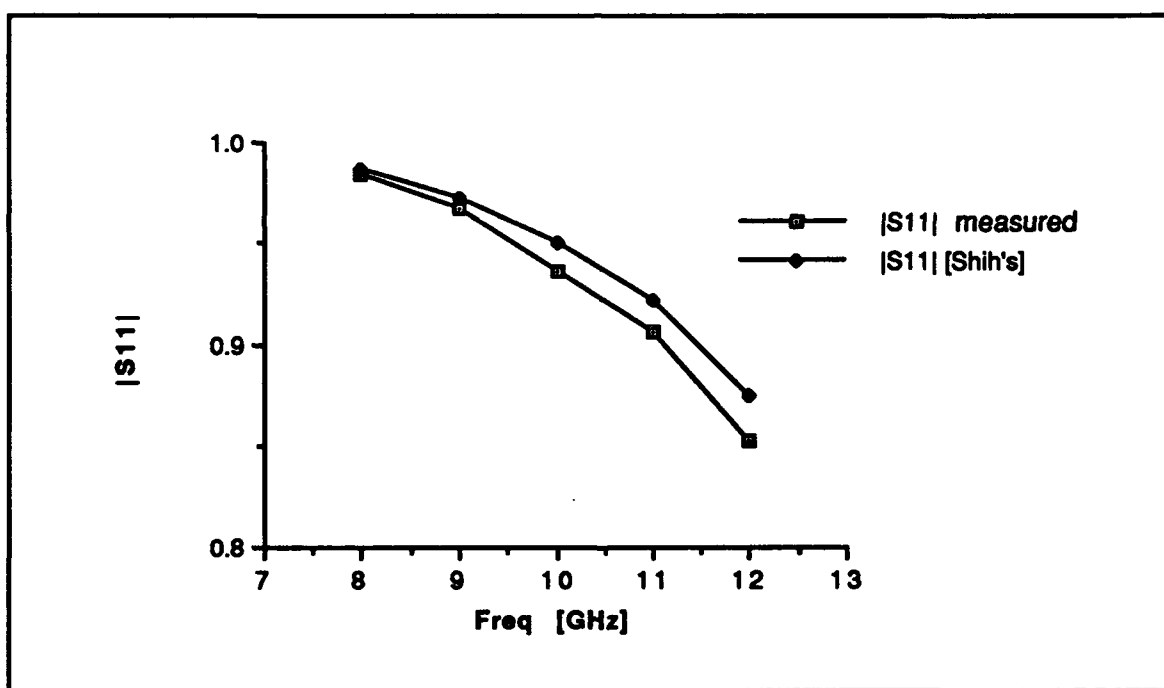


Figure 11 Magnitude $|S_{11}|$ versus Frequency for the measured and Shih's data in the X band for $T=200$ mils and $t=45$ mils.

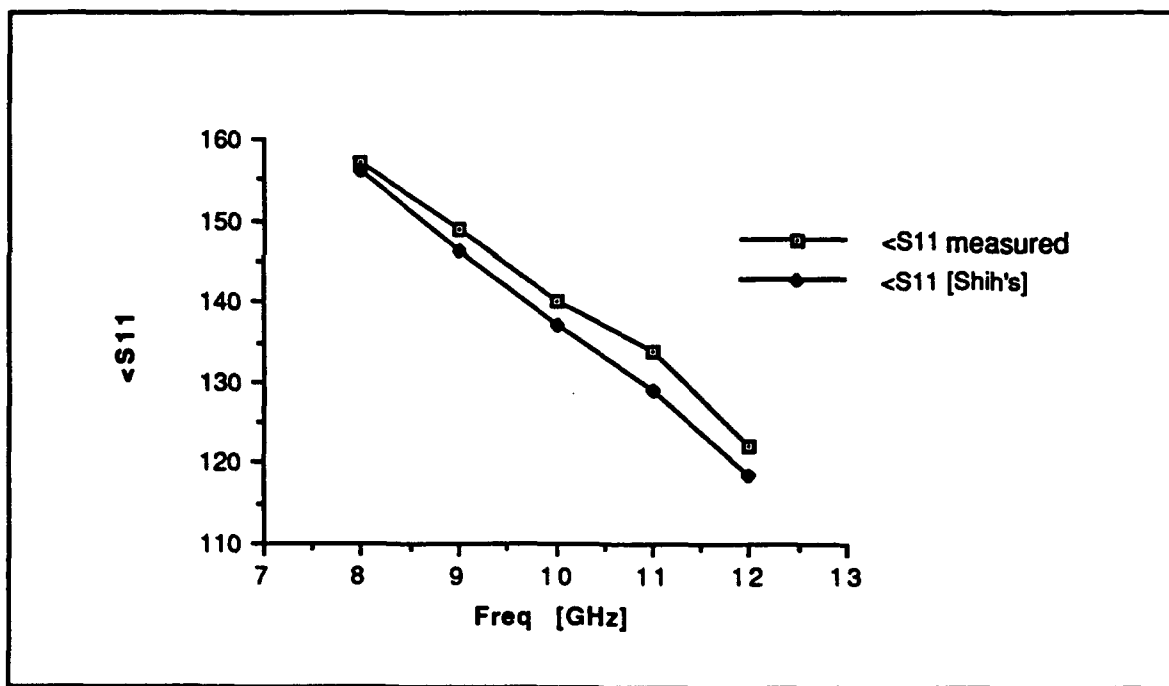


Figure 12. Phase versus Frequency for the measured and Shih's data in the X band for $T=200$ mils and $t=45$ mils.

IV. EXPERIMENTAL VALIDATION

The most accurate method to validate the CAD model is to compare the results obtained from the model to what was observed experimentally. In order to do that, a filter was used, which already exists in the NPS laboratory and works in the X band having four inductive strips i.e, three resonators (Figure 13). The dimensions of this filter are $T_1=90$, $T_2=250$, $T_3=240$, $T_4=90$ mils, $R_1=558$, $R_2=540$, $R_3=540$ mils and metal thickness $t=2$ mils, where, R_1 , R_2 , R_3 are the distances between the inductive strips. In order to validate the model, a Touchstone circuit file was created for a filter having three resonators; this file is shown in Figures 14, 15, and 16. In Figure 17, one can see the measured filter response. Figure 18 gives the predicted response of the finline filter model which has the same dimensions as the X band filter.

Additionally, three filters are simulated, the responses of which are given by Vahldieck, et al [Ref.11]. Table 3 gives the specifications of these filters. Figures 19, 21, and 23 show the filter responses obtained by Vahldieck, et al. Figures 20, 22, 24 show the filter responses predicted by the finline filter model. As shown from all the above comparisons, the model responses agree quite well with the experimental responses.

In order to observe the influence of thickness, Figure 73 and 74 in Appendix C show the filters responses predicted by the finline model for the Ka and E band filters with zero thickness. The comparison of Figures 73 and 20 shows that when the metal thickness is zero, the central frequency of the filter response shifts down 1.5 GHz. for the Ka band filter. Also the comparison of figures 74 and 23 shows that when the metal thickness is zero, the central frequency for the E band filter shifts down 2.4 GHz.

TABLE 3. FILTERS SPECIFICATIONS

Frequency	Thickness	T1=T4	T2=T3	R1=R3	R2
Ku Band	35.43 mils	88.11 mils	350.98 mils	413.54 mils	415.27 mils
Ka Band	20.07 mils	39.72 mils	152.36 mils	188.11 mils	188.58 mils
E Band	3.937 mils	24.13 mils	77.87 mils	75.23 mils	75.47 mils

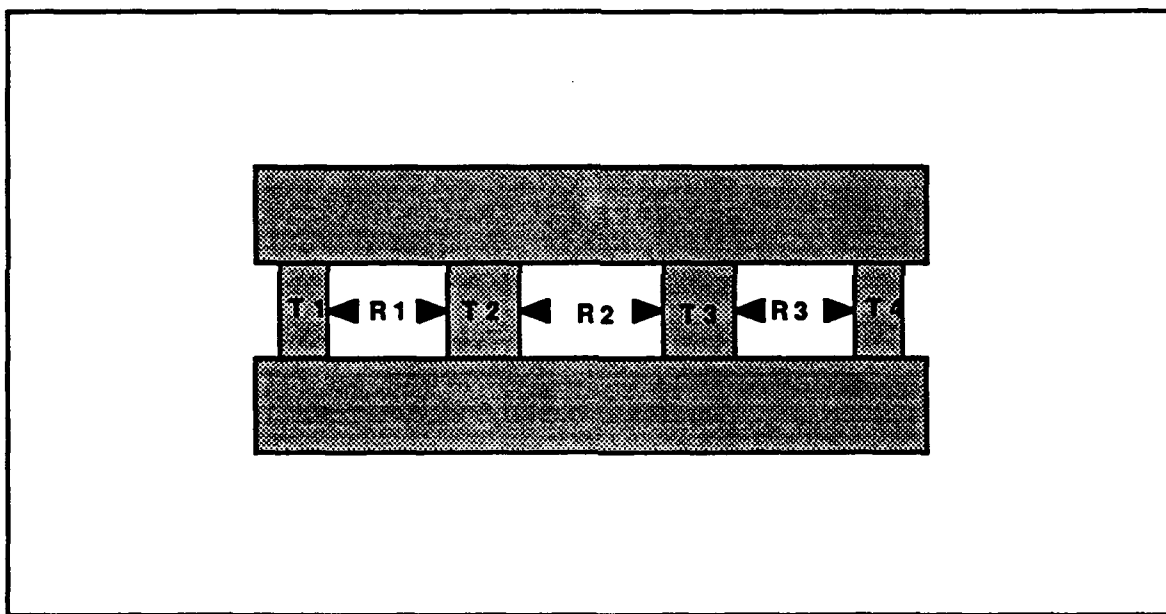


Figure 13. Filter with three resonators.

```

USER:    DIMITRIS DARIOTIS
! DATE:   JUNE-4-90
! CIRCUIT: MODEL OF FINLINE FILTER CONSISTING OF FOUR INDUCTIVE
!          STRIPS THREE RESONATORS.STRIPS HAVE FINITE THICKNESS
!          AND ARE CENTERED IN THE WAVEGUIDE WITH W/B=1
! COMMENT: THIS MODEL WORKS FOR ALL FREQUENCY BANDS. TO
!          WORK THE MODEL, THE PARAMETERS THAT MUST BE DEFINED
!          ARE STRIP LENGTH, METAL THICKNESS DIMENSIONS OF THE
!          WAVEGUIDE AND THE OPERATING FREQUENCY.

```

```

DIM
FREQ GHZ
RES OH
IND NH
CAP PF
LNG MIL
TIME PS
COND /OH
ANG DEG

```

```

VAR

```

```

A=900

```

```

B=400

```

```

k=2.5

```

```

T1=90

```

```

T2=250

```

```

T3=240

```

```

T4=90

```

```

R1=558

```

```

R2=540

```

```

R3=540

```

```

!THICKNESS OF THE STRIP

```

```

!STRIP LENGTH No1

```

```

!STRIP LENGTH No2

```

```

!STRIP LENGTH No3

```

```

!STRIP LENGTH No4

```

```

!DISTANCE BETWEEN STRIPS No1

```

```

!DISTANCE BETWEEN STRIPS No2

```

```

!DISTANCE BETWEEN STRIPS No3

```

```

EQN

```

```

Tov2A=T1/2

```

```

!MODEL PARAMETERS

```

```

Tov2B=T2/2

```

```

!MODEL PARAMETERS

```

```

Tov2C=T3/2

```

```

!MODEL PARAMETERS

```

```

Tov2D=T4/2

```

```

!MODEL PARAMETERS

```

```

Aov2=0.5*(A-k)

```

```

! FORMULAS FOR THE FACTORS A1 AND A2

```

```

D1=(2.3258+6.0338*EXP(-0.0797*280*k/A))*B/140

```

```

D2=(0.53542+1.0103*EXP(-0.1197*280*k/A))*B/140

```

```

! FORMULAS FOR THE INDUCTANCE

```

```

La=D1-D2*LOG(280*T1/A)

```

```

Lb=D1-D2*LOG(280*T2/A)

```

Figure 14. Finline Filter Model Program.

```

Lc=D1-D2*LOG(280*T3/A)
Ld=D1-D2*LOG(280*T4/A)
! FORMULA FOR THE CAPACITANCE
C=0.5*(A/B)*(A/280)*0.0008297
CKT
! STRIP No1
CAP 1 0 C^C
IND 1 0 L^La
RWG 1 2 A^Aov2 B^B L^Tov2A ER=1 RHO=0.64
DEF2P 1 2 A
A 1 2
A 1 2
A 3 2
A 3 2
DEF2P 1 3 STRIPA
! RESONATOR No1
RWG 1 2 A^A B^B L^R1 ER=1 RHO=.64
DEF2P 1 2 RESOA
! STRIP No2
CAP 1 0 C^C
IND 1 0 L^Lb
RWG 1 2 A^Aov2 B^B L^Tov2B ER=1 RHO=0.64
DEF2P 1 2 B
B 1 2
B 1 2
B 3 2
B 3 2
DEF2P 1 3 STRIPB
! RESONATOR No2
RWG 1 2 A^A B^B L^R2 ER=1 RHO=0.64
DEF2P 1 2 RESOB
! STRIP No3
CAP 1 0 C^C
IND 1 0 L^Lc
RWG 1 2 A^Aov2 B^B L^Tov2C ER=1 RHO=0.64
DEF2P 1 2 C
C 1 2
C 1 2
C 3 2
C 3 2
DEF2P 1 3 STRIPC

```

Figure 15. Finline Filter Model program (cont.).

```

! RESONATOR No3
RWG 1 2 A^A B^B L^R3 ER=1 RHO=0.64
DEF2P 1 2 RESOC
! STRIP No4
CAP 1 0 C^C
IND 1 0 L^Ld
RWG 1 2 A^Aov2 B^B L^Tov2D ER=1 RHO=0.64
DEF2P 1 2 D
D 1 2
D 1 2
D 3 2
D 3 2
DEF2P 1 3 STRIPD
RWGT 1 A^A B^B ER=1 RHO=1
DEF1P 1 WEDGE
STRIPA 1 2
RESOA 2 3
STRIPB 3 4
RESOB 4 5
STRIPC 5 6
RESOC 6 7
STRIPD 7 8
DEF2P 1 8 FINFILT
TERM
FINFILT WEDGE WEDGE
PROC!
OUT
FINFILT DB[S11] GR1
FINFILT DB[S12] GR1
FREQ
SWEEP 8 12 0.01
SWEEP 9.7 11.5 0.01
GRID
RANGE 8 12 0.4
GR1 -60 20 10
OPT!
TOL!

```

Figure 16. Finline Filter Model program (cont.).

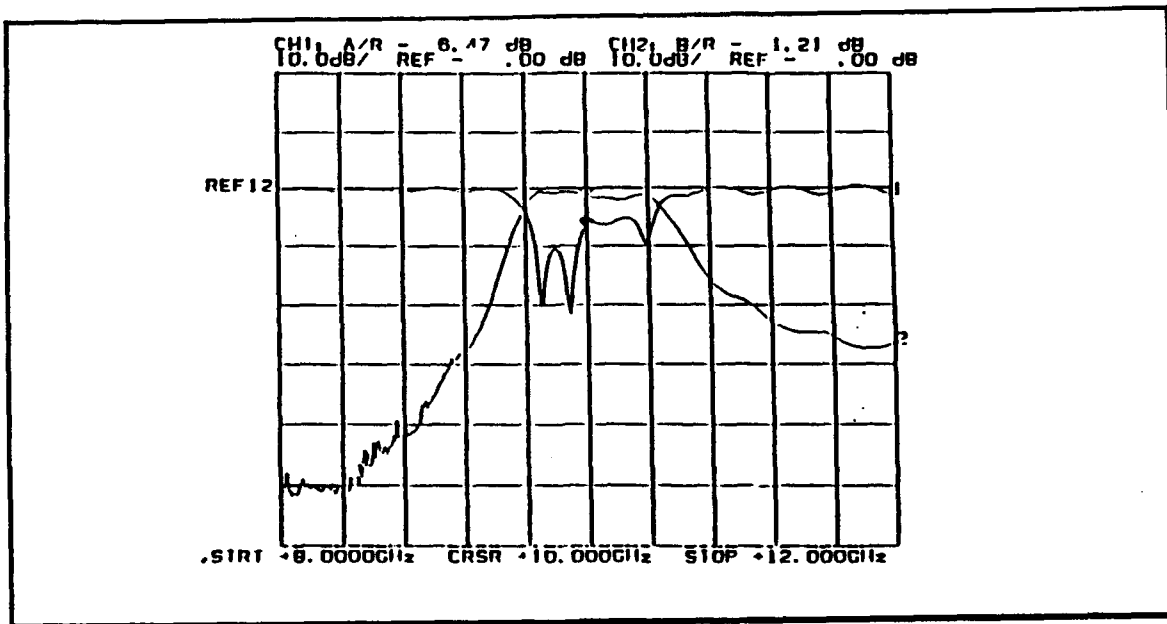


Figure 17. Experimental response for the X-Band filter [Ref 9].

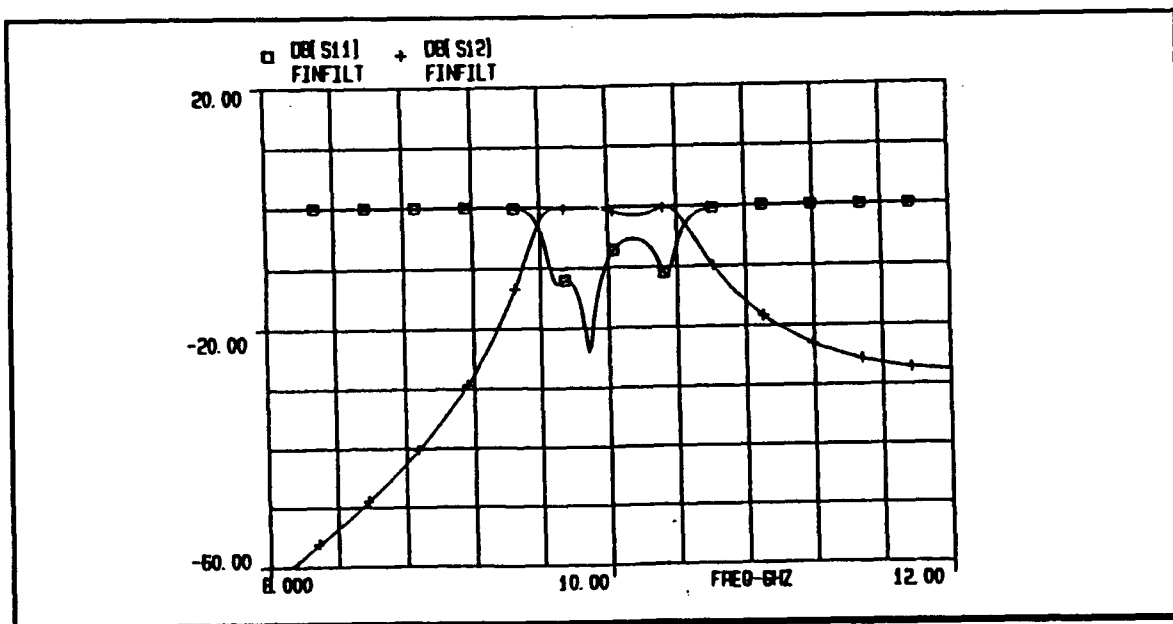


Figure 18. Filter response from the finline filter model Touchstone program.

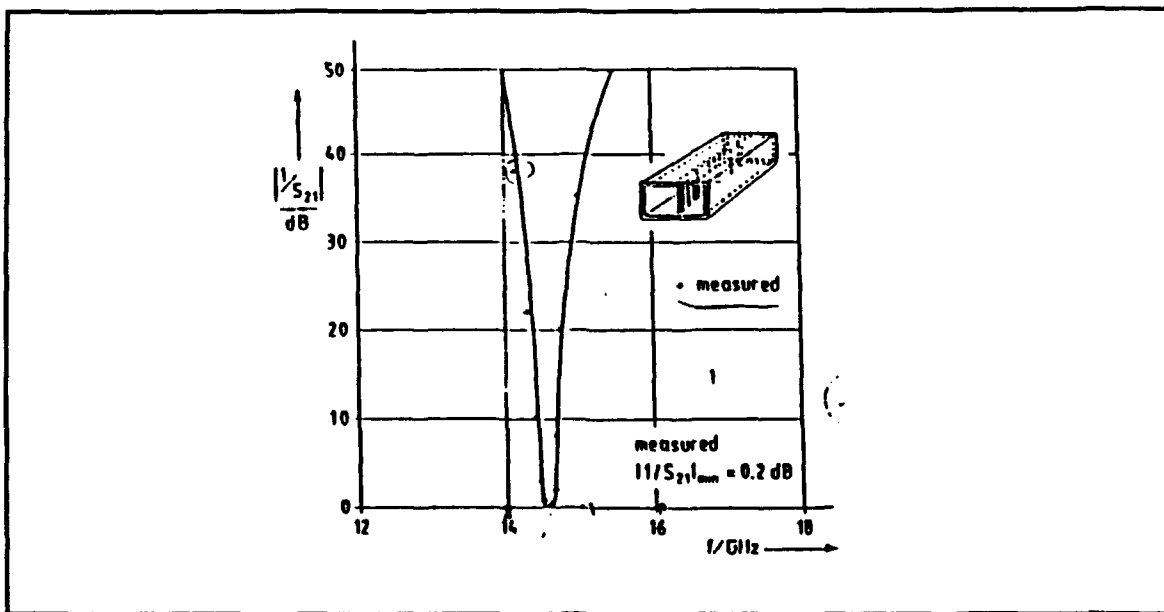


Figure 19. Experimental response for the Ku Band filter [Ref 11].

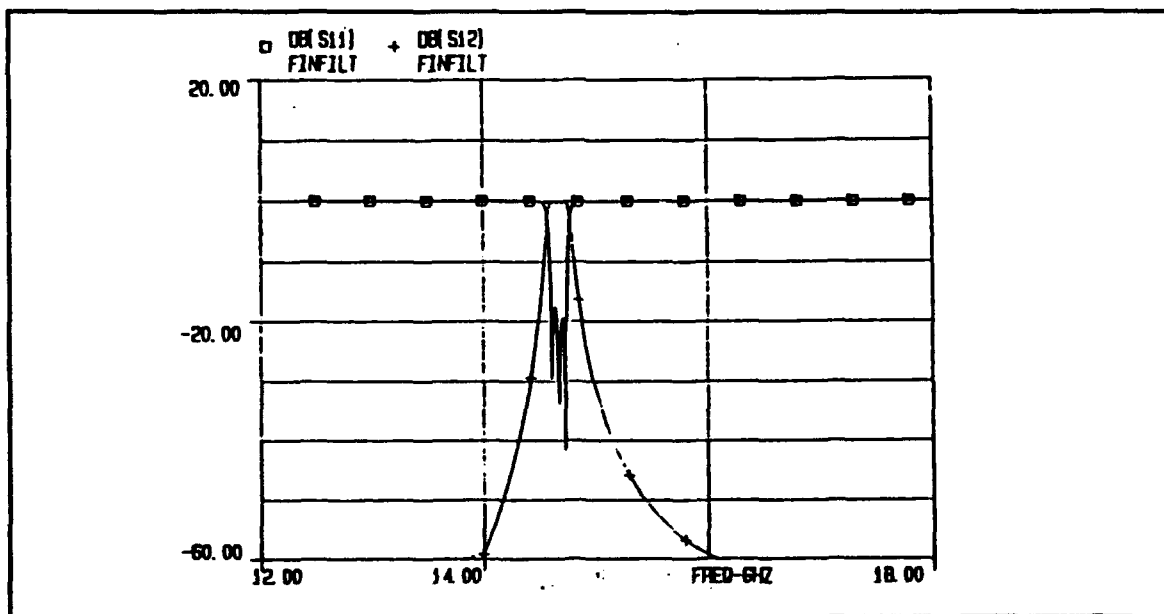


Figure 20. Model response for the Ku Band filter.

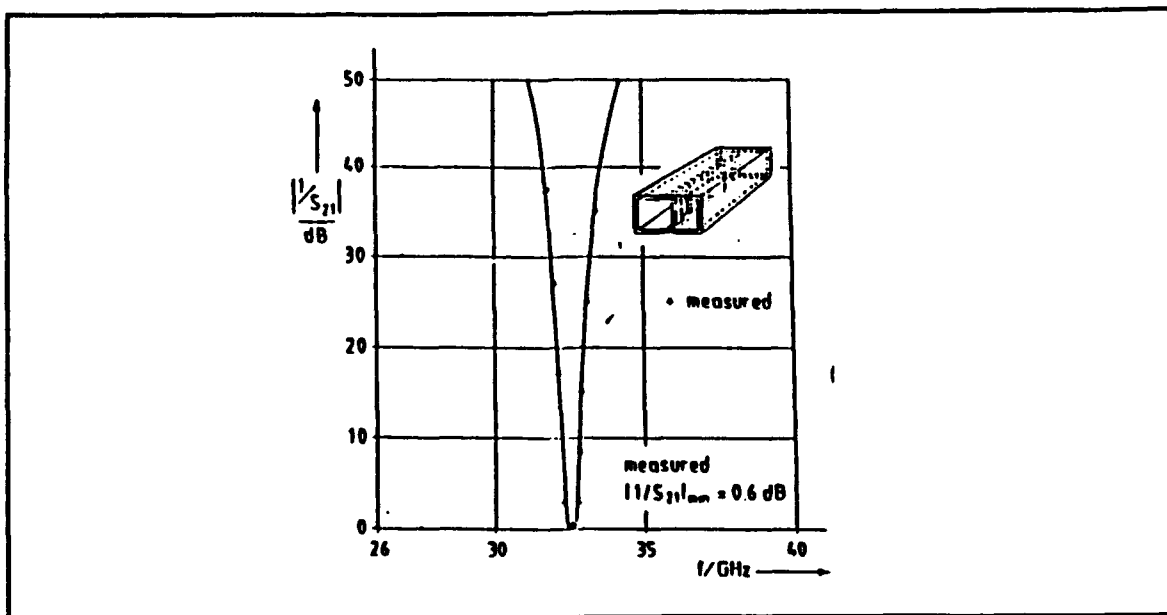


Figure 21. Experimental response for the Ka band filter [Ref 11].

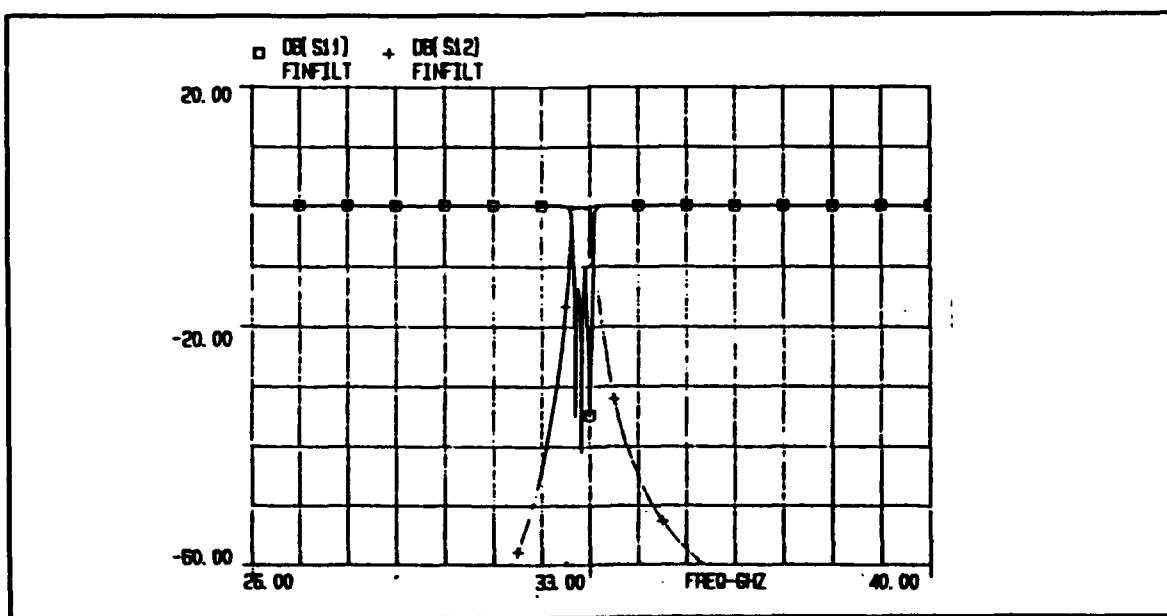


Figure 22. Model response for the Ka Band filter.

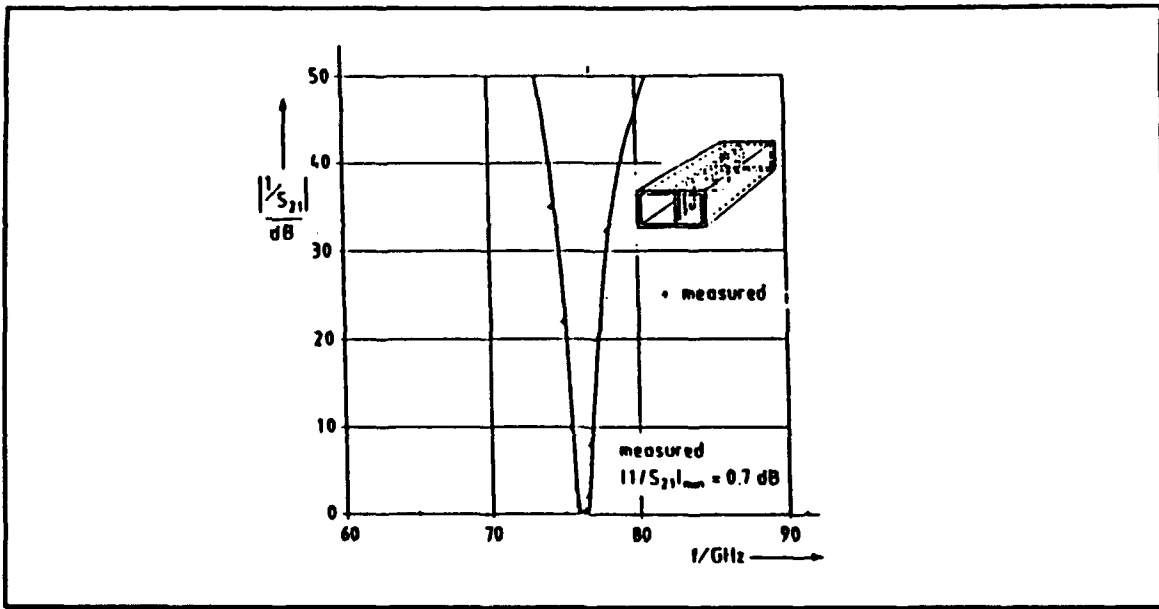


Figure 23. Experimental response for the E Band filter [Ref 11].

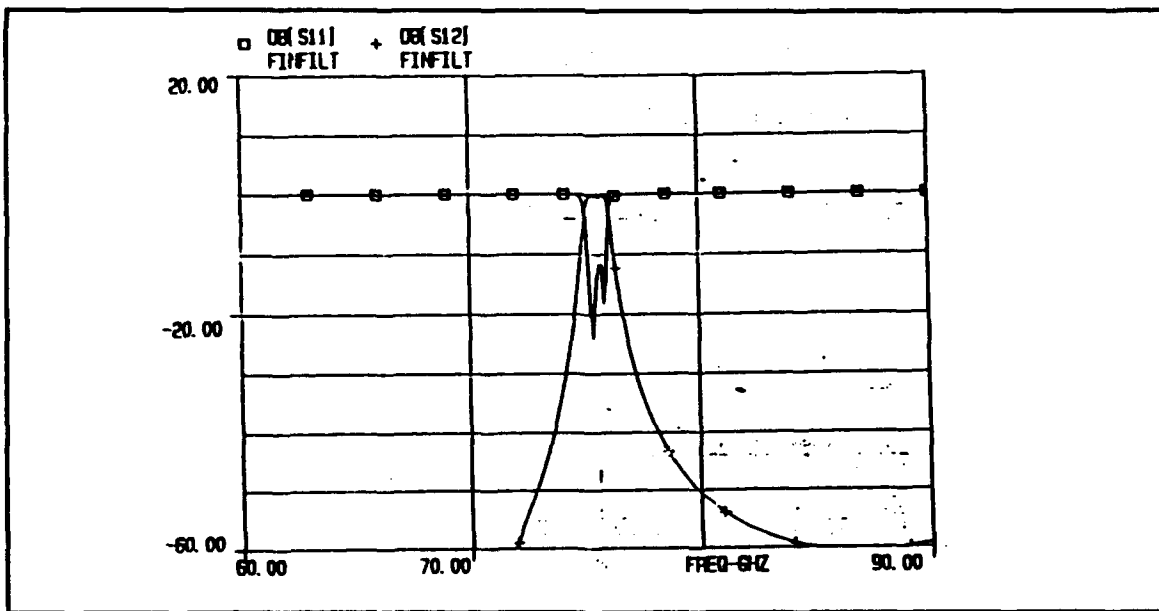


Figure 24. Model response for the E Band filter.

V. CONCLUSIONS AND RECOMMENDATIONS

A. CONCLUSIONS

This thesis describes a CAD model for the inductive strip with finite metal thickness which is centered in a finline with $w/b=1$. The starting point for this model was the curves of magnitude and phase of the reflection coefficient, S_{11} , for inductive strips with finite metal thickness derived from Shih's work for the Ka band [Ref. 10]. The data were in the range $0.01 < T/a < 0.7$ and $0 < t/a < 0.17$. As described in the chapters of Model Accuracy and Experimental Validation, Shih's data are very close to the data measured in the laboratory and to the data generated by the spectral domain method as well. Also, the experimental responses of various existing filters were close to the responses predicted by the model. The above agreement leads to the conclusion that the CAD model described here for millimeter wave applications can be used.

B. RECOMMENDATIONS

The successful match of the model results to the results obtained in the laboratory, recommends that the work in the Microwave Department of NPS continue in the following areas:

1. Develop a model for strips centered in finline with $w/b < 1$, and finite metal thickness.
2. Develop a model for inductive strips which are off-center with $w/b < 1$, and finite metal thickness.
3. Investigate the effect of a dielectric substrate for strips with $w/b < 1$, and finite metal thickness.

APPENDIX A. S-DATA

TABLE 4. S-DATA FOR STRIP LENGTH T=0.1 MM.

	t=0 mils		t=1 mil		t= 2 mils		t=5 mils		t=50 mils	
Freq	S11	θ11	S11	θ11	S11	θ11	S11	θ11	S11	θ11
26	0.641	128.02	0.679	131.36	0.7125	133.75	0.7708	138.53	0.9708	165.28
30	0.504	117.99	0.545	120.85	0.579	123.24	0.6458	127.54	0.9416	159.07
36	0.391	109.39	0.425	111.78	0.450	113.69	0.516	117.51	0.887	150.95
40	0.333	105.57	0.366	107.67	0.391	108.91	0.450	112.73	0.8416	145.22

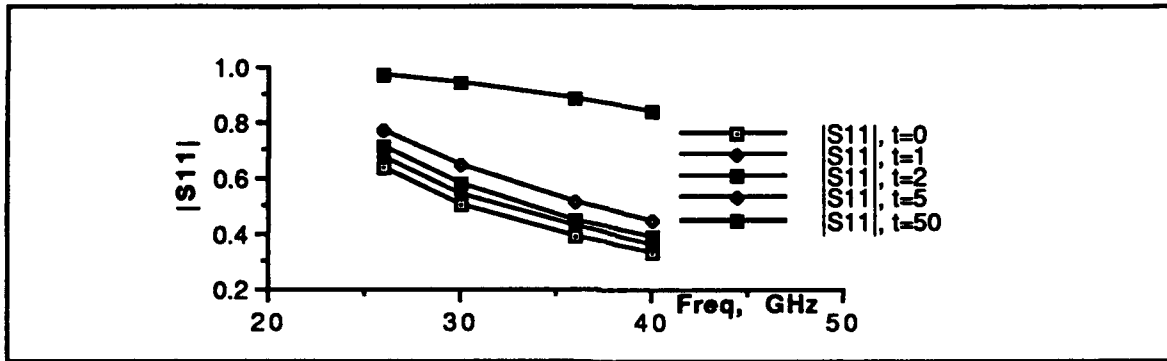


Figure 25. Magnitude of S11 versus frequency for strip length T=0.1 mm

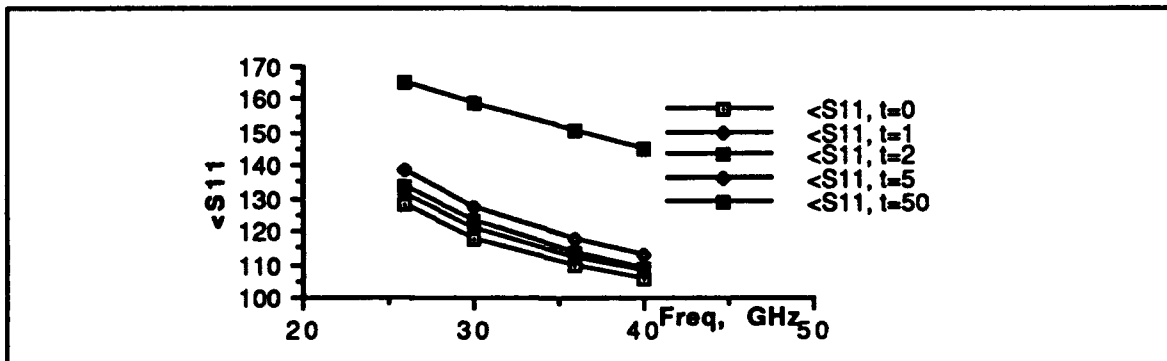


Figure 26. Angle θ11 versus frequency for strip length T=0.1mm.

TABLE 5. S-DATA FOR STRIP WITH LENGTH T=0.2 MM.

	t=0 mils		t=1 mil		t=2 mils		t=5 mils		t=50 mils	
Freq	S11	Θ11	S11	Θ11	S11	Θ11	S11	Θ11	S11	Θ11
26	0.725	133.75	0.754	135.66	0.775	137.57	0.8208	141.40	0.975	166.24
30	0.5958	121.81	0.629	124.20	0.650	126.11	0.704	130.41	0.950	159.55
36	0.466	111.78	0.4958	113.31	0.5208	114.64	0.5708	118.47	0.908	151.43
40	0.408	106.05	0.433	107.96	0.4525	109.15	0.500	112.73	0.866	145.70

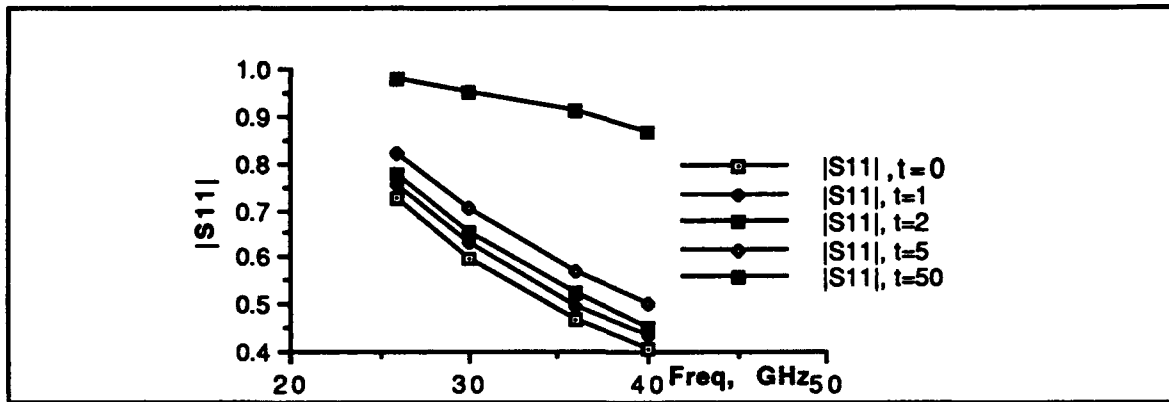


Figure 27. Magnitude of S11 versus frequency for strip length T=0.2 mm.

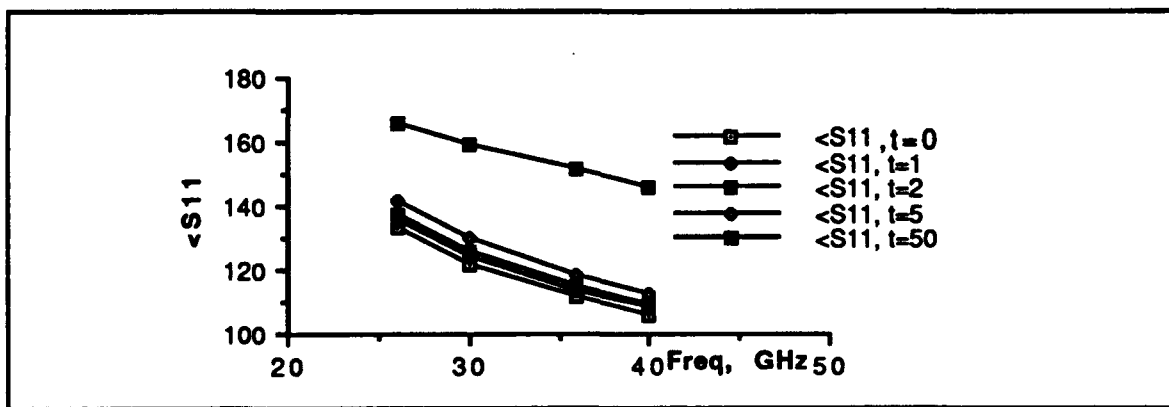


Figure 28. Angle Θ11 versus frequency for strip length T=0.2 mm.

TABLE 6. S-DATA FOR STRIP LENGTH T=0.5 MM.

	t=0mils		t=1mil		t=2mils		t=5mils		t=50mils	
Freq	S11	∠11	S11	∠11	S11	∠11	S11	∠11	S11	∠11
26	0.850	140.44	0.866	141.87	0.875	143.31	0.900	146.65	0.991	166.72
30	0.7458	127.07	0.766	128.69	0.783	130.41	0.816	133.75	0.975	160.50
36	0.625	112.73	0.6375	114.17	0.654	116.08	0.695	119.42	0.95	152.38
40	0.5375	104.61	0.558	106.05	0.575	107.96	0.616	111.30	0.916	146.65

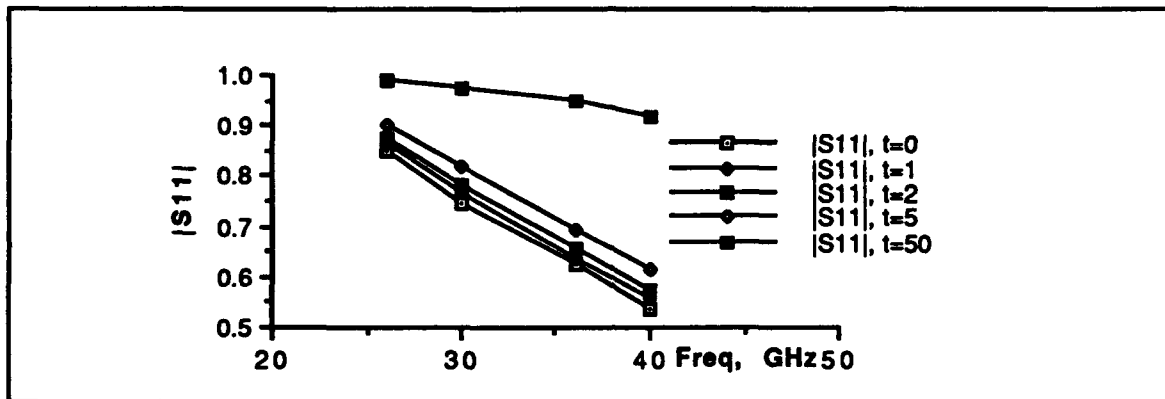


Figure 29. Magnitude of S11 versus frequency for strip length T=0.5 mm.

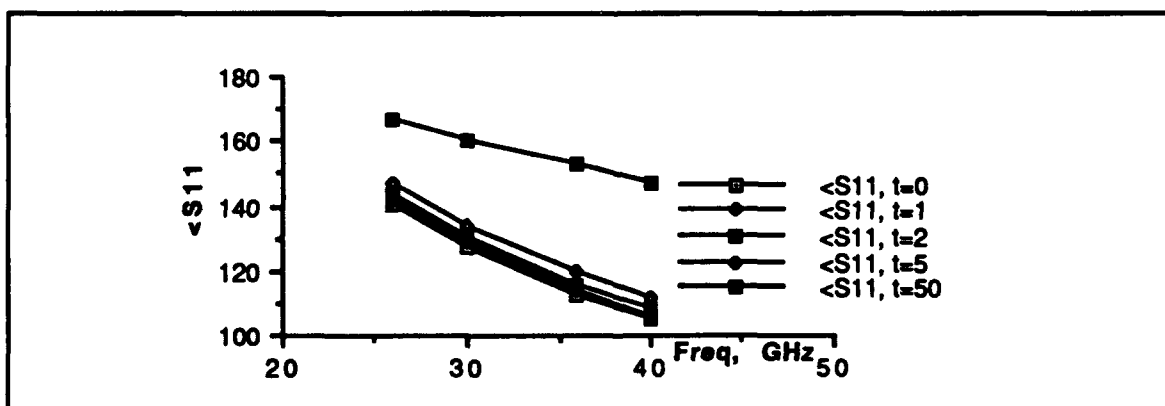


Figure 30. Angle ∠11 versus frequency for strip length T=0.5mm.

TABLE 7. S-DATA FOR STRIP LENGTH T=1MM.

	t=0 mils		t=1 mil		t=2 mils		t=5 mils		t=50 mils	
Freq	S11	∠11	S11	∠11	S11	∠11	S11	∠11	S11	∠11
26	0.933	144.74	0.941	146.17	0.945	147.13	0.954	149.52	0.995	167.19
30	0.8708	130.41	0.833	131.84	0.887	133.28	0.908	136.62	0.9875	161.94
36	0.762	111.78	0.775	113.69	0.7875	115.12	0.816	119.42	0.966	153.34
40	0.679	100.31	0.691	102.23	0.708	103.75	0.737	107.96	0.958	146.94

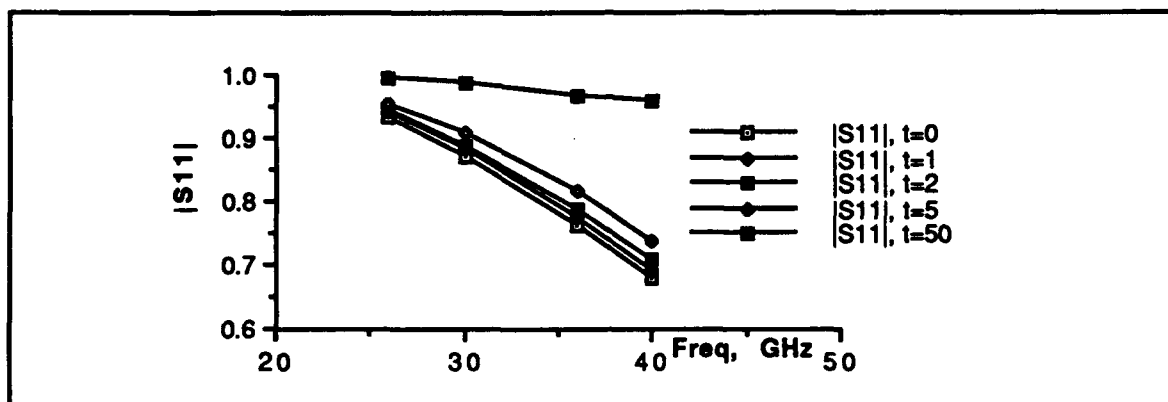


Figure 31. Magnitude S11 versus frequency for strip length T=1mm.

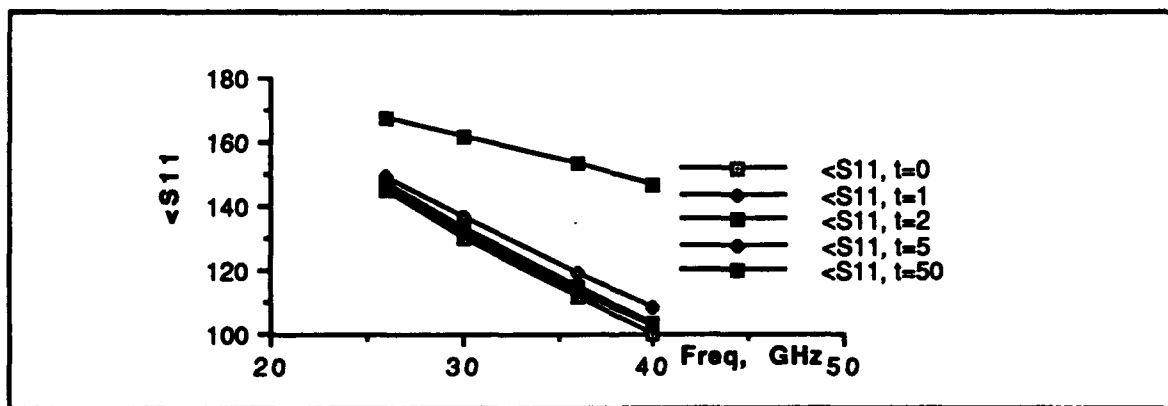


Figure 32. Angle ∠11 versus frequency for strip length T=1 mm.

TABLE 8. S-DATA FOR STRIP LENGTH T=2 MM.

	t=0 mils		t=1 mil		t=2 mils		t=5 mils		t=50 mils	
Freq	S11	∠11	S11	∠11	S11	∠11	S11	∠11	S11	∠11
26	0.983	147.61	0.987	148.56	0.989	149.04	0.991	151.43	0.996	167.86
30	0.966	132.32	0.968	134.23	0.972	135.19	0.973	138.15	0.986	162.13
36	0.904	109.87	0.912	111.78	0.916	113.69	0.920	117.99	0.976	153.82
40	0.833	94.108	0.841	95.06	0.85	97.45	0.851	102.70	0.966	146.65

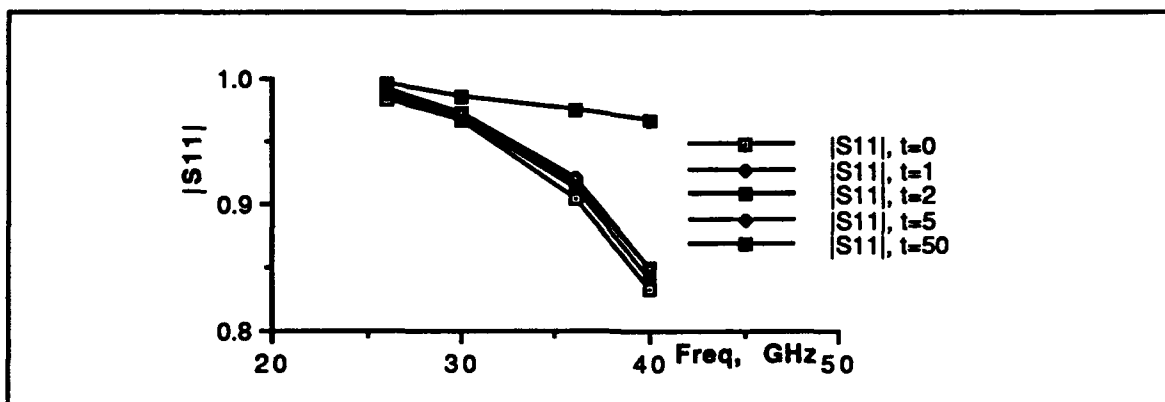


Figure 33. Magnitude of S11 versus frequency for strip length T=2 mm.

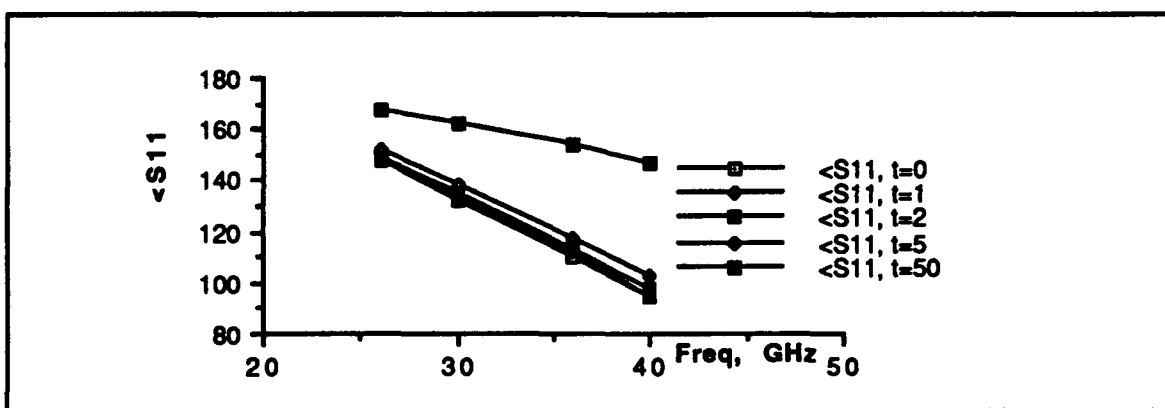


Figure 34. Angle ∠11 versus frequency for strip length T=2 mm.

TABLE 9. S-DATA FOR STRIP LENGTH T=5 MM.

	t=0 mils		t=1 mil		t=2 mils		t=5 mils		t=50 mils	
Freq	S11	Θ11	S11	Θ11	S11	Θ11	S11	Θ11	S11	Θ11
26	0.995	148.08	0.996	149.04	0.997	150.00	0.998	152.38	0.999	167.96
30	0.985	132.80	0.986	134.71	0.987	135.66	0.988	138.50	0.997	162.42
36	0.975	108.91	0.976	110.82	0.977	112.70	0.978	117.5	0.995	153.82
40	0.965	85.98	0.966	88.85	0.967	91.7	0.968	97.45	0.993	146.03

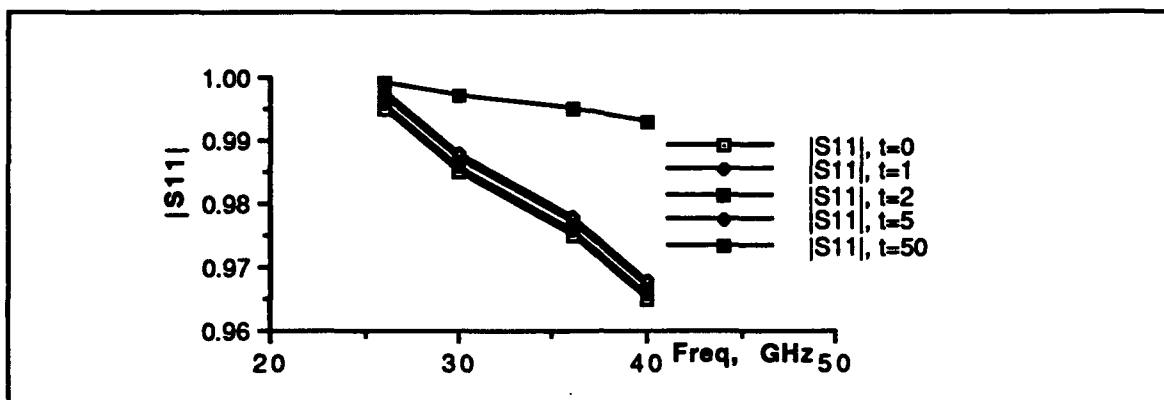


Figure 35. Magnitude for S11 versus frequency for strip length T=5 mm.

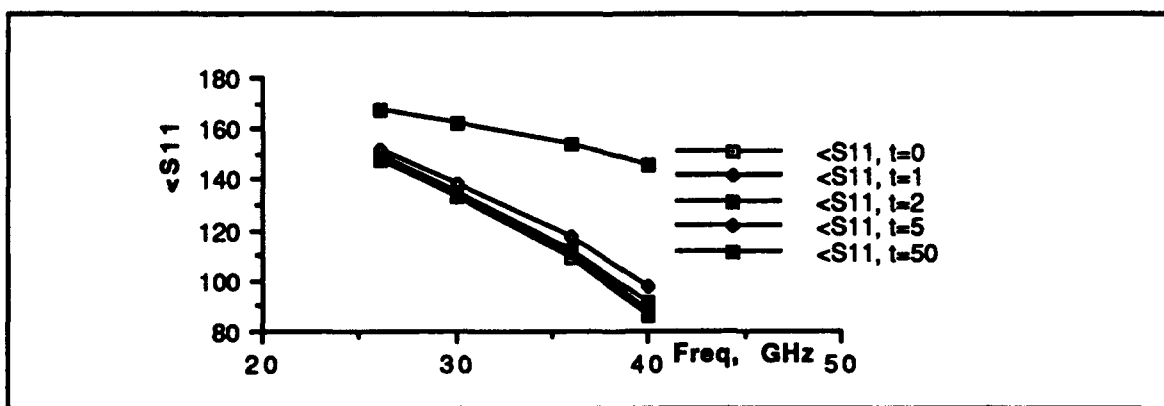


Figure 36. Angle Θ11 versus frequency for strip length T=5 mm.

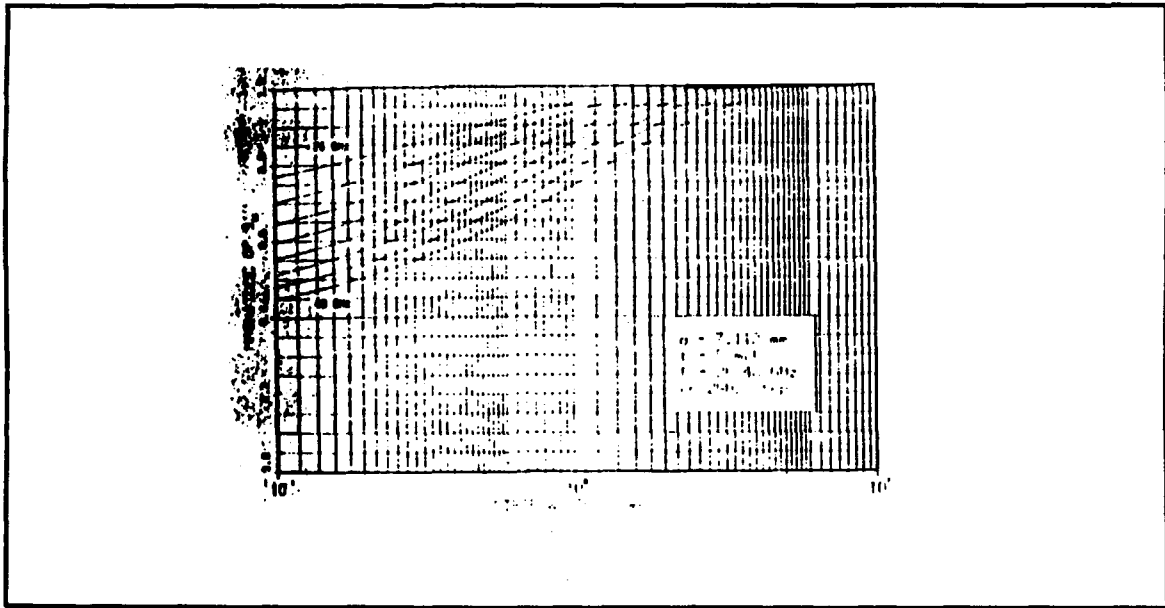


Figure 37. Magnitude of S11 for strip with thickness $t=5$ mils [Ref 10].

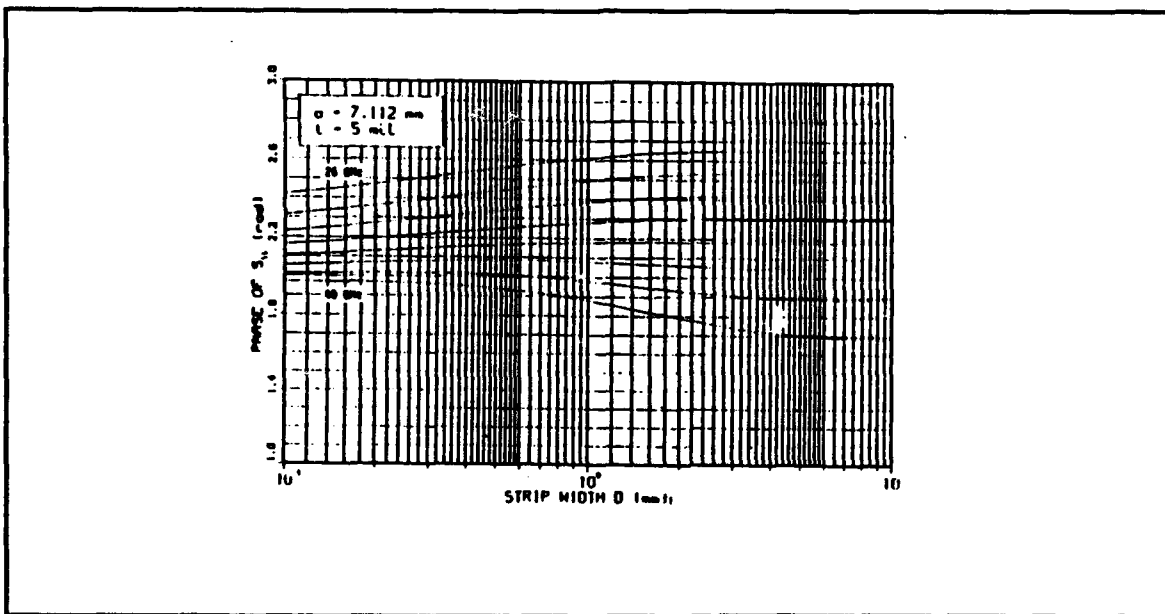


Figure 38. Angle of the S11 for strip with thickness $t=5$ mils [Ref 10].

APPENDIX. B. MAGNITUDE, ANGLE, SMITH CHART PLOT OF MODEL AND DATA

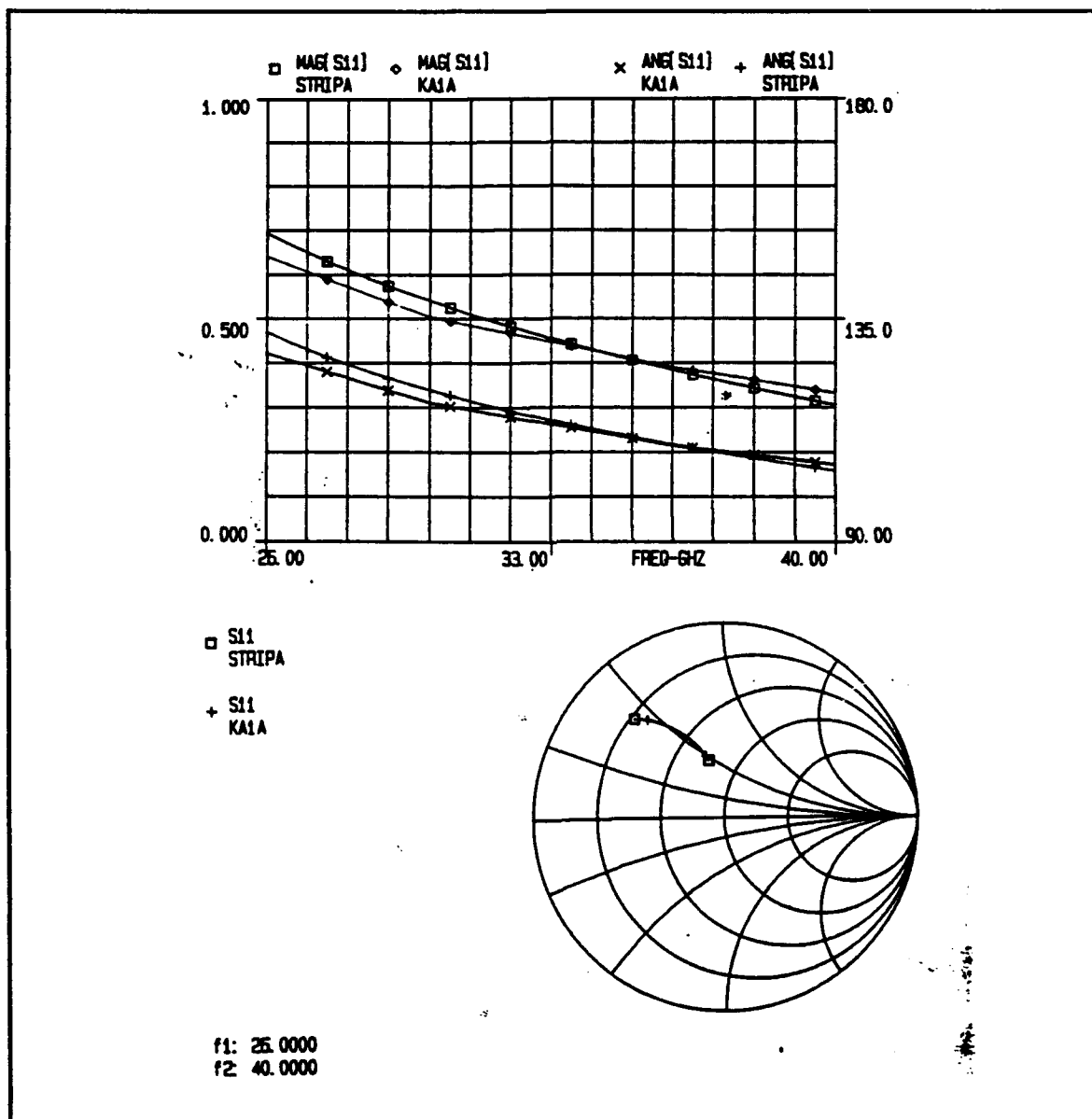


Figure 39. Plots for WR(28), $w/b=1$, $T=0.1$ mm, $t=0$ mils.

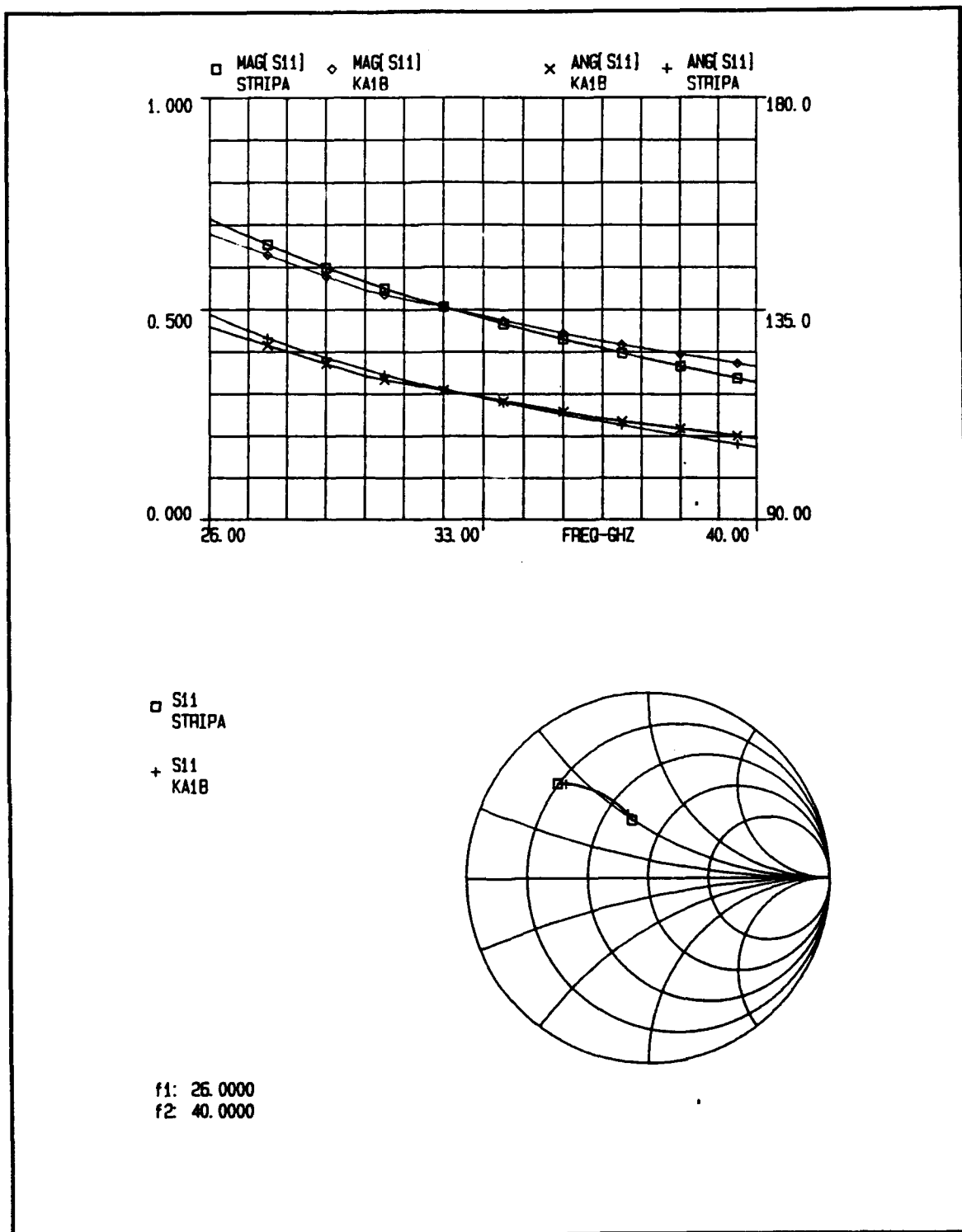


Figure 40. Plots for WR(28), $w/b=1$, $T=0.1$ mm, $t=1$ mils.

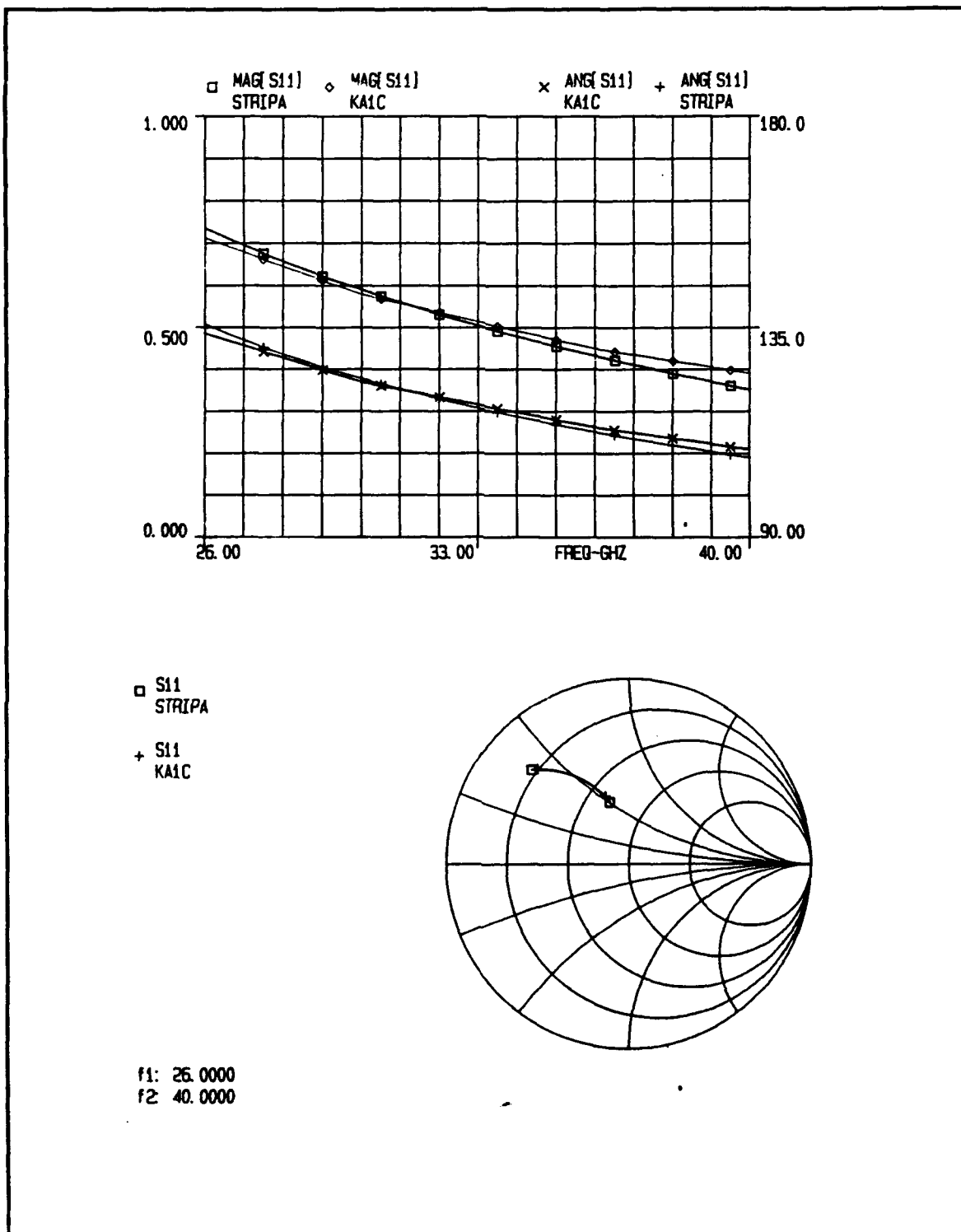
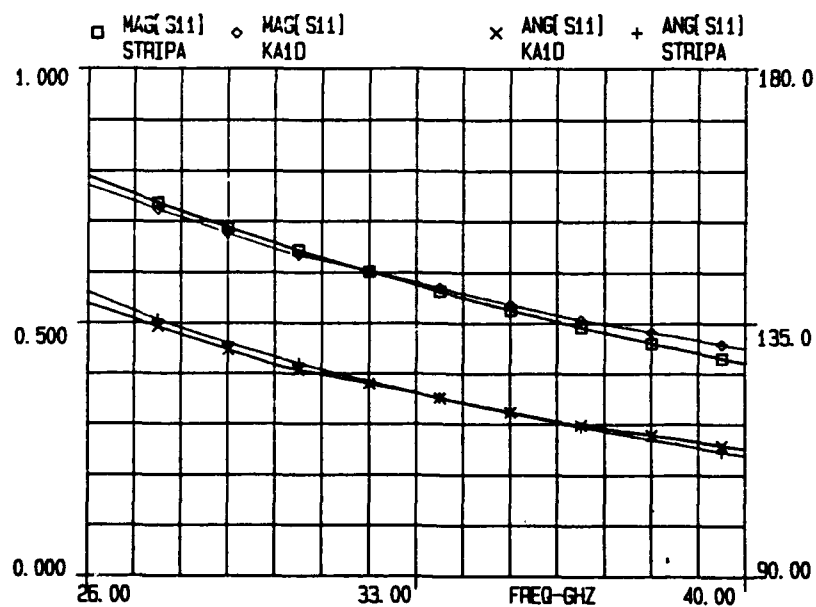
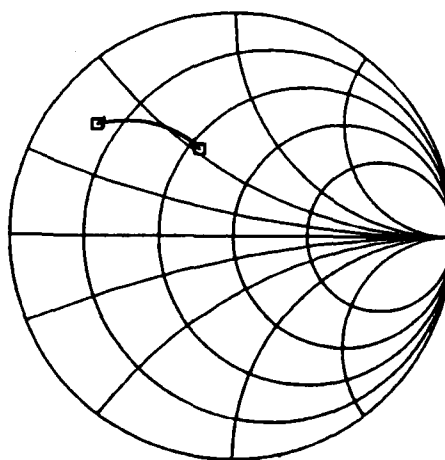


Figure 41. Plots for WR(28), $w/b=1$, $T=0.1$ mm, $t=2$ mils.



□ S11
STRIPA
+ S11
KA1D



f1: 26.0000
f2: 40.0000

Figure 42. Plots for WR(28), $w/b=1$, $T=0.1$ mm, $t=5$ mils.

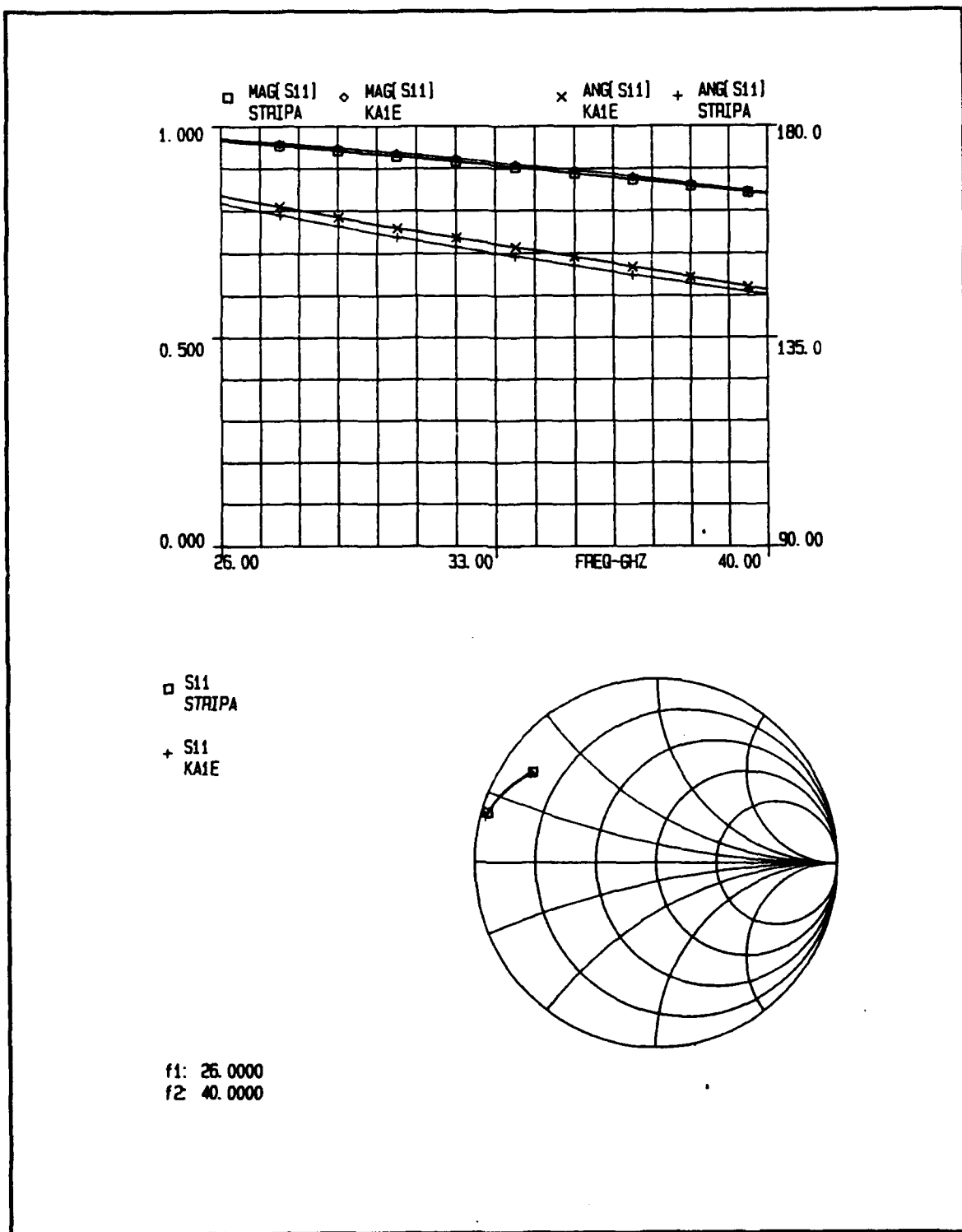
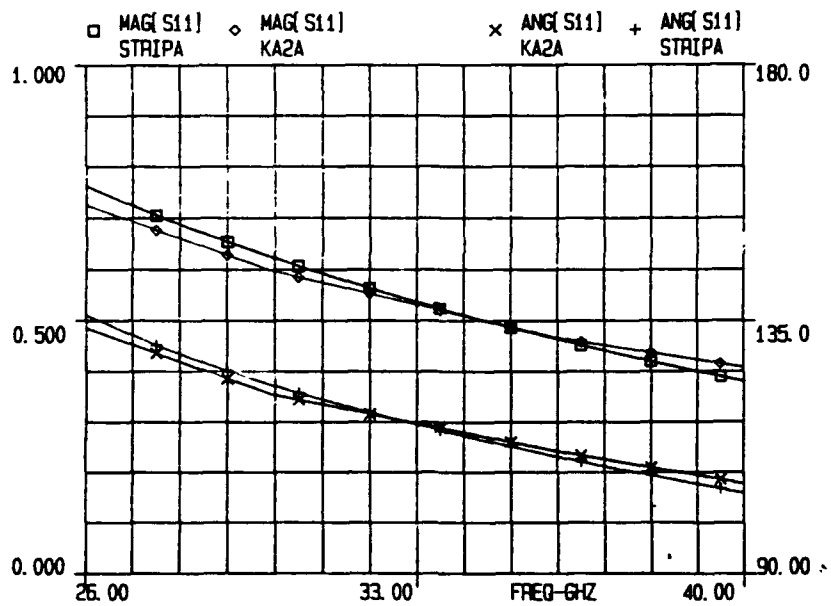
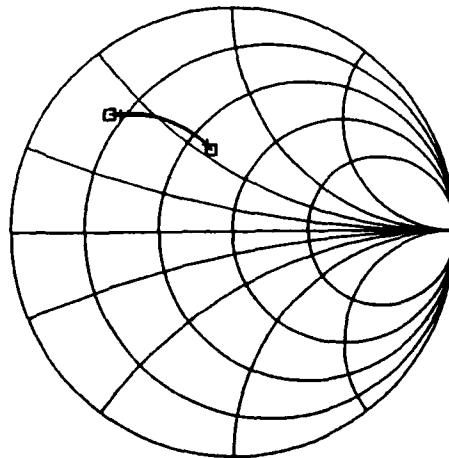


Figure 43. Plots for WR(28), $w/b=1$, $T=0.1$ mm, $t=50$ mils.

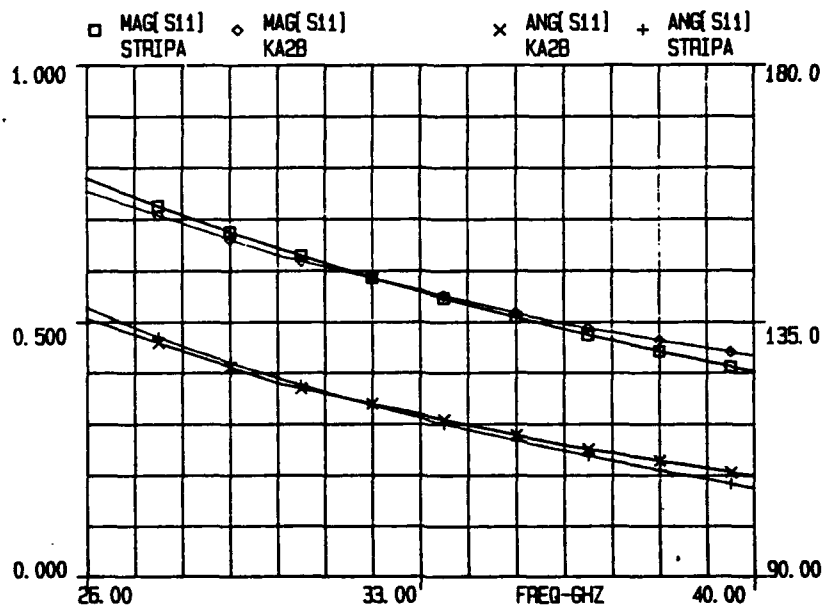


□ S11
STRIPA
+ S11
KA2A



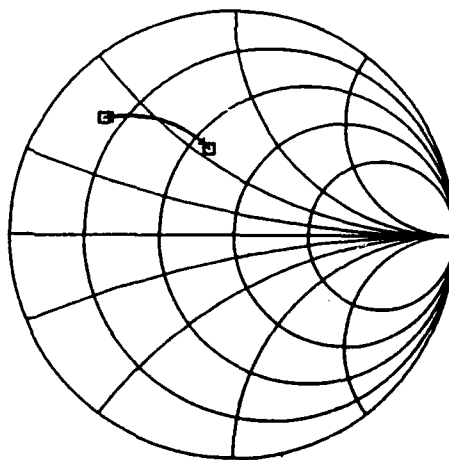
f1: 26.0000
f2: 40.0000

Figure 44. Plots for WR(28), $w/b=1$, $T=0.2$ mm, $t=0$ mils.



□ S11
STRIPA

+ S11
KA2B



f1: 26.0000
f2: 40.0000

Figure 45. Plots for WR(28), $w/b=1$, $T=0.2$ mm, $t=1$ mils.

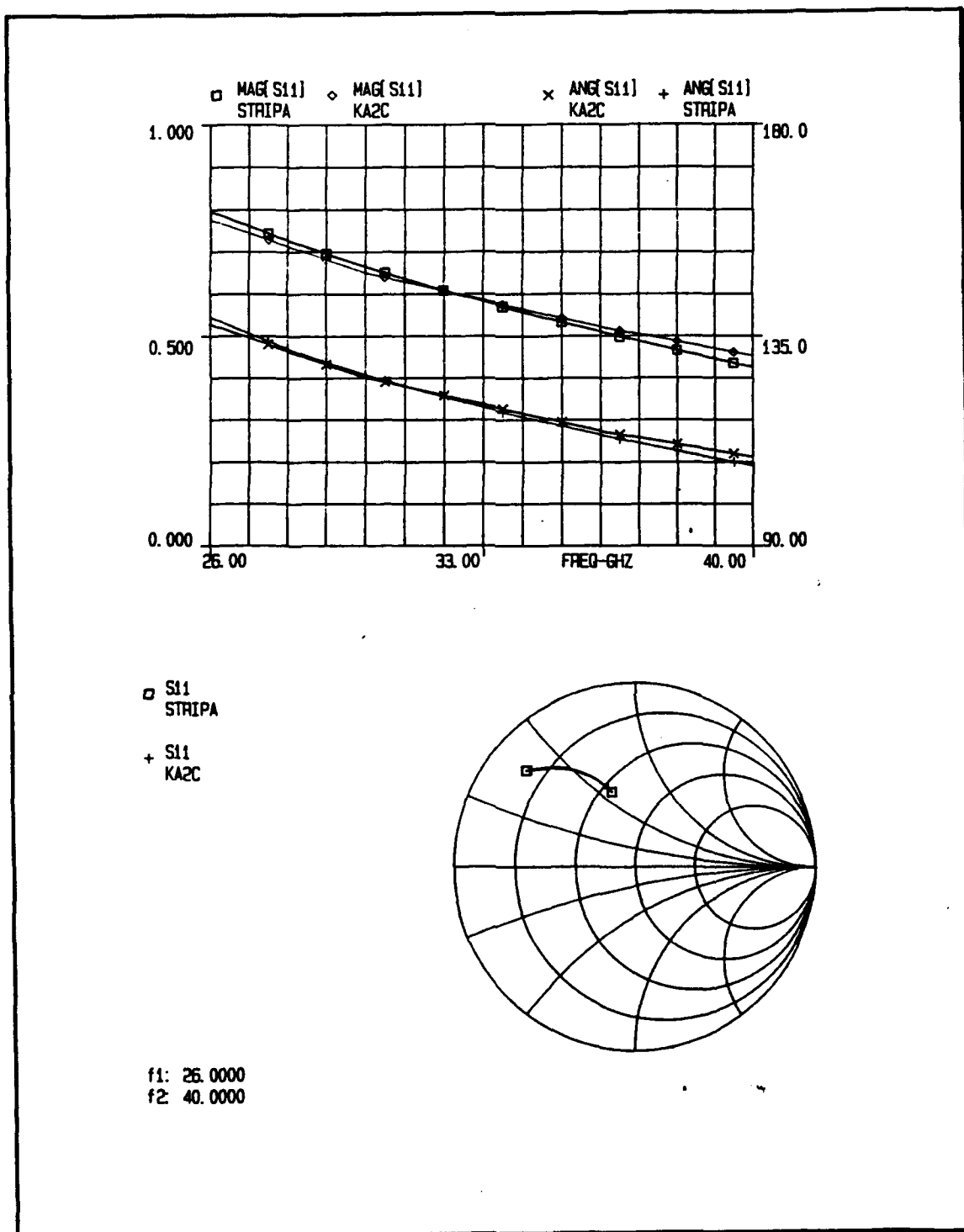
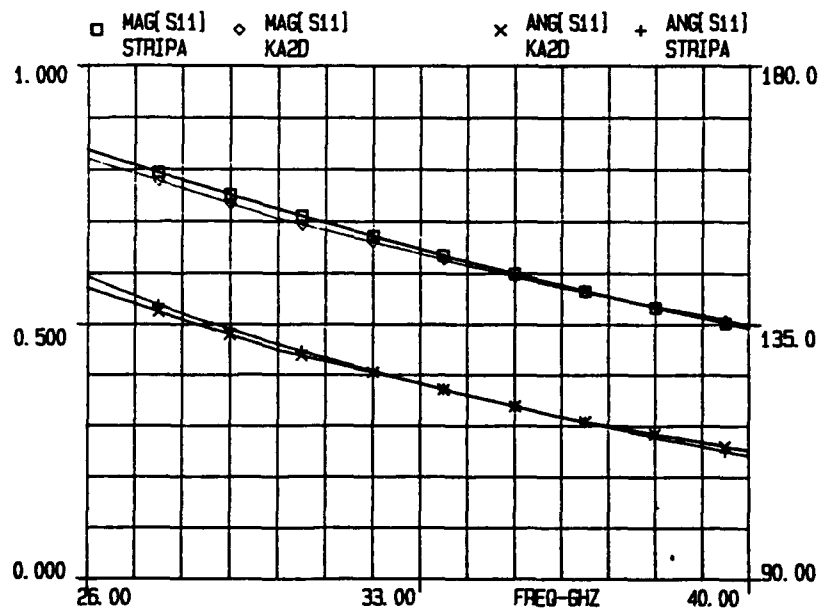
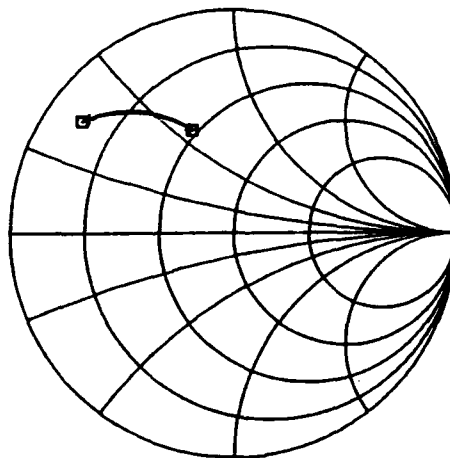


Figure 46. Plots for WR(28), $w/b=1$, $T=0.2$ mm, $t=2$ mils.

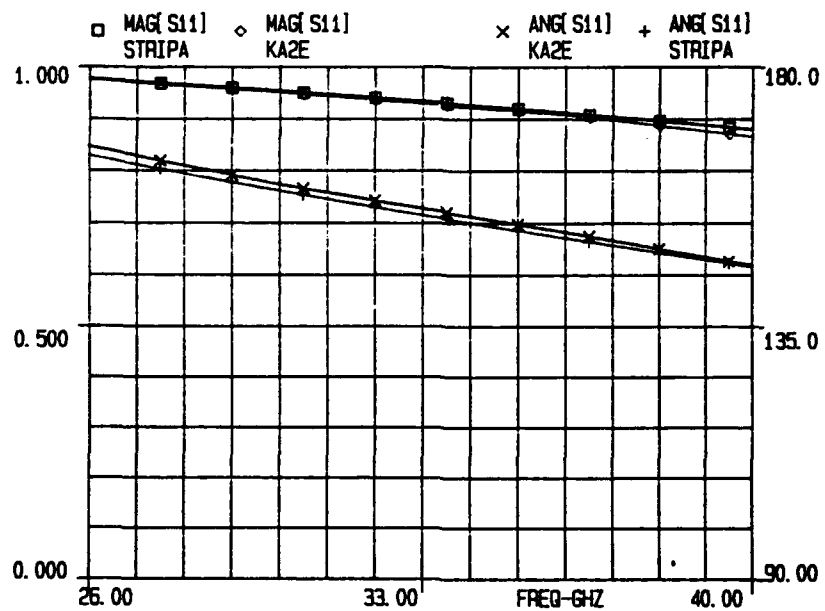


□ S11
STRIPA
+ S11
KA2D

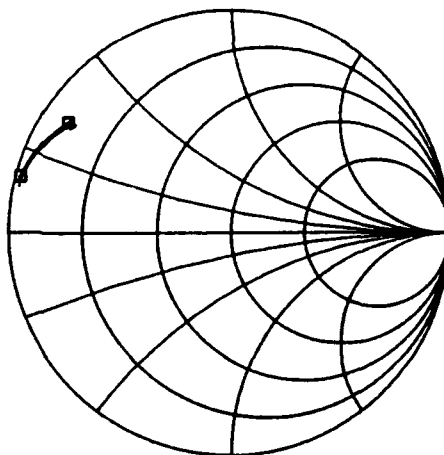


f1: 26.0000
f2: 40.0000

Figure 47. Plots for WR(28), $w/b=1$, $T=0,2$ mm, $t=5$ mils.



□ S11 STRIPA
+ S11 KA2E



f1: 26.0000
f2: 40.0000

Figure 48. Plots for WR(28), T=0.2 mm, t=50 mils.

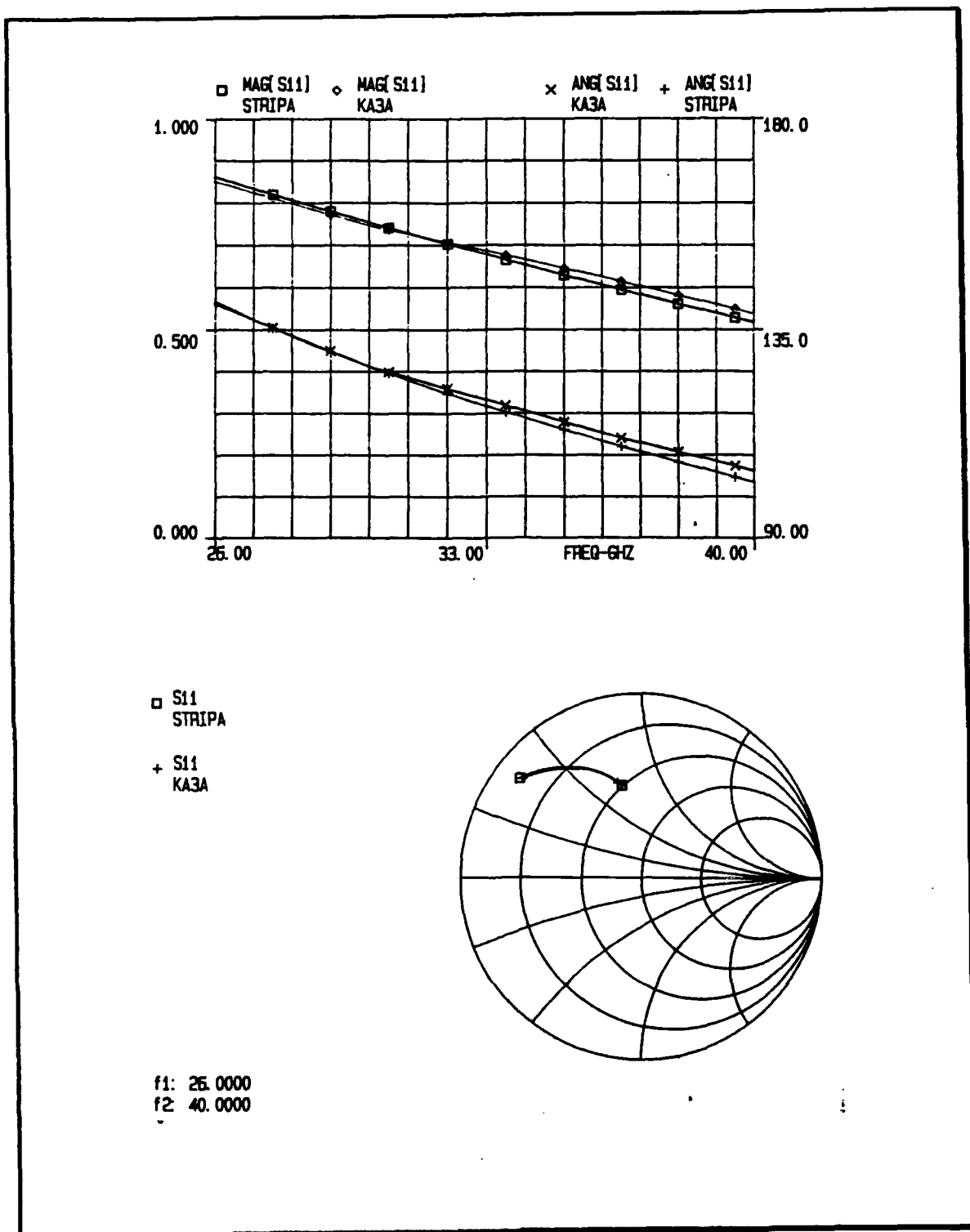


Figure 49. Plots for WR(28), $w/b=1$, $T=0.5$ mm, $t=0$ mils.

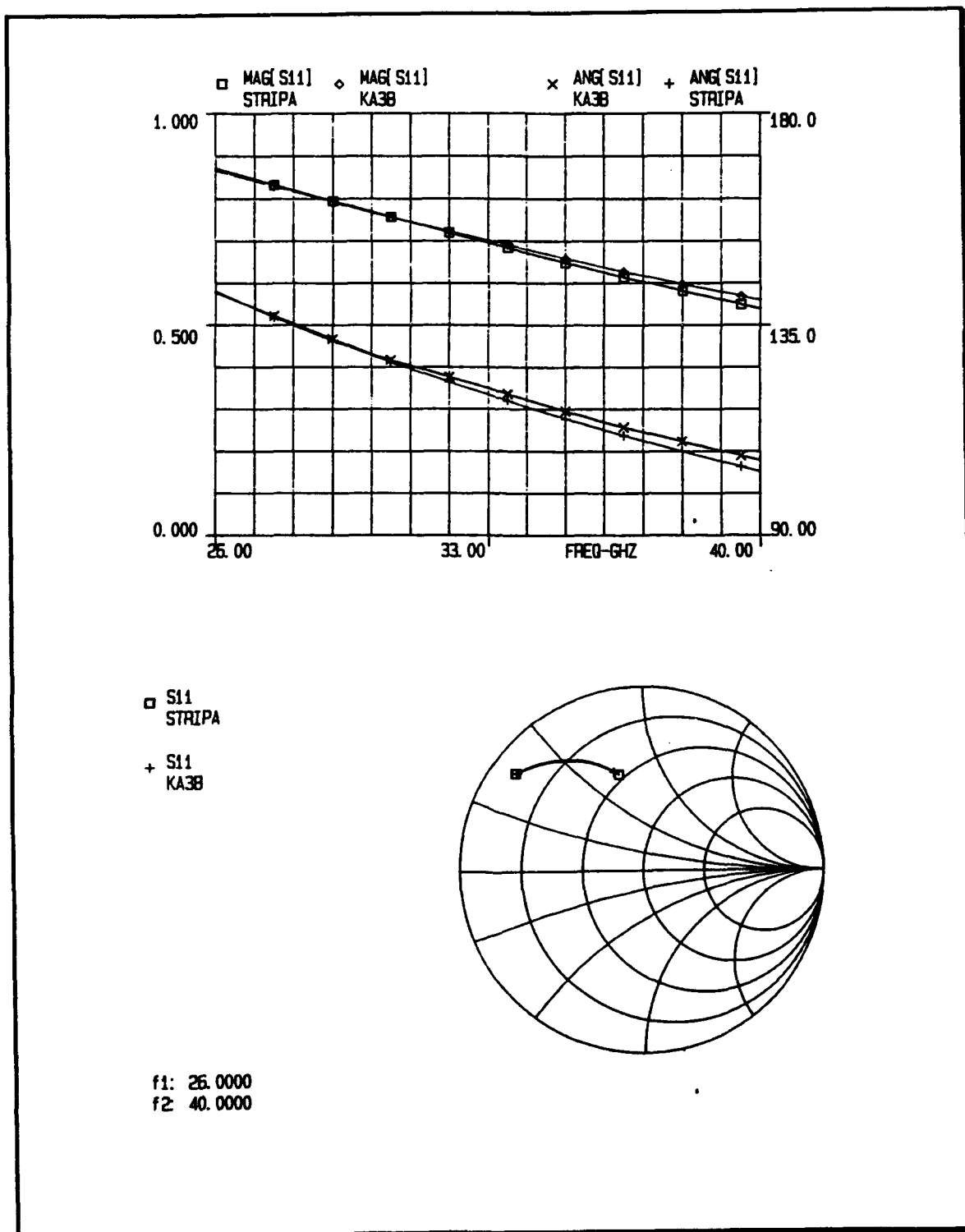


Figure 50. Plots for WR(28), $w/b=1$, $T=0.5$ mm, $t=1$ mils.

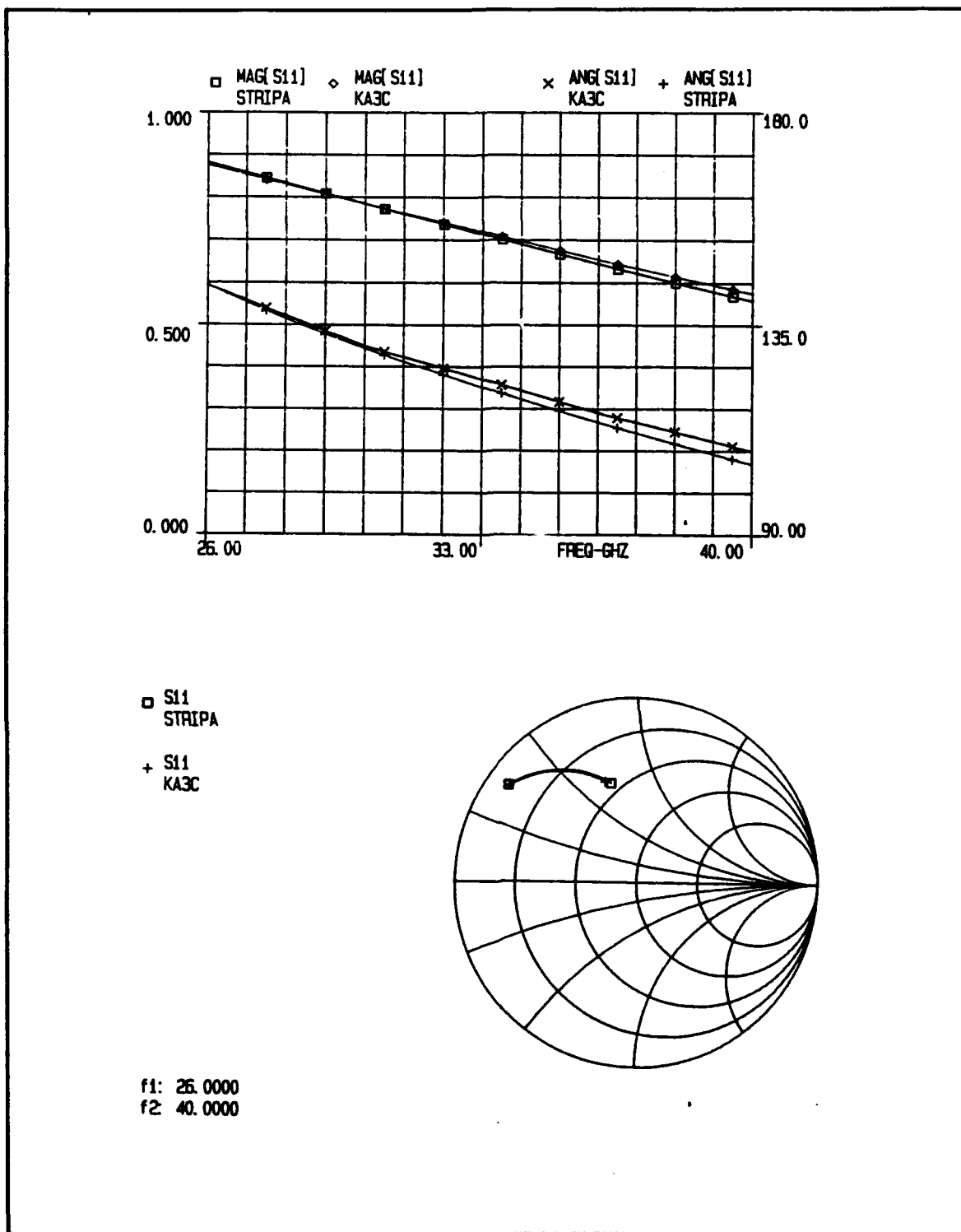


Figure 51. Plots for WR(28), $w/b=1$, $T=0.5$ mm, $t=2$ mils.

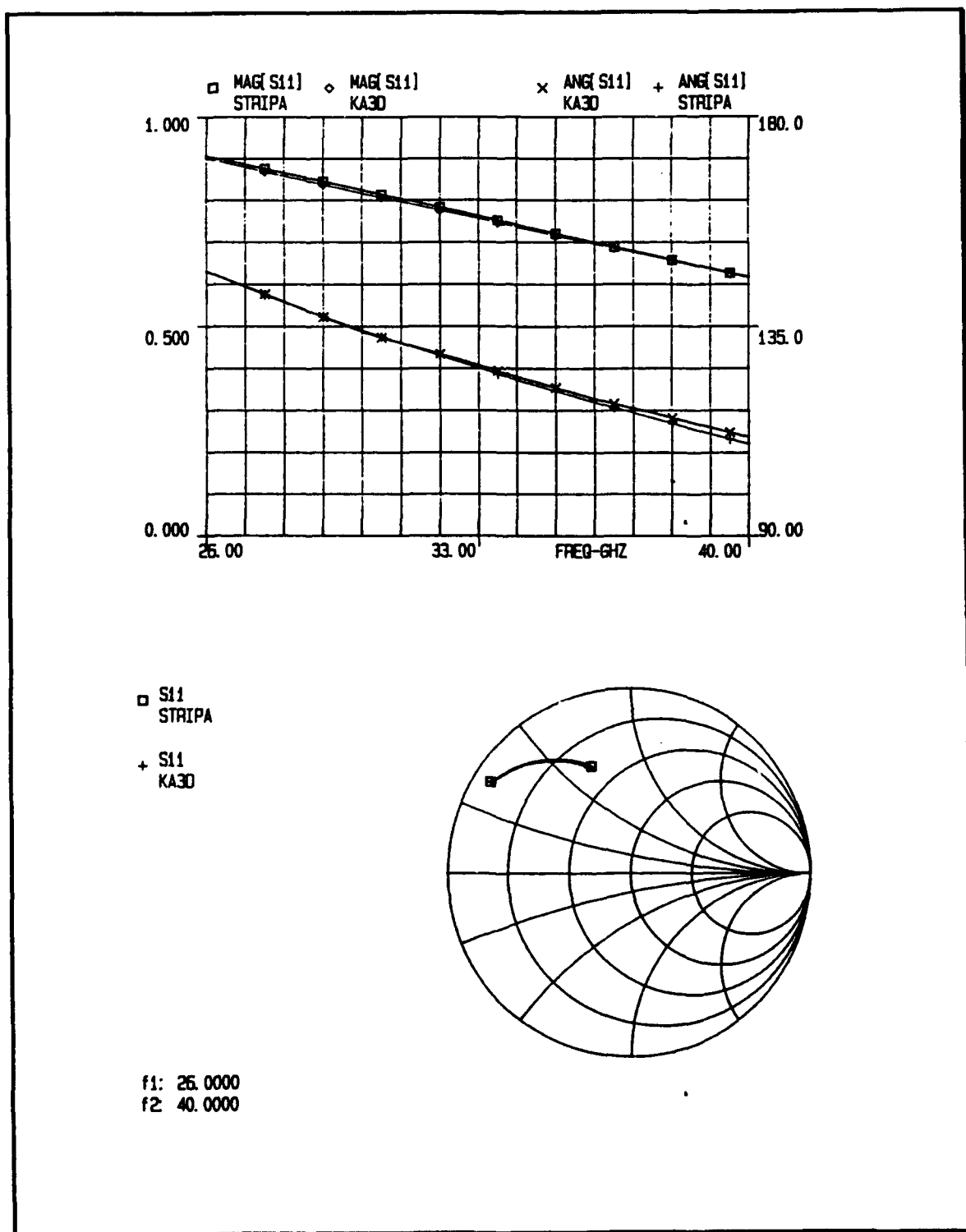
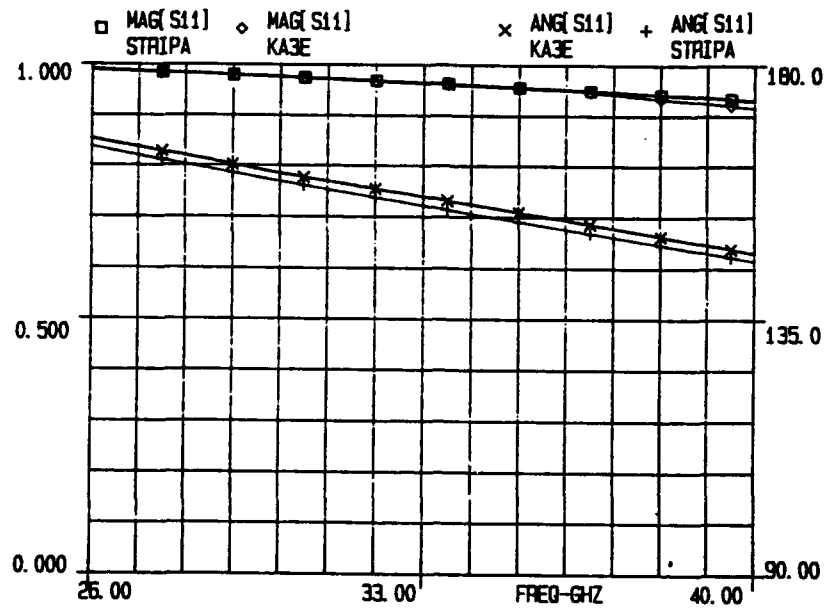
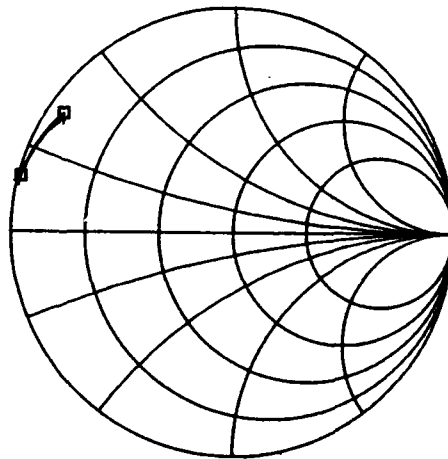


Figure 52. Plots for WR(28), $w/b=1$, $T=0.5$ mm, $t=5$ mils.



□ S11
STRIPA

+ S11
KA3E



f1: 26.0000
f2: 40.0000

Figure 53. Plots for WR(28), $w/b=1$, $T=0.5$, $t=50$ mils.

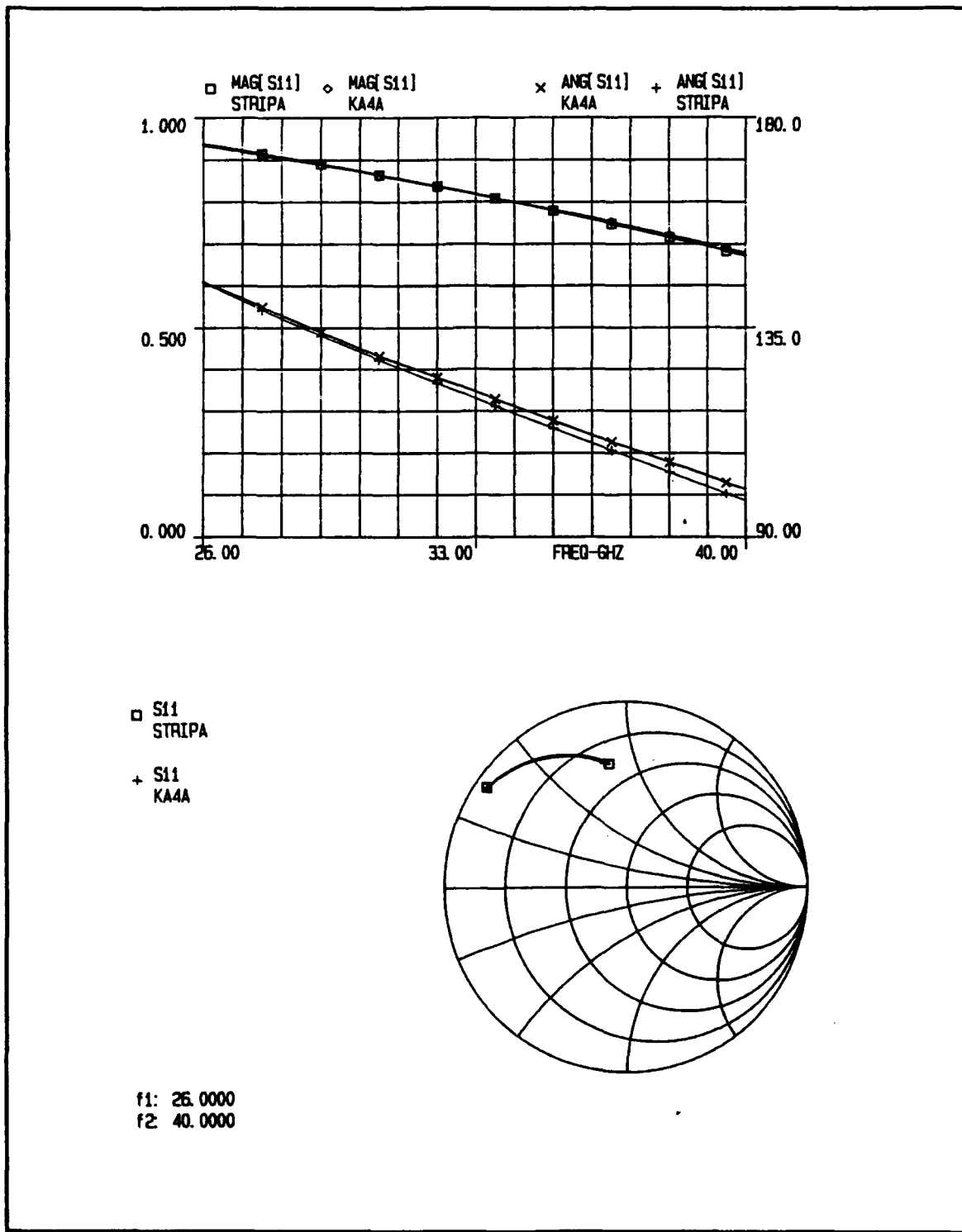


Figure 54. Plots for WR(28), $w/b=1$, $T=1$ mm, $t=0$ mils.

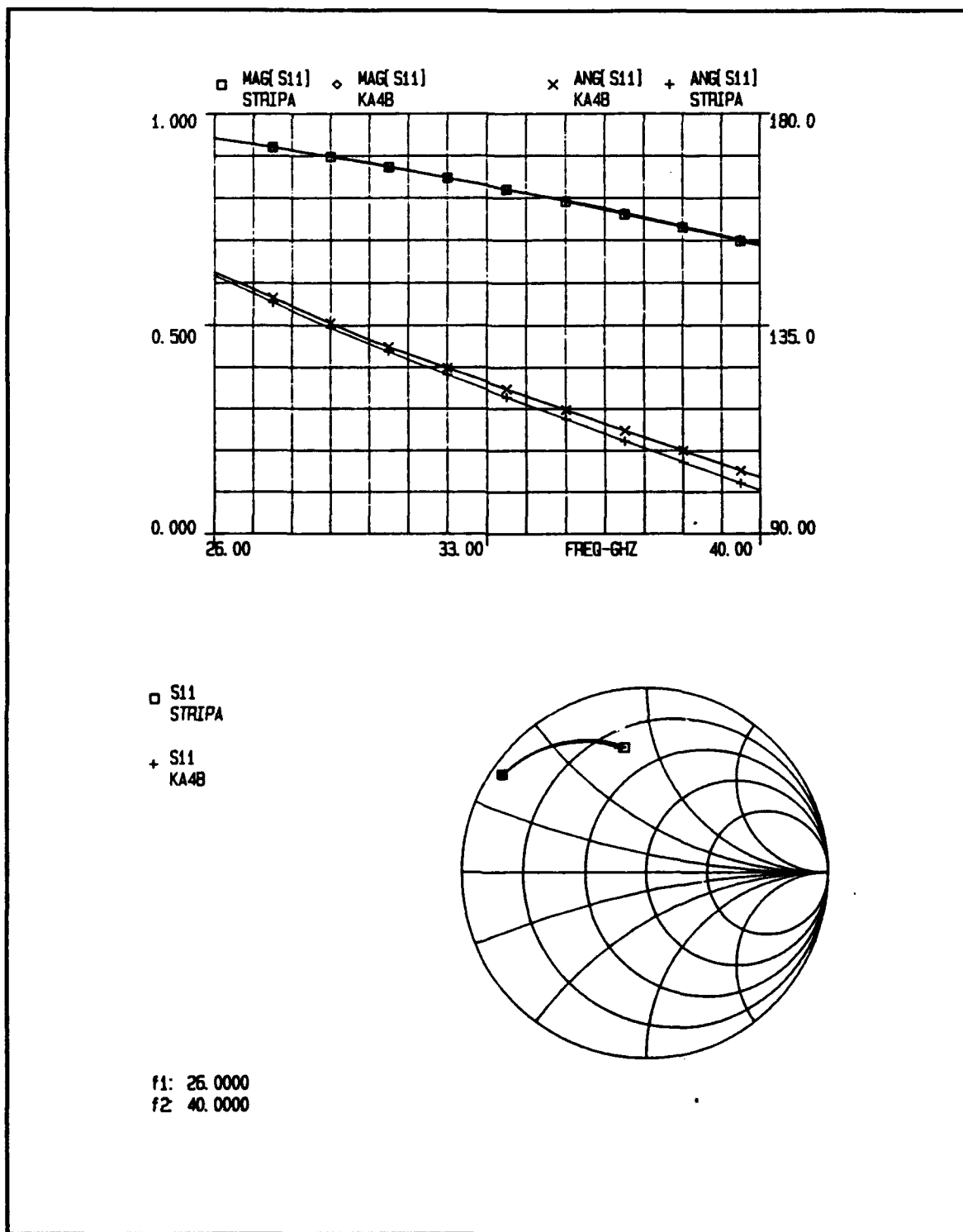


Figure 55. Plots for WR(28), $w/b=1$, $T=1$ mm, $t=1$ mils.

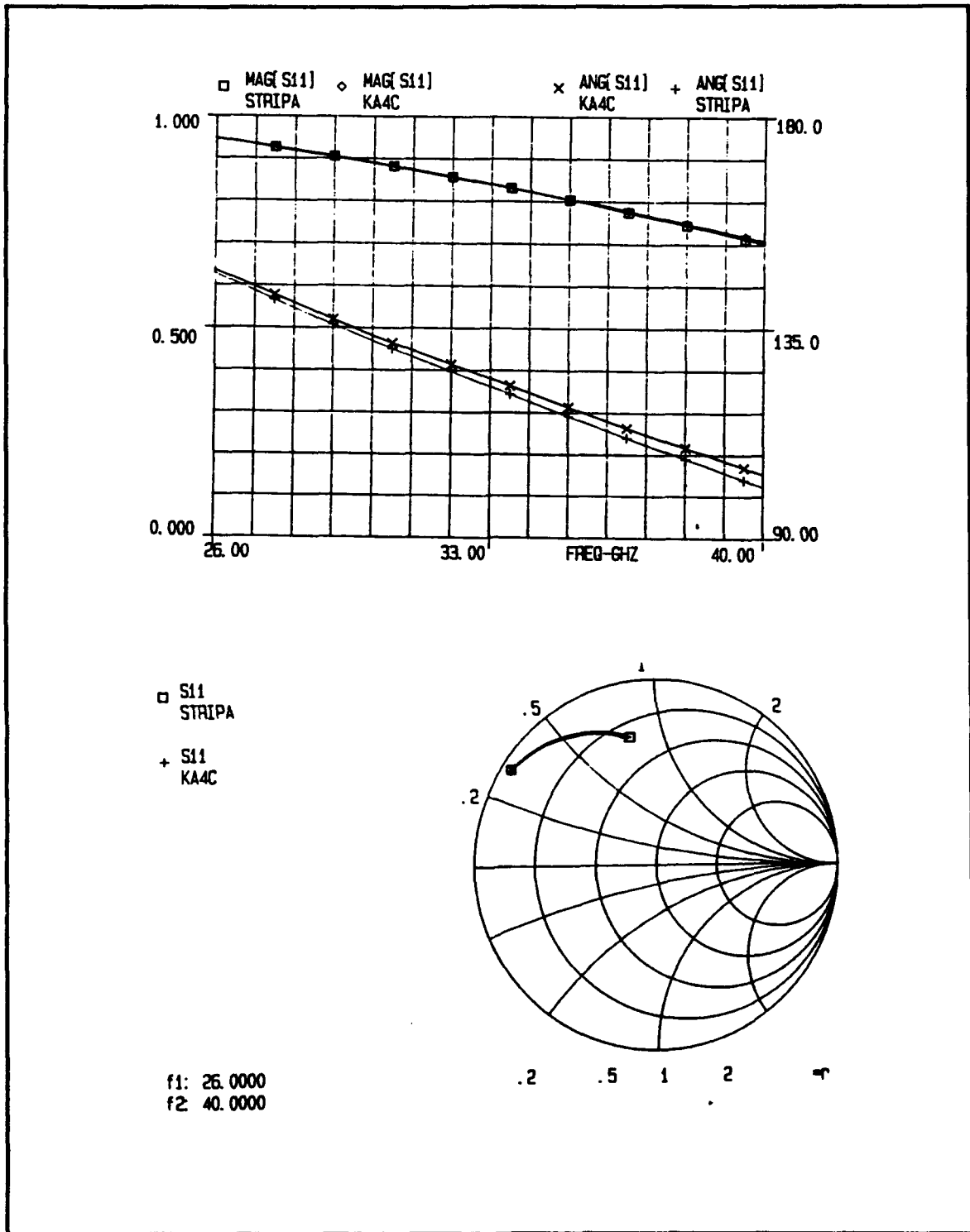


Figure 56. Plots for WR(28), $w/b=1$, $T=1$ mm, $t=2$ mils.

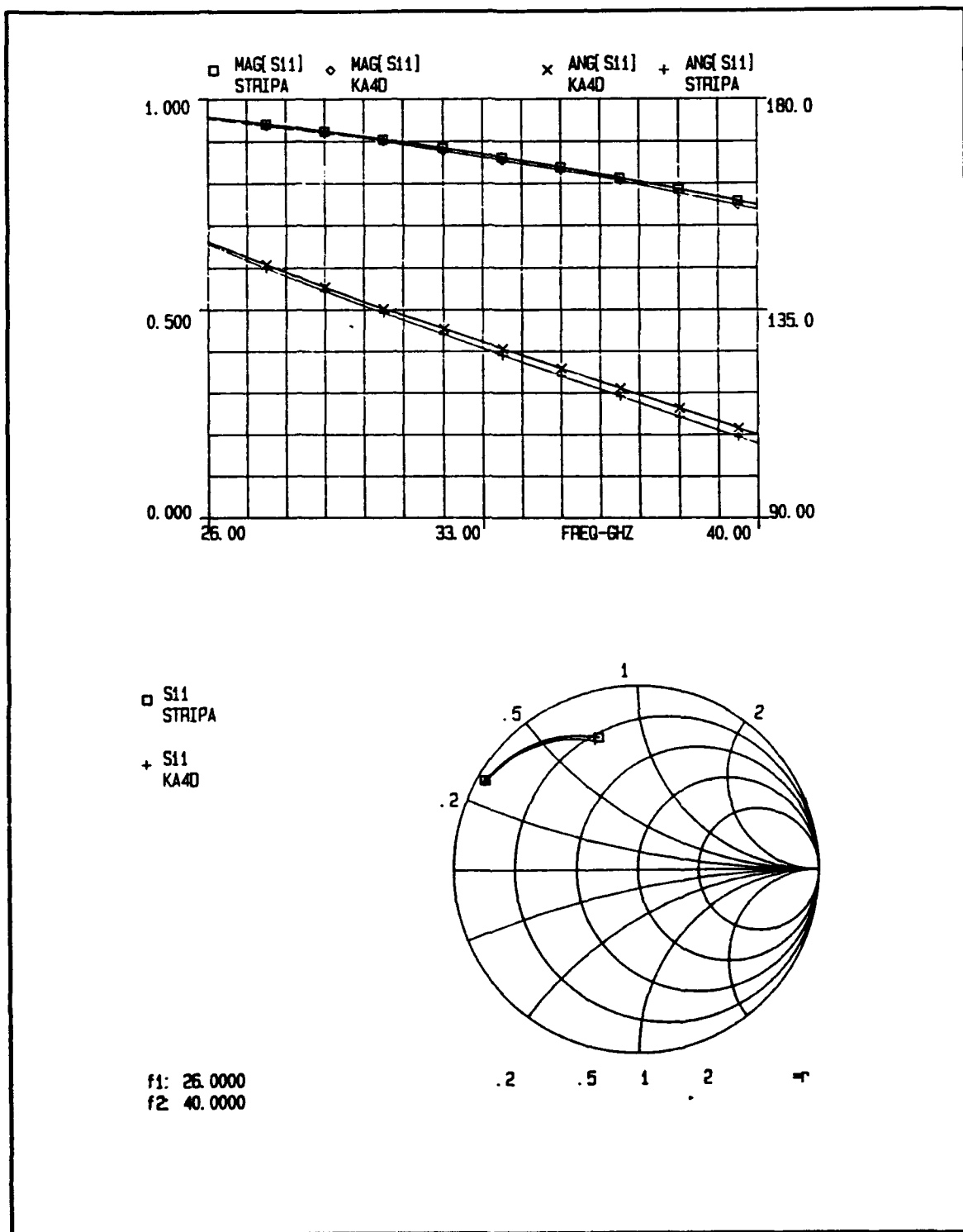


Figure 57. Plots for WR(28), $w/b=1$, $T=1\text{mm}$, $t=5$ mils.

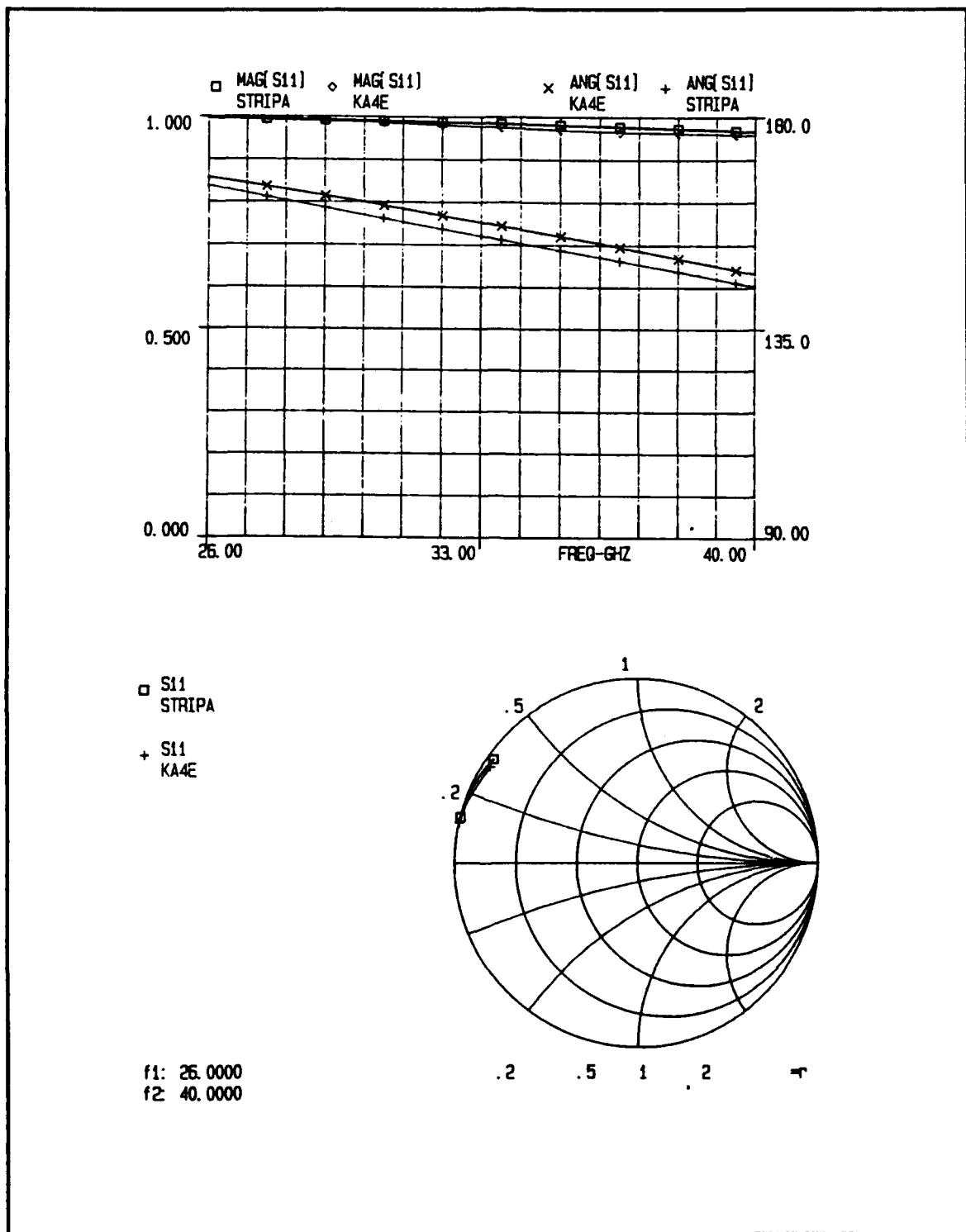


Figure 58. Plots for WR(28), $w/b=1$, $T=1$ mm, $t=50$ mils.

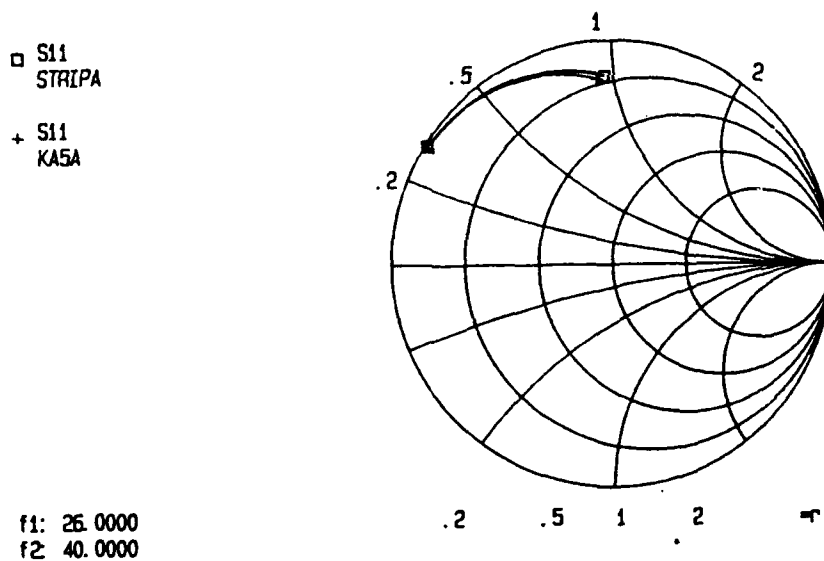
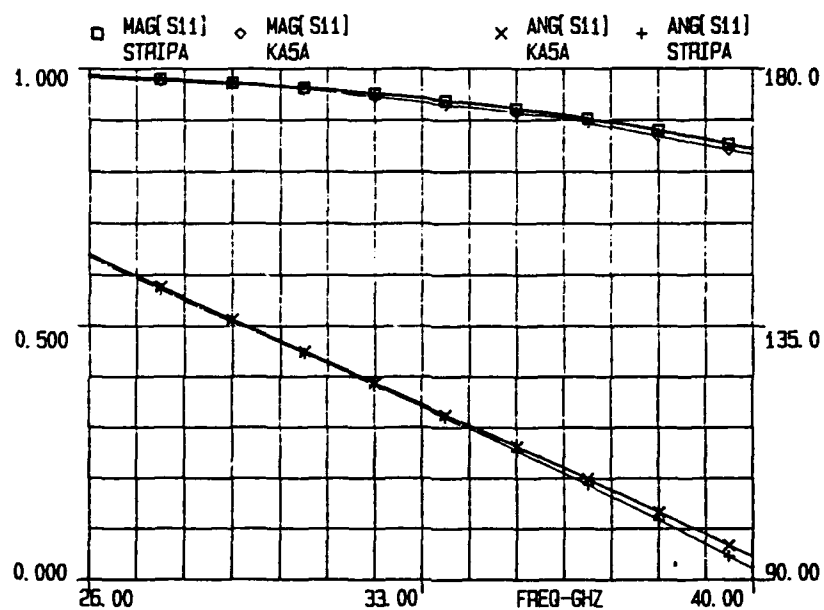


Figure 59. Plots for WR(28), $w/b=1$, $T=2$ mm, $t=0$ mils.

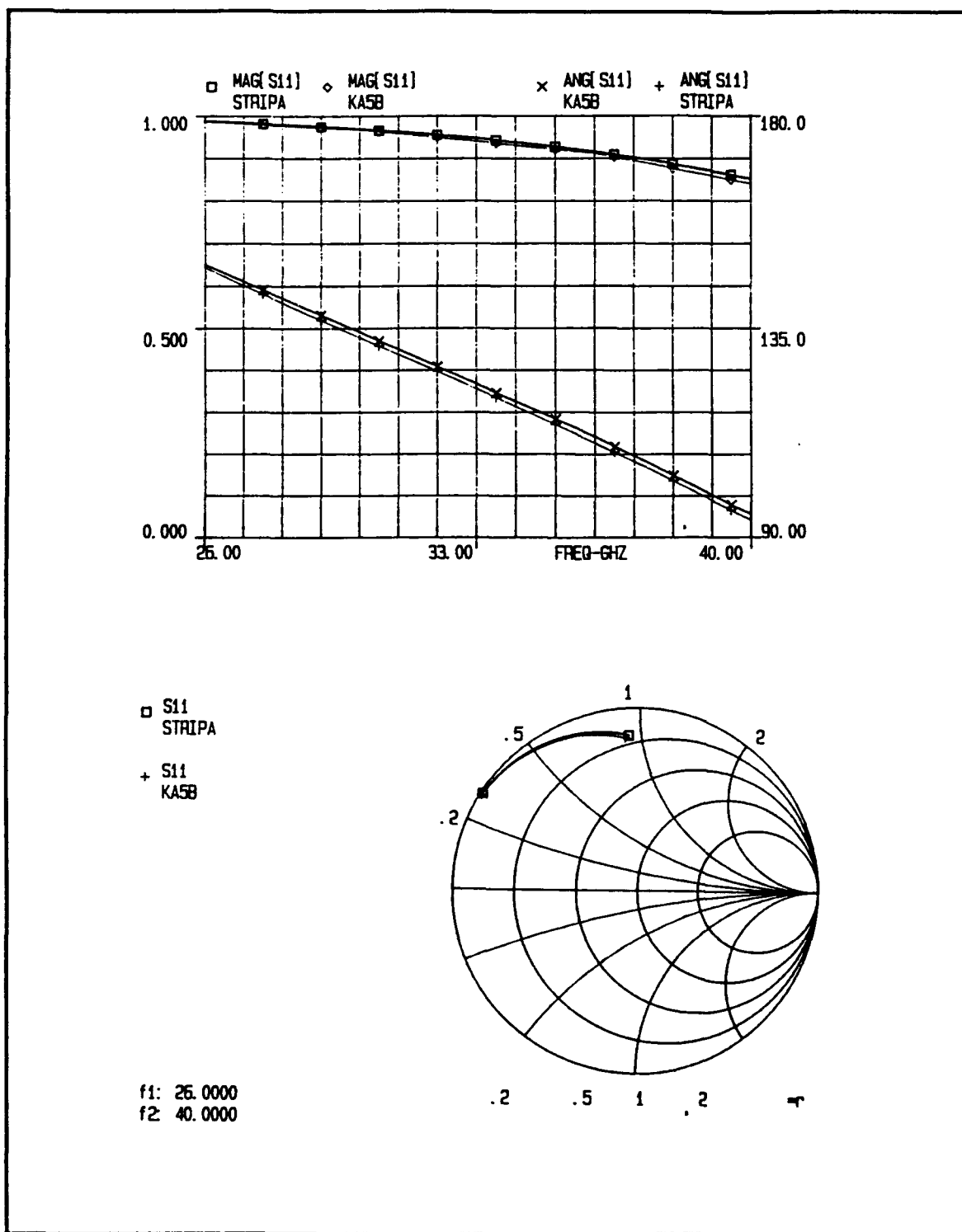
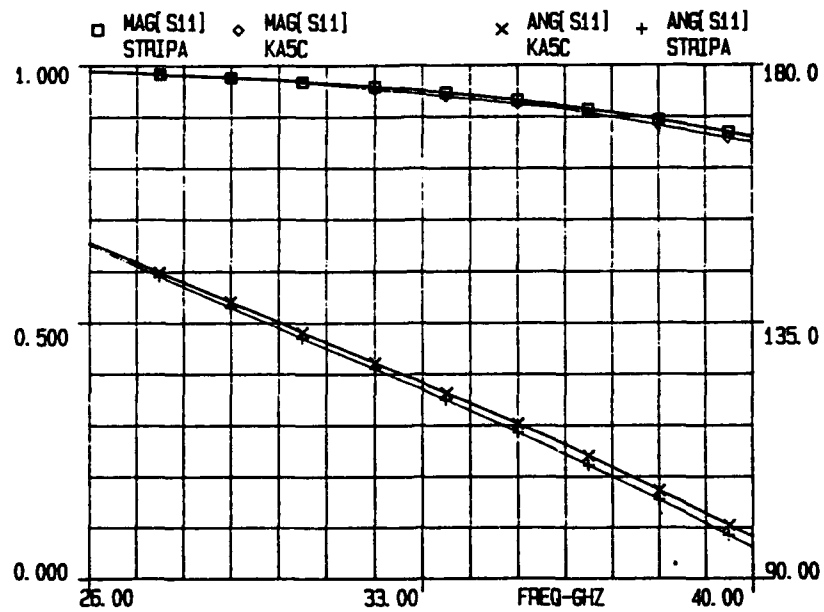
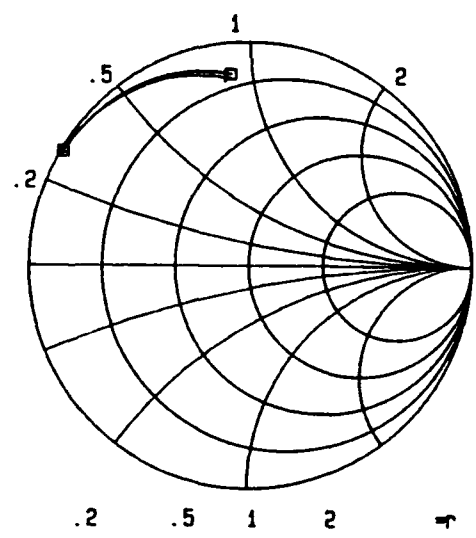


Figure 60. Plots for WR(28), $w/b=1$, $T=2\text{mm}$, $t=1$ mils.



□ S11 STRIPA
 + S11 KA5C



f1: 26.0000
 f2: 40.0000

Figure 61. Plots for WR(28), w/b=1, T=2 mm,t=2 mils

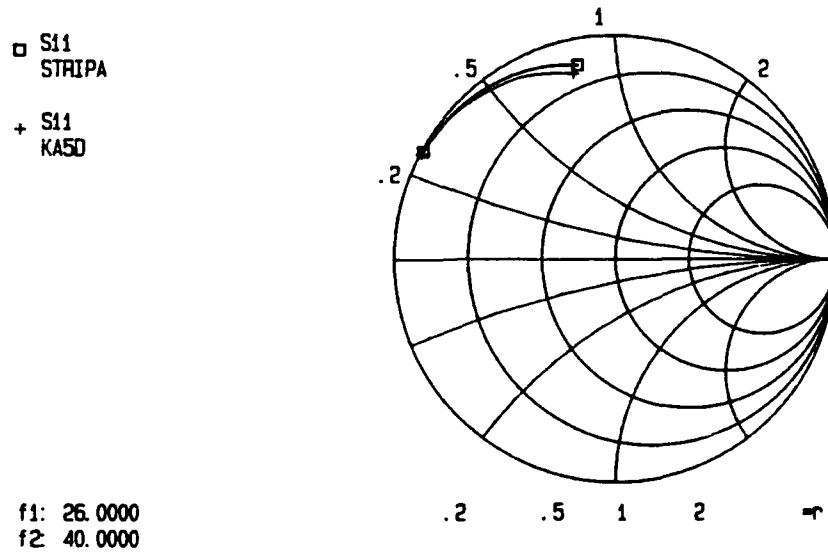
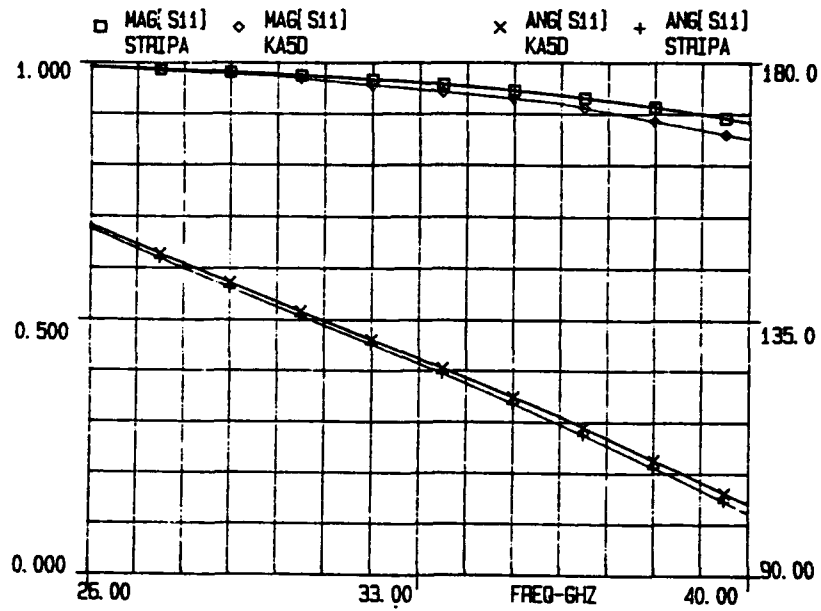


Figure 62. Plots for WR(28), $w/b=1$, $T=2$ mm, $t=5$ mils.

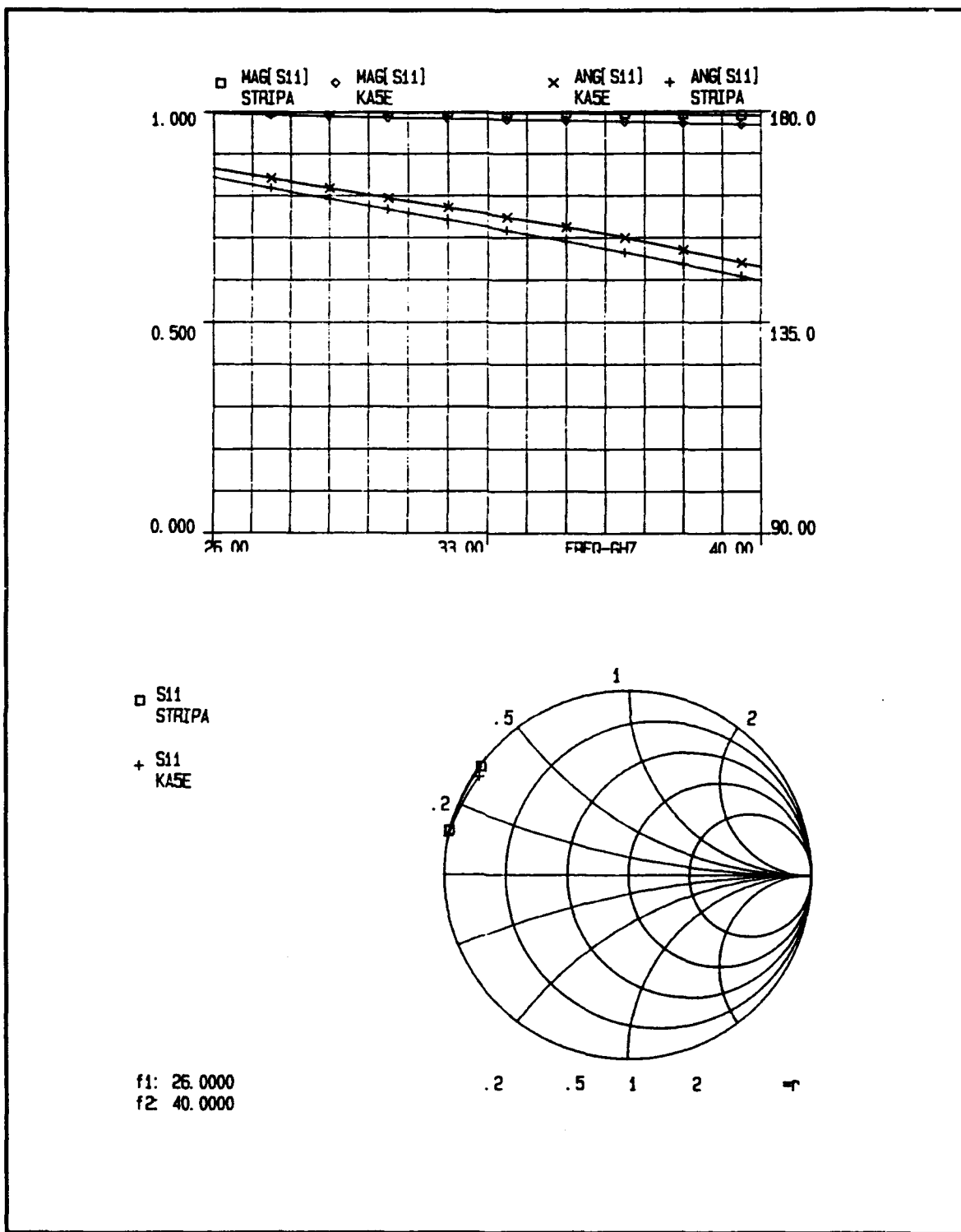


Figure 63. Plots for WR(28), $w/b=1$, $T=2$ mm, $t=50$ mils.

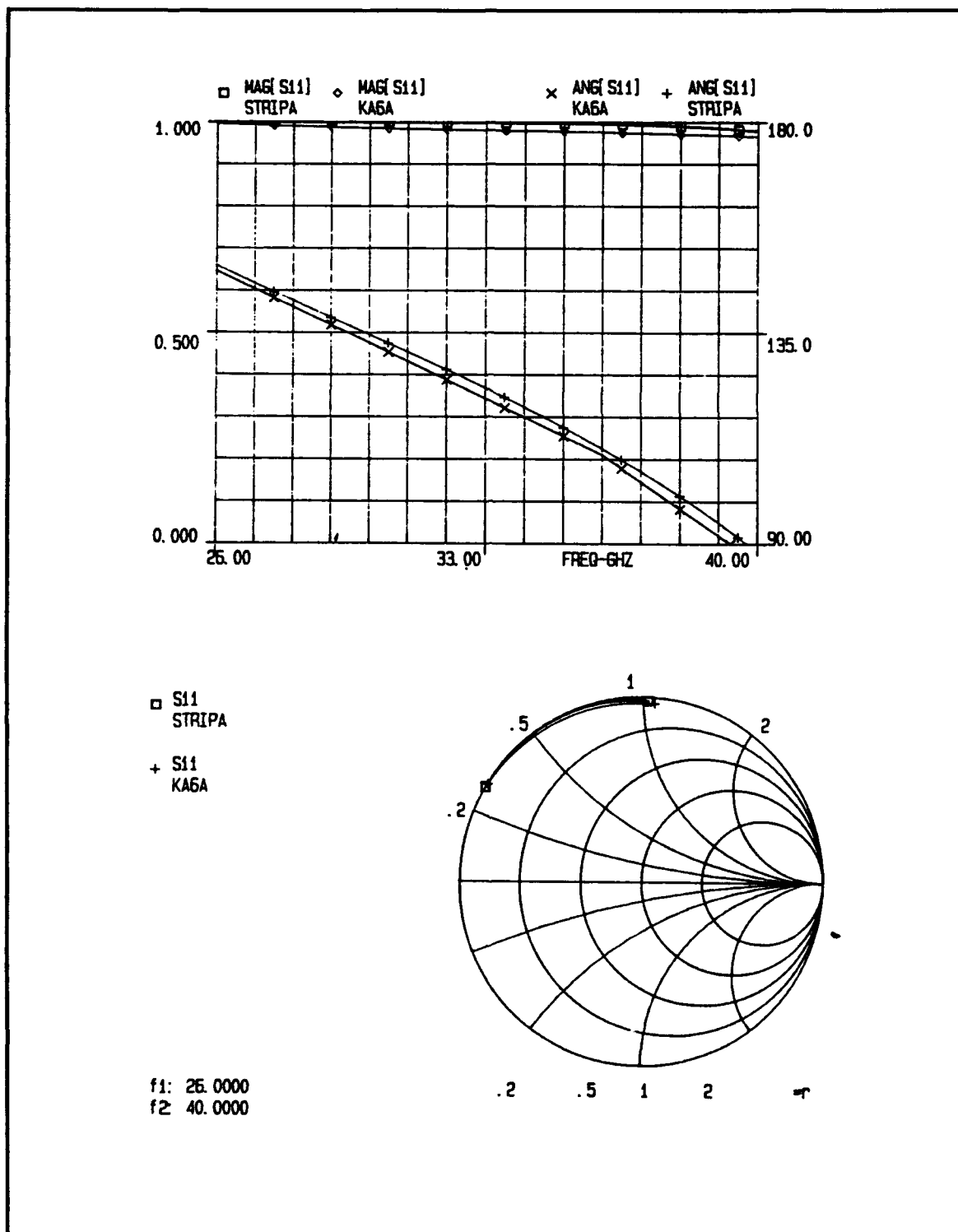
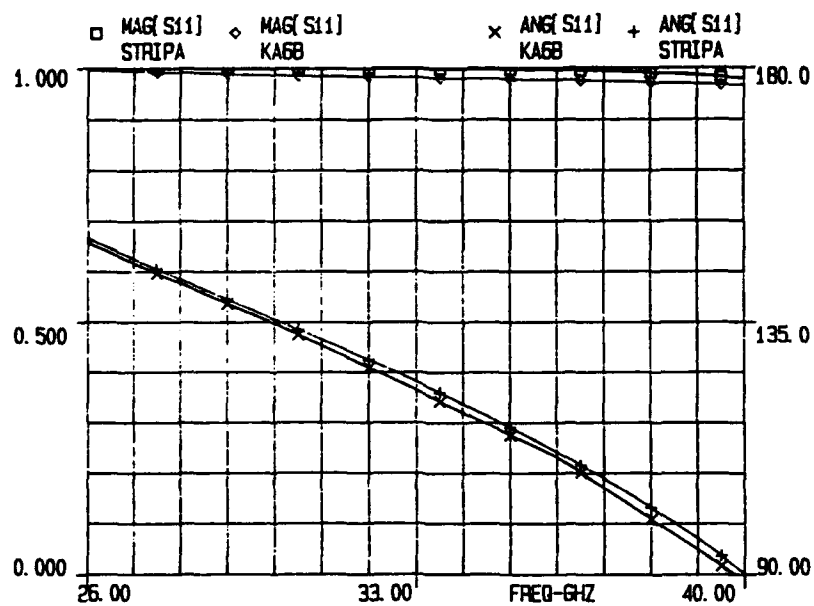


Figure 64. Plots for WR(28), $w/b=1$, $T=5$ mm, $t=0$ mils.



□ S11 STRIPA
 + S11 KA6B

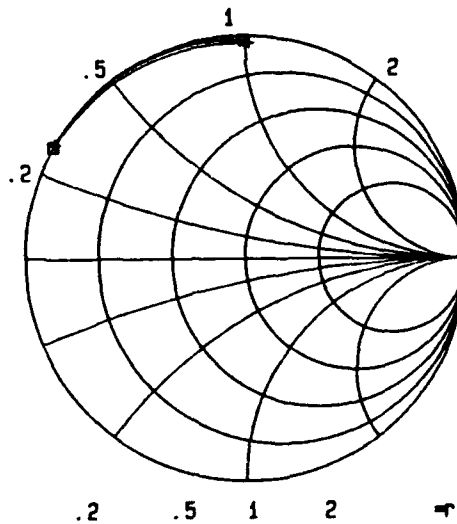


Figure 65. Plots for WR(28), $w/b=1$, $T=5$ mm, $t=1$ mils.

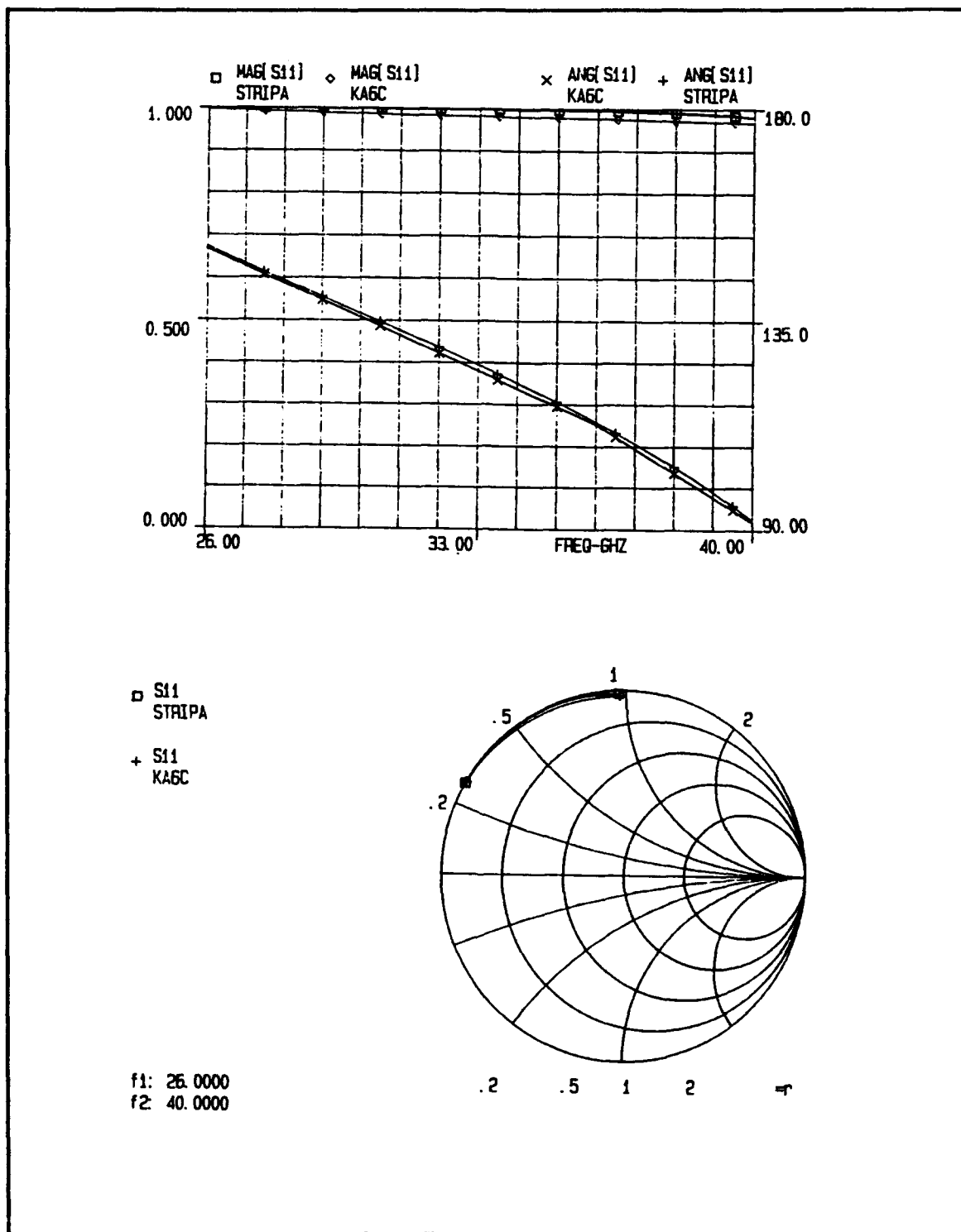


Figure 66. Plots for WR(28), w/b=1, T=5 mm, t=2 mils.

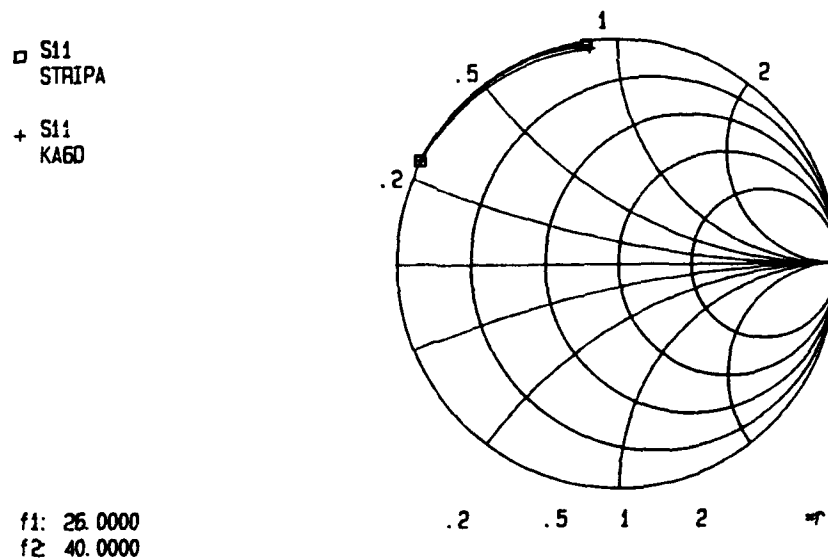
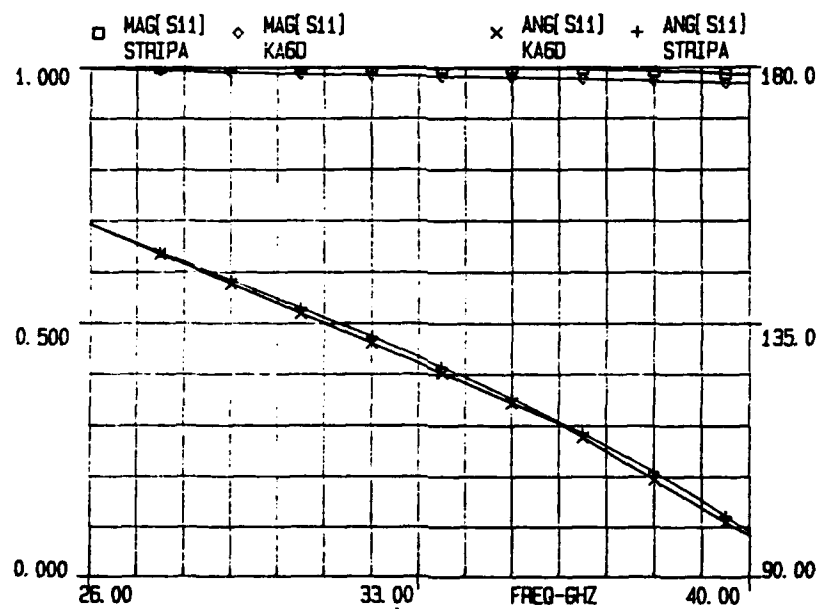


Figure 67. Plots for WR(28), $w/b=1$, $T=5$ mm, $t=5$ mils.

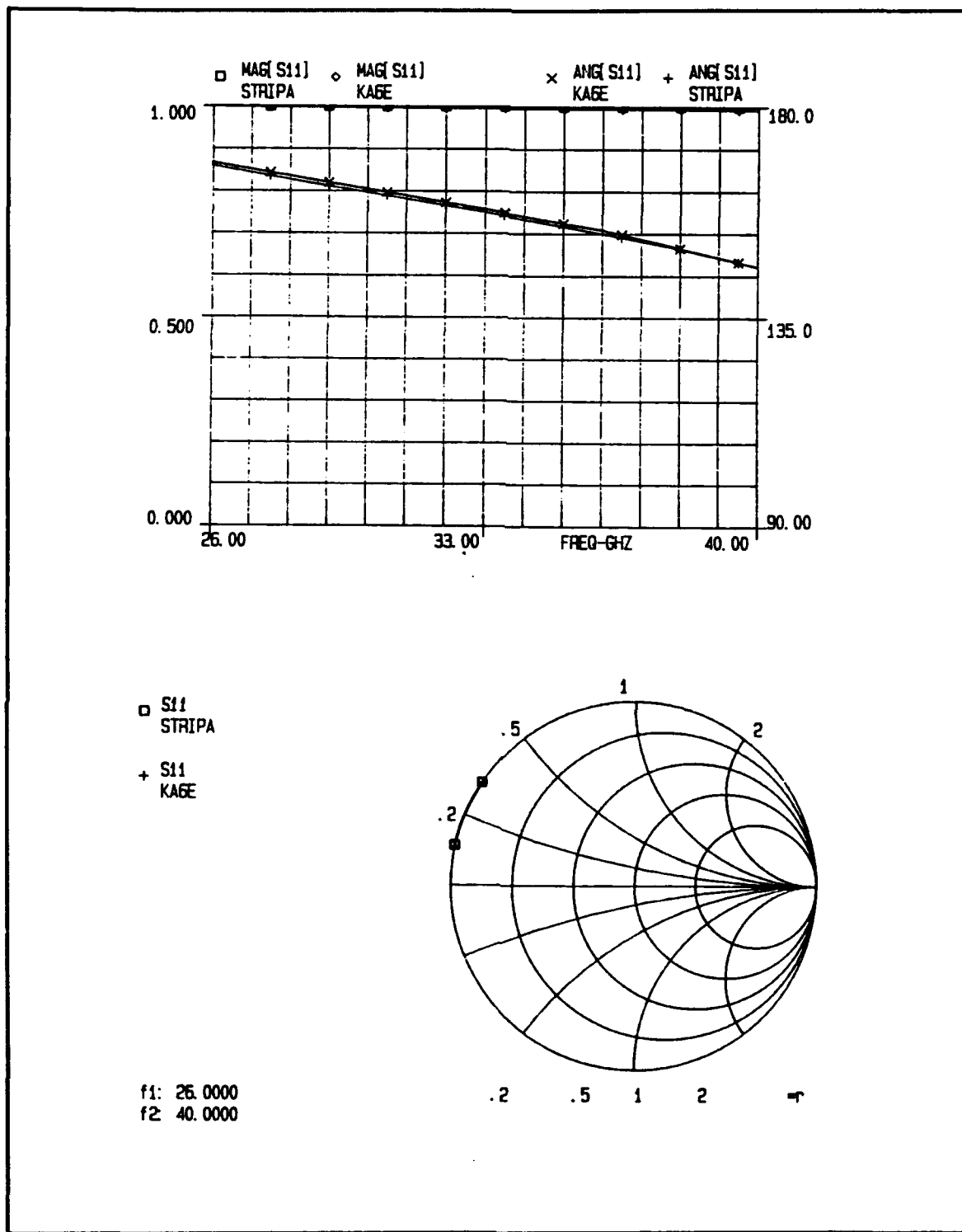


Figure 68. Plots for WR(28), $w/b=1$, $T=5$ mm, $t=50$ mils.

APPENDIX C.

TABLE 10. S-DATA FOR WR(28), w/b=1, T=15 MILS t=0 MILS

Frequency	S11	Θ_{11}	S12	Θ_{11}
26.10	0.826	139.116	0.563	49.116
28.10	0.764	131.876	0.645	41.876
30.10	0.706	125.705	0.708	35.705
32.10	0.652	120.272	0.758	30.272
34.10	0.601	115.390	0.799	25.390
36.10	0.553	110.937	0.833	20.937
38.10	0.509	106.831	0.860	16.831

TABLE 11. S-DATA FOR WR(28), w/b=1, T=15 MILS, t=0 MILS FROM [REF.10].

Frequency	S11	Θ_{11}	S12	Θ_{12}
26.10	0.8494	141.7676	0.5277	51.7676
28.10	0.7883	134.39	0.6152	44.1739
30.10	0.7316	128.3203	0.6817	38.3204
32.10	0.6795	122.6251	0.7337	32.6250
34.10	0.6323	117.8790	0.7748	27.8790
36.10	0.5878	114.1348	0.8090	24.1348
38.10	0.5476	110.2852	0.8367	20.2852

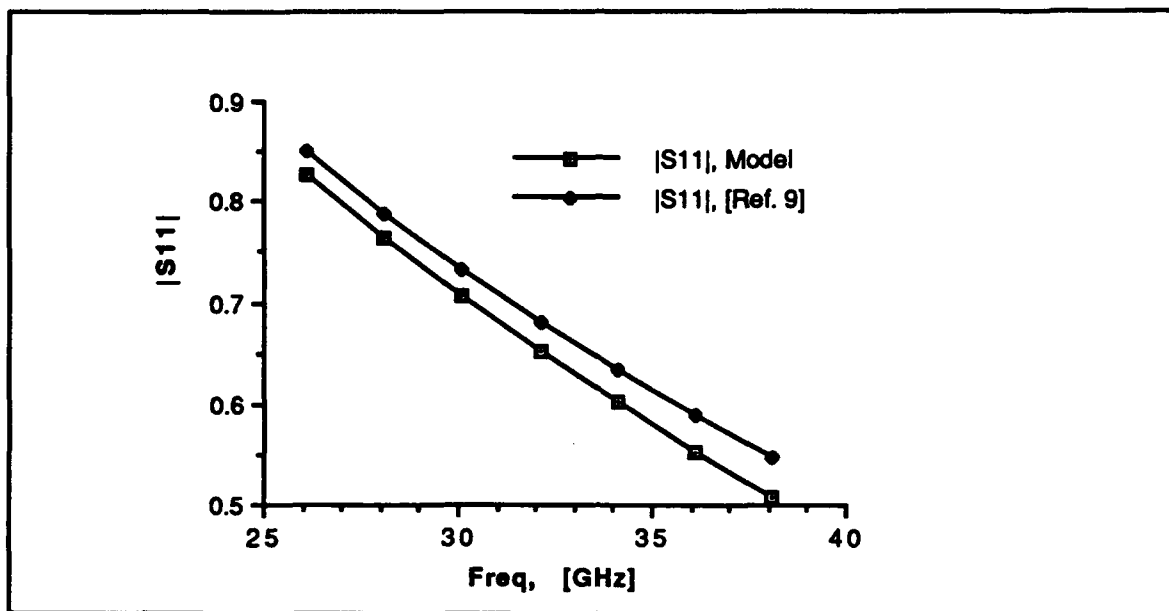


Figure 69. Magnitude for WR(28) with $w/b=1$, $T=15$ mils, $t=0$ mils.

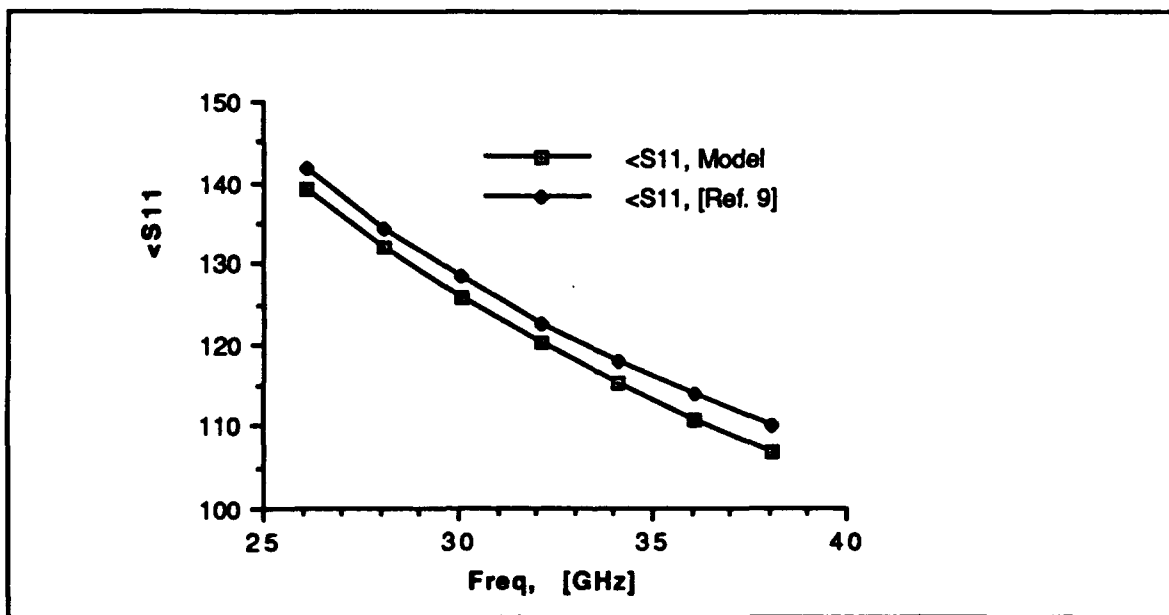


Figure 70. Angle for WR(28) with $w/b=1$, $T=15$ mils, $t=0$ mils.

TABLE 12. S-DATA FOR WR(8), w/b=1, T=30 MILS, t=0 MILS FROM [REF. 9].

Frequency	 S11 	∠11	 S12 	∠11
90	0.9956	151.3653	0.0937	61.3653
95	0.9933	145.6700	0.1157	55.6700
100	0.9901	140.0274	0.1404	50.0274
105	0.9862	134.8595	0.1658	44.8594
110	0.9808	130.0079	0.1948	40.0079
115	0.9741	124.0489	0.2263	34.0489
120	0.9653	118.6172	0.2611	28.6172
125	0.9540	112.5001	0.3000	22.5001
130	0.9382	106.5411	0.3461	16.5411
135	0.9184	99.6856	0.3957	9.6856
140	0.8914	92.3555	0.4532	2.3555

TABLE 13. S-DATA FOR WR(8), w/b=1, T=30 MILS, t=0 MILS.

Frequency	 S11 	Θ11	 S12 	Θ12
90	0.995	149.153	0.00998	50.153
95	0.993	143.611	0.1181	53.611
100	0.990	138.230	0.1410	48.23
105	0.986	132.877	0.1667	42.877
110	0.981	127.460	0.1940	37.46
115	0.974	121.907	0.2265	31.907
120	0.966	116.153	0.2585	26.153
125	0.955	110.141	0.2966	20.141
130	0.942	103.814	0.3356	13.814
135	0.924	97.118	0.3823	7.118
140	0.901	90.005	0.4338	0.005

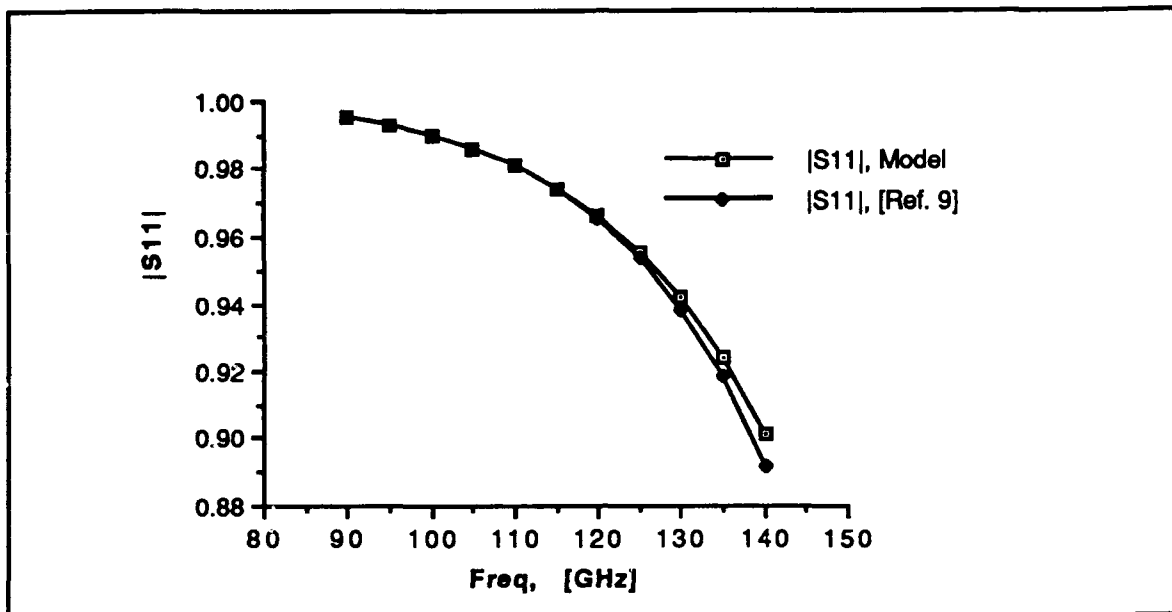


Figure 71. Magnitude for WR(8) with $w/b=1$, $T=30$ mils, $t=0$ mils.

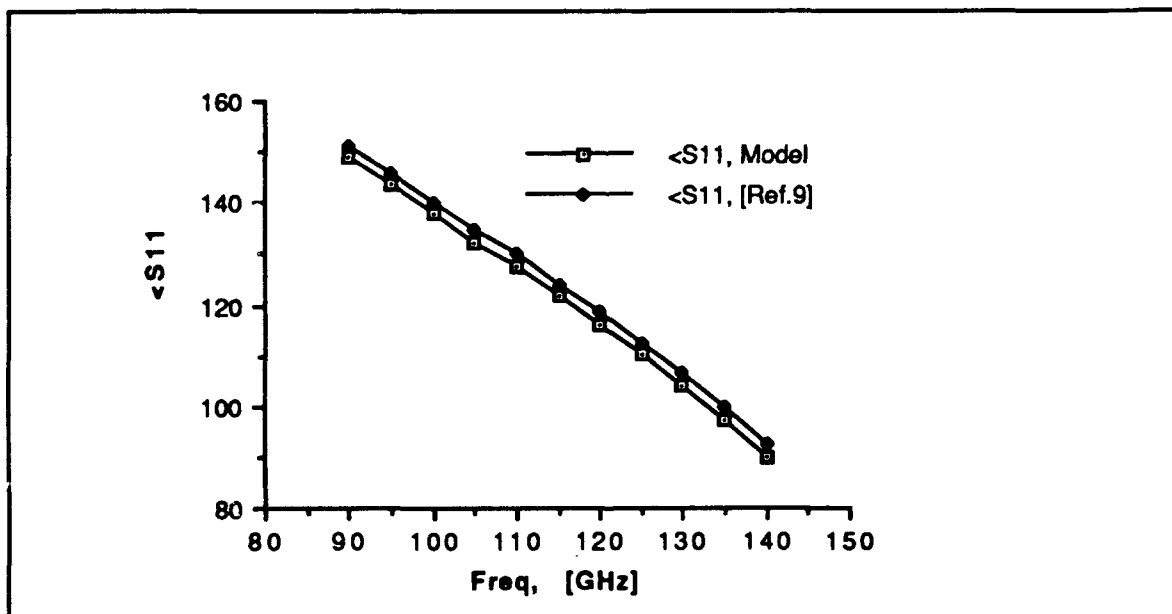


Figure 72. Angle for WR(8) with $w/b=1$, $T=30$ mils, $t=0$ mils.

TABLE 14. WORST ERROR FOR METAL THICKNESS $t=0$ MILS.

Strip length	S11 (Match) Max Error	S11 (model) Max Error
0.1 mm	9.5%	8%
0.2 mm	9%	6.8%
0.5 mm	3.15%	3.9%
1 mm	0.29%	1%
2 mm	0.84%	1.2%
5 mm	1.2%	1.3%

TABLE 15. WORST ERROR FOR METAL THICKNESS $t=1$ MILS.

Strip length	S11 (Match) Max Error	S11 (Model) Max Error
0.1 mm	10%	10%
0.2 mm	8.3%	7.1%
0.5 mm	1.9%	3.7%
1 mm	1.3%	0.57%
2 mm	1.54%	1.1%
5 mm	1.34%	1.34%

TABLE 16. WORST ERROR FOR METAL STRIP $t=2$ MILS.

Strip length	S11(match) Max Error	S11(Model) Max Error
0.1 mm	10%	9.8%
0.2 mm	4.6%	5.6%
0.5 mm	1.21%	2.8%
1 mm	0.56%	0.7%
2 mm	1.29%	1%
5 mm	1.24%	1.3%

TABLE 17. WORST ERROR FOR METAL THICKNESS $t=5$ MILS.

Strip length	S11(match) Max Error	S11(Model) Max Error
0.1 mm	6.4%	6.3%
0.2 mm	3.2%	1.6%
0.5 mm	0.4%	0.5%
1 mm	1.76%	1.4%
2 mm	2%	2%
5 mm	1.1%	1.6%

TABLE 18. WORST ERROR FOR METAL THICKNESS $t=50$ MILS.

Strip length	S11(match) Max Error	S11(Model) Max Error
0.1 mm	0.95%	0.5%
0.2 mm	1.6%	1.5%
0.5 mm	2.4%	1.5%
1 mm	1.5%	0.8%
2 mm	2.6%	2%
5 mm	0.6%	0.6%

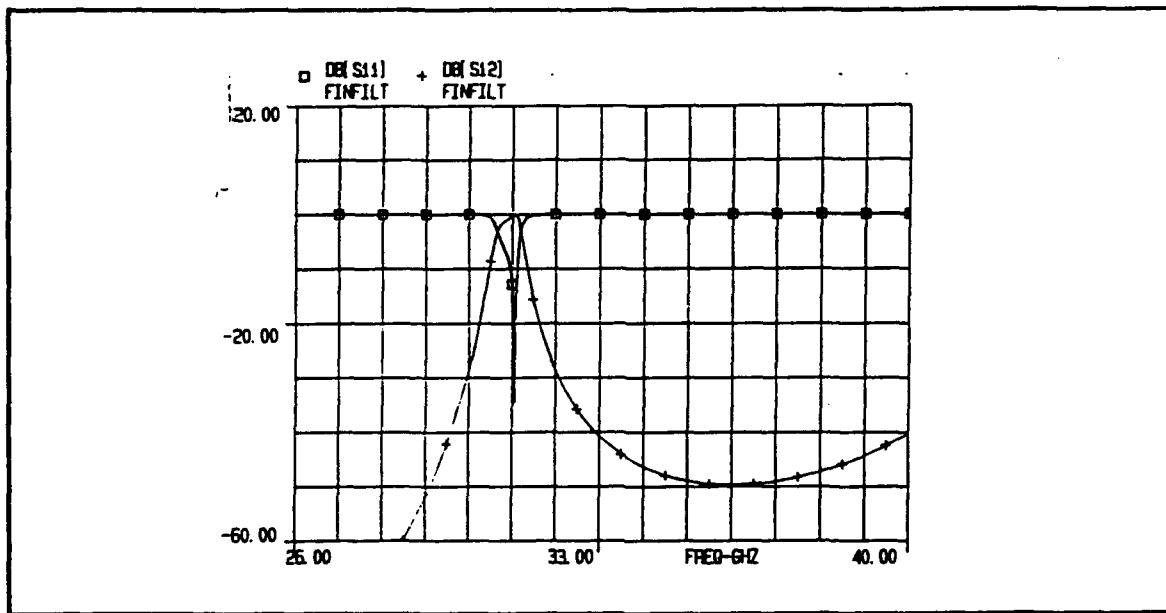


Figure 73. Model response for the Ka band filter with $t=0$ mils.

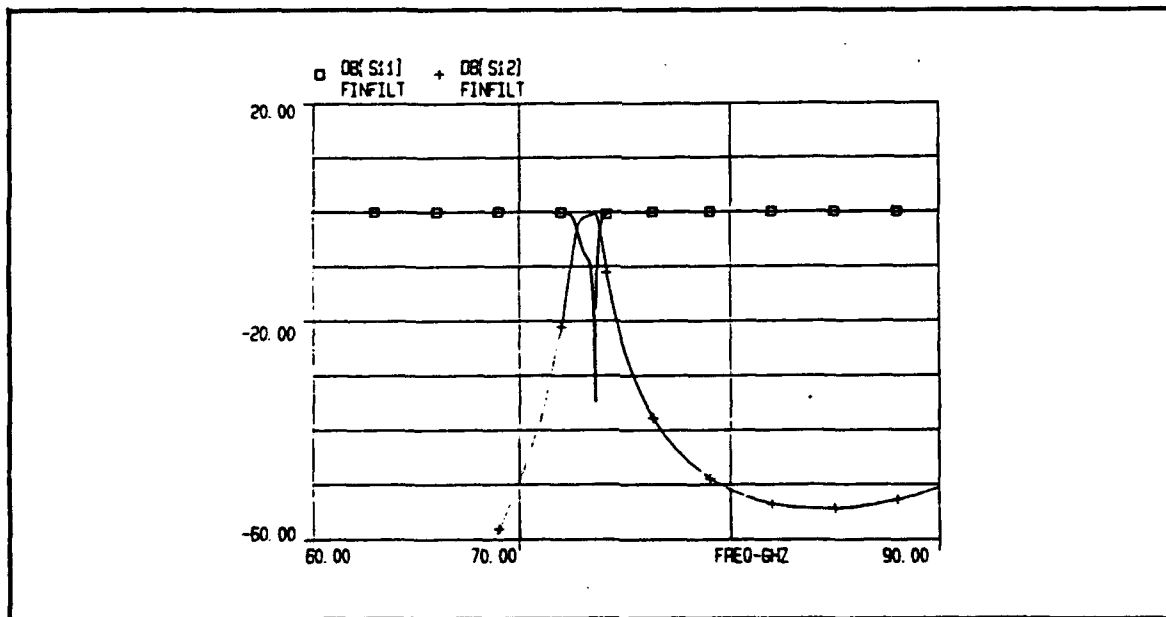


Figure 74. Model response for the E band filter with $t=0$ mils.

REFERENCES

- [1] P. J. Meier, "*Integrated finline millimeter components*," IEEE Trans. Microwave Theory and Tech., vol. MTT-22, pp. 1209-1216, Dec 1974.
- [2] J. B. Knorr and P. M. Shayda, "*Millimeter-wave finline characteristics*," IEEE Trans. Microwave Theory and Tech., vol. MTT-28, pp. 737-743, Jul 1980.
- [3] G. S. Miller, "*An experimental investigation of several finline discontinuities*," M. S. thesis, Naval Postgraduate School, Monterey, CA, Dec 1980.
- [4] J. B. Knorr, "*Equivalent reactance of a shorting septum in a finline: theory and experiment*," IEEE Trans. Microwave Theory and Techniques, vol. MTT-29, pp. 1196-1202, Nov 1981.
- [5] J. C. Deal, "*Numerical computation of the scattering coefficients of an inductive strip in a finline*," M. S. thesis, Naval Postgraduate School, Monterey, CA, Mar 1984.
- [6] J. B. Knorr and J. C. Deal, "*Scattering coefficients of an inductive strip in a finline: theory and experiment*," IEEE Trans. Microwave Theory and Tech. , vol. MTT-33, pp. 1011-1017, Oct 1985.
- [7] J. B. Knorr, "*A CAD model for the inductive strip in finline*," technical report NPS 62-88-013, Naval Postgraduate School, Monterey, CA, Aug 1988.
- [8] J. B. Knorr, "*CAD models for inductive strips in homogeneous finline: the methodology*," technical report NPS 62-90-007, Naval Postgraduate School, Monterey, CA, Mar 1990.
- [9] M. Morua, "*A CAD models for the inductive strips in homogeneous finline*," M. S. thesis, Naval Postgraduate School, Monterey, CA, Jun 1990.
- [10] Yi-Chi Shih, "*Design of waveguide E-plane filters with all-metal inserts*," IEEE Trans. Microwave Theory and Tech., vol. MTT-32, pp. 695-704, Jul 1984.

- [11] R. Vahldieck, J. Bornemann, F. Arndt, D. Grauerholz, "*Optimized waveguide E-plane metal insert filters for millimeter-wave applications,* " IEEE Trans. Microwave Theory and Tech., vol. MTT-31, pp. 66-69, Jan 1988.

INITIAL DISTRIBUTION LIST

	No. Copies
1. Defense Technical Information Center Cameron Station Alexandria, VA 22304-6145	2
2. Library, Code 52 Naval Postgraduate School Monterey, CA 93943-5100	2
3. Chairman, Code EC Naval Postgraduate School Department of Electrical and Computer Engineering Monterey, CA 93943-5000	1
4. Director, Research Administration, Code 81 Naval Postgraduate School Monterey, CA 93940-5000	1
5. Professor Jeffrey B. Knorr, Code EC/Ko Department of Electrical and Computer Engineering Naval Postgraduate School Monterey, CA 93943-5000	2
6. Professor Rama Janaswamy, Code EC/Js Department of Electrical and Computer Engineering Naval Postgraduate School Monterey, CA 93943-5000	1
7. Dimitrios Dariotis Kifisias 38 Ambelokipoi 11526 Athens Greece	3
8. Embassy of Greece Naval Attache 2228 Massachusetts Ave., N.W. Washington, D.C. 20008	3